Definition of Process Zones and Connectivity in Catchment Scale NPS Processes

Report to the
WATER RESEARCH COMMISSION

by

S Lorentz[1], J Miller[2], P Lechler[3], G Mackin[4] M Lord[2],
J Kollongei[1], J Pretorius[1], K Ngeleka[1], N Zondi[1] J le Roux[5]

[1]School of Bioresources Engineering and Environmental Hydrology
University of KwaZulu-Natal, Pietermaritzburg

[2]Institute of Watershed Research and Management,
Western Carolina University

[3]Bureau of Mines and Geology
University of Nevada, Reno

[4]Department of Mathematics & Statistics
University of Northern Kentucky

[5]Institute for Soil, Climate and Water,
Agricultural Research Council, Pretoria

WRC Report No.1808/1/11
ISBN No 978-1-4312-0112-9

February 2011

DISCLAIMER

This report has been reviewed by the Water Research Commission (WRC) and approved for publication. Approval does not signify that the contents necessarily reflect the views and policies of the WRC, nor does mention of trade names or commercial products constitute endorsement or recommendation for use.

The research in this report emanated from a project funded by the Water Research Commission (WRC) entitled:

'Definition of Process Zones and Connectivity in Catchment Scale NPS Processes'.

The Reference Group responsible for this project consisted of the following persons:

Mr M du Plessis	WRC (Chairman)
Dr N Jovanovic	CSIR
Dr W de Clercq	Stellenbosch University
Mr KP Taylor	Department of Agriculture
Prof KL Bristow	CSIRO, Townsville, Australia
Prof A Görgens	Sigma Beta Consulting
Mr TJ Matsetela	NAFU

The financing of the project by the Water Research Commission and the guidance, advice and assistance of the Reference Group is gratefully acknowledged, particularly the guidance and introductions instigated by Prof Bristow. Interpretation of the soil survey by Dr Pieter le Roux and his team (University of the Free State) is also gratefully acknowledged. The authors would also like to acknowledge the kind co-operation, use and access to their land of the farmers in the Mkabela catchment, particularly Mr Werner Schröder.

EXECUTIVE SUMMARY

Successful prediction of agricultural non-point source pollution (NPS-P) requires an understanding and quantification of the sources and pathways of sediment and nutrients in the landscape and stream network. The migration of NPS-P is often dominated by controls and connectivity features in the catchments and so this work aims at observation, description and quantification of the processes for water, sediment and nutrient delivery in a research catchment, the Mkabela catchment near Wartburg, KwaZulu-Natal. These processes include land based connectivity and stream reach barriers and controls. The catchment selected comprises a predominant sugar cane land use, but includes areas of vegetable cropping, forestry and pastures. The landscape is dominated by Natal Group Sandstone geology and the stream network has numerous impoundments, wetlands and hydraulic controls at road crossings and changes in gradient or bed type.

The methods applied to the understanding of the NPS-P migration included:

- Sediment source fingerprinting, where surface soils were sampled and downstream deposition profiles cored to deduce the source, timing and controls dominant in the migration of sediments;
- Geophysical and soil pedological surveys to determine dominant pathways of water, sediment and nutrient migration in the contributing hillslopes;
- Stable isotopes of water and nutrient sampling to illustrate flow pathways, controls and connectivity in contributing hillslopes and the stream network.

Soil and sediment profiles were sampled in May 2008 and nutrient, sediments and isotopes were sampled in the stream network at various spatial and temporal scales between 2009 and 2011.

The combined process zone-sediment tracing analysis resulted in the following conclusions.

- The study catchment is composed of a series of distinct process zone types, each characterized by differences in their ability to produce, transfer, and store sediment. The nature and spatial arrange of the process zones within the basin show that it can be subdivided into three subcatchments, referred to here as upper, mid- and lower subcatchments. The three subcatchments differ in their tendencies to transport and store sediment and nutrients.

- The construction of a drainage ditch through the upstream most wetland significantly altered the geomorphic and hydrologic connectivity of the catchment. Prior to its construction, sediments (and associated nutrients) were largely deposited within wetlands which encompassed a majority of the valley floors within the upper catchment. Sediments delivered to the mid-catchment area were generally transported downstream as a result of confined flows and steep channel gradients which often include bedrock reaches. There is very little storage within the reach, except within local dams.

- Following construction of the ditch across the upper most wetland, sediments could be transported from the headwaters of the catchment, through downstream wetlands and dams (reservoirs) and to a low-gradient alluvial channel boarded by an extensive riparian zone. Thus, the axial drainage system is geomorphically and hydrologically connected during most events throughout the study basin. However, current rates of sediment deposition within the downstream most riparian wetlands is extremely high, approaching 10 cm/yr, suggesting that this reach limits the further downstream movement of sediment.

- The complex interactions between runoff, soil type and characteristics, and land-use (among other factors) appear to create temporal and spatial variations in sediment provenance. Silt- and clay-rich layers found within the wetland and reservoir deposits appear to have been derived from the erosion of fine-grained, valley bottom soils which are frequently utilized as vegetable fields. The deposits tend to exhibit elevated concentrations of Cu and Zn, presumably from the use of fertilizers which contain both elements. Coarser-grained deposits within the wetland and reservoir presumably result from the erosion of sandier hillslope soils extensively utilized for sugar cane. Erosion of these upland cane fields presumably occurs during relatively high magnitude runoff events that are capable of transporting sand-sized sediment off the slopes, and which create dam (reservoir) deposits lacking significant quantities of silt- and clay-sized particles. Therefore, sediment source, as might be expected, varies as a function of runoff magnitude.

- Sediment source determination on multiple cores from the wetland demonstrated that sediment partitioning during transport not only produced deposits of varying sedimentological and chemical characteristics, but deposits

consisting of sediment from different source areas. As a result, within highly variable depositional environments, multiple cores should be collected and analyzed to determine sediment provenance.

Nutrient loading and isotopic tracing behaviours reflect the following:

- The nutrient (NO_3-N and P) transport in the catchment mirrors the sediment migration through the channel system. However, the relationship between sediment and P is poor, suggesting that much of the P transport in contributing hillslopes is in a dissolved phase and may occur in the subsurface.

- The loads of nutrients between the Bridge 1 and Bridge 2 section reflect the bedrock control, where contributions from sugar cane hillslopes between these stations are not retained, even in the short wetland upstream of Bridge 2. Isotope ratios reveal that impounded tributaries are often effective in retaining event water. However mixing and disturbance of the resident nutrients and sediments results in elevated outflow concentrations during events.

- The dominant contribution mechanism for nutrients in the landscape appears to be in the subsurface, in lateral discharge in the intermediate layer between the sandy soil and bedrock.

- Event water, carrying high nutrient loads, dominates the responses at the field scale, while low flows reflect the groundwater concentrations of N and P throughout the catchment.

Future understanding of the connectivity and controls in the Mkabela and other catchments would be improved by further sediment fingerprinting to the lower parts of the catchment and identification of nutrient tracers to identify the sources and track the movement and deposition of applied fertilizers. An increase in the frequency of sampling stream responses of isotopes, nutrients and sediments during events would improve the understanding and quantification of the connectivity between land units and stream. While the hydropedological assessment of hilsllope response types has allowed for the definition of hillslope water generation mechanisms in this study, improved monitoring of the hilsllope water and nutrient responses would be invaluable in quantifying the links between land units and stream and the nature of nutrient migration.

TABLE OF CONTENTS

LIST OF FIGURES

LIST OF TABLES

1. INTRODUCTION

Successful prediction of non-point source pollution (NPS-P) requires an understanding and quantifying of the sources and pathways of potential pollutant in the landscape and stream network. However, the migration of NPS-P is dominated by controls and connectivity features in the catchments and these often belie traditional methods of simulation. Nevertheless, a clear understanding of the process mechanisms of these connectivity and control features, based on observation, can lead to their identification and inclusion in estimating NPS-P in ungauged basins. This project, therefore, aims at developing and applying techniques to identify and quantify nutrient and sediment source zones, quantify the translation of these pollutants through the landscape and quantify the impact of control features on the transfer of pollutants through a stream system.

Specific project aims are to:

- Delineate, characterize and quantify sediment and nutrient process zones in the Mkabela research catchment, near Wartburg, KwaZulu-Natal;
- Define the dynamics and connectivity of the process zones by observing water, and nutrient fluxes and by physical and geochemical fingerprinting of sediments;
- Define and quantify the impact of NPS pollution controls such a riparian zones, wetlands and reservoirs on the migration of sediments and solutes through the catchment; and
- Develop and propose algorithms for inclusion in simulation models to allow for the NPS dynamics in process zones and control features.

In this study we develop a description of the processes for water, sediment and nutrient delivery in the Mkabela research catchment (Figure 1), based on a combination of investigative techniques. No single method is likely to uncover all the nuances of the landscape and stream connectivity and controls. Therefore, the following suite of techniques has been applied over a period of three years (2008-2011):

- Field observations and mapping led to the delineation and description of process zones within the catchment;
- Geophysics and hydropedology surveys were conducted to describe the hillslope water generating mechanisms and controls;
- Stable isotopes of water (^{18}O and ^{2}H), were sampled a various scales in the nested sub-catchments to reveal sources and pathways of hydrological response;

- Sediment fingerprinting was used to identify and quantify the sources, conveyance and depositional history of sediments from landscape to stream;
- Hydrometry, together with nutrient and suspended solids sampling in the stream network, led to an understanding of the continuity and responses of NPS-P to rainfall events and low flow sequences and
- Trace nutrient fingerprinting was used to identify sources and pathways of fertilizer product from field to stream.

The study concludes with suggestions for improved application of the techniques and identification of mechanisms requiring detailed study.

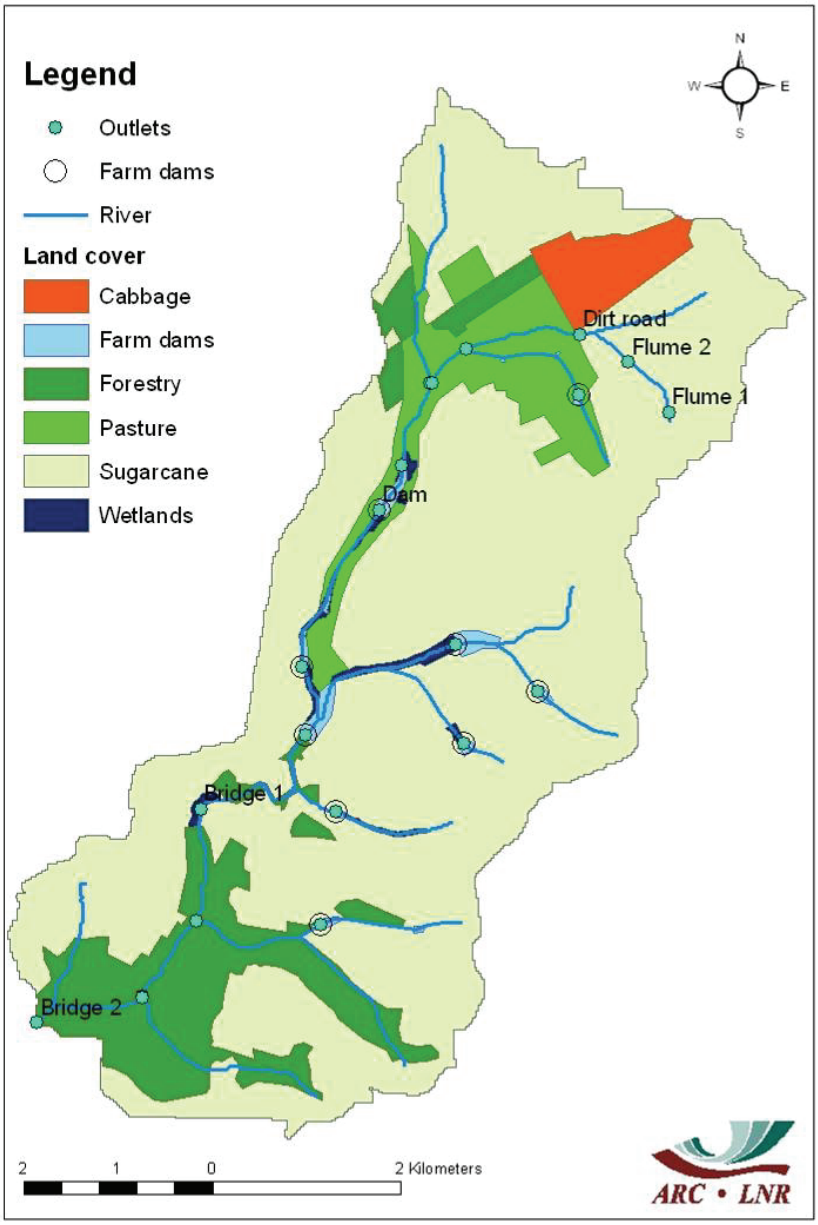

Figure 1. The Mkabela research catchment, showing land use.

2. PROCESSES ZONE DESCRIPTION

2.1 Background and Study Area

Historically, examination of fluvial processes, including sediment transport, focussed on moderate to low-gradient, alluvial rivers (Grant and Swanson, 1995), and sediment was assumed to move semi-systematically through the drainage system. This classical continuum view has be replaced in recent years by a segmented perspective of a drainage network, resulting in the increased use of hierarchical classification systems for the analysis and management of riverine environments (Frissell et al., 1986; Kishi et al., 1987; Grant et al., 1990; Montgomery and Buffington, 1993; Grant and Swanson, 1995, Brierley and Fryirs, 2005). While proposed classification systems differ in their specifics, the unifying theme is that drainage networks consist of channel and valley floor environments that can be subdivided into progressively smaller units, each of which are morphologically homogeneous with respect to landforms, processes, and the controlling factors of geology, vegetation, substrate, and hillslope influences (Gant and Swanson, 1995). Commonly included categories range from localized channel-scale units (defined on the basis of various river bed features such as pools, riffles, bars, etc.), reach scale units (defined according to the nature of both the channel and valley floor), and larger scale units ranging up to and beyond the entire drainage basin. Application of the hierarchal approach for management purposes has focused on reach-scale units, often referred to as process zones (or alternatively, a river style by Fryirs and Brierley, 2001). Inherent within the hierarchal systems approach is the perception that process zones (as well as units defined at other scales) differ in their ability to produce, transport, and store sediment. For example, some zones, such as hillslope hollows (u-shaped depressions on the hillslope) serve as significant sediment sources, whereas others, including confined bedrock channels, serve predominantly as conduits of sediment transport. The predominant geomorphic process (es), then, vary between the various process zones. Differences in sediment production, transport, and storage are considered important because they lead to differences in the behavior (type, rate, and magnitude of erosional and depositional processes) between zone types (Brierley and Fryirs, 2005). Confined bedrock channels, for example, are unlikely to undergo the same type of adjustment to a decrease in sediment load as are unconfined alluvial channels bounded by wide valley floors. Process zones therefore represent a fundamental unit of watershed management that allows distinct strategies to be developed for specific parts of the drainage network.

Two concepts closely linked to the hierarchal view of river systems are those of coupling and connectivity. Coupling dictates how upstream geomorphic responses to environmental change affect those downstream (and vice versa) (Brunsden, 1993; Harvey 1997, 2001, 2002; Hooke, 2003). Along well-coupled rivers, erosional and depositional responses are transmitted between juxtaposed zones, whereas the effects of environmental change along poorly coupled systems are spatially limited. Manifestations of coupling are governed by sediment connectivity, defined by Hooke (2003) as the ability of sediment to pass through a channel network (i.e., from one defined zone to another). Hooke (2003) proposed a five category classification system describing the degrees of reach-scale connectivity. The classification is primarily based on the nature of the sediment sources as well as stream competence (and therefore discharge and grain size under consideration). Categories defined by Hooke (2003) include unconnected, partially connected, connected, potentially connected (competent but lacking a suppy of sediment), and disconnected.

In light of the above, the source(s), transport, and storage of NPS pollution are likely to depend on the hierarchal structure (morphometry) of the watershed and the connectivity between process zones and other hierarchal units. To our knowledge, however, the utilization of a hierarchal approach, which has the ability to effectively determine the spatial and causal linkages between human activities, watershed-scale processes, and channel conditions, has not been applied to the investigation of NPS pollution.

2.2 Delineation, Characterization and Mapping of Process Zones

The utilized hierarchical classification system was modified from that presented by Montgomery and Buffington (1993) and Grant and Swanson (1995) to fit the characteristics of the catchment in the KwaZulu-Natal Midlands. Field and cartographic observations indicated that the catchment could be subdivided into channel units (defined on channel bed features and the underlying substrate), process zones (defined on differences in valley shape, valley floor landforms, and substrate type), and subcatchment units (defined according to changes in basin and valley morphometry). The utilized classification system is presented in Figure 2. General characteristics of the process zones are presented in Table 1, whereas photographs of selected zone types are shown in Figure 3. The processes zones were initially defined on the basis of geomorphic criteria including their position on the landscape, dimensions and cross-sectional form of the feature, composition and nature of the bounding materials (bedrock vs. sediment; sediment size, stratification, etc.), and relief/gradient of the included terrain. It is important to recognize that while zone types were defined geomorphically, each type exhibits specific traits with regards to geomorphic processes (including erosion and deposition), and hydrologic sources and sinks.

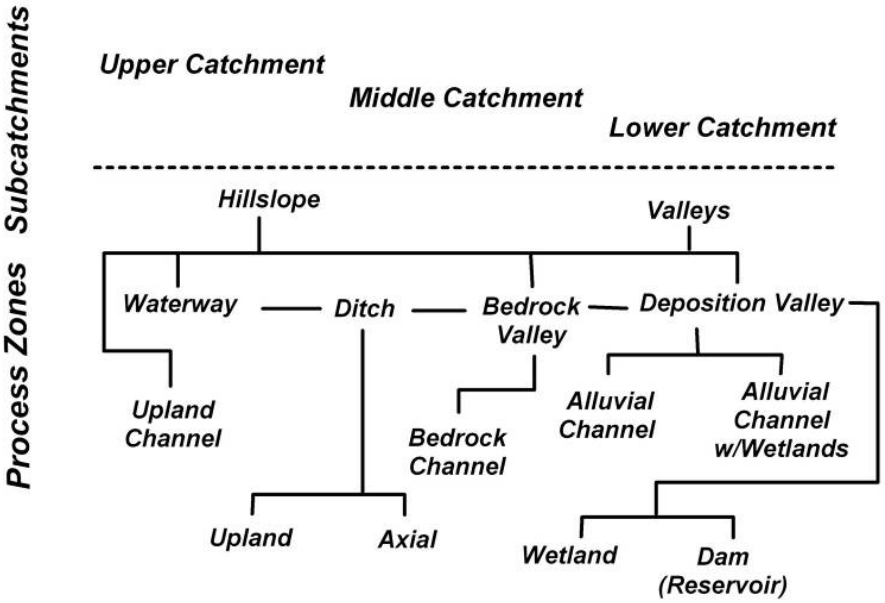

Figure 2. System used to classify process zones.

Table 1. Summary of Process Zones and their general characteristics

Process Zone	**Character**	**Dominant Process**
Waterways	• Man-made, typically in upland areas • Slope parallel • Wide, shallow channel • V. little sediment storage • Grass covered channel bed	• Sediment transport over "rough" bed • Predominantly a zone of recharge (?)
Ditch	• Man-made, trapezoidal channel • Valley parallel, slope perpendicular (axial), slope Parallel (upland) • Relatively low gradient • Channel bed – sediment	• Sediment transport through low gradient, but efficient channel • Recharge zone
Wetland Valley (with channel)	• Natural, flat-lying alluvial & lacustrine fill • Wide valley • May or may not exhibit through flowing channel	• Sediment deposition & storage • Groundwater discharge
Alluviated Valley (with riparian wetlands)	• "Natural" flat, alluvial valley floor of varying width • Narrow, deep channel form • May or may not be bordered by riparian wetlands	• Sediment transport through channel • Sediment storage on floodplain • Dominated by groundwater discharge
Bedrock Channel	• Narrow, bedrock controlled valley • Steep channel, with multiple knickpoints present • V. little sediment storage	• Sediment transport through highly competent channel

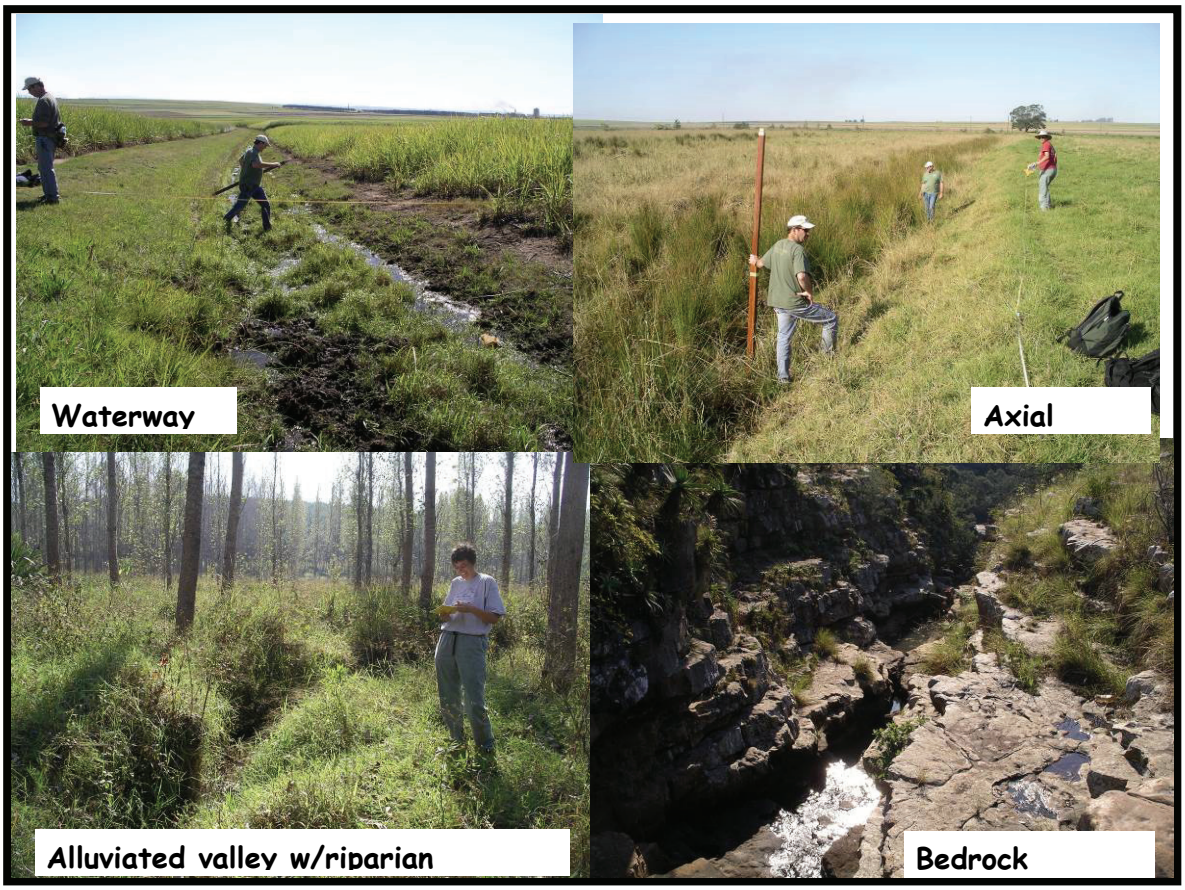

Figure 3. ***Examples of selected process zones; see Table 1 for zone characteristics.***

2.3 Process Zone Deductions from Geophysics and Soil Surveys

Delineation and mapping of process zones utilized an iterative approach where distinct reaches of the drainage network were classified and mapped on 2007 georectified SPOT images, with the aid of stereoscopic viewing of 2004, 1:10,000 aerial photographs. Once mapped, the geo-rectified and field checked data provided spatial information on the type and distribution of the process zones and the ability of the drainage network to transfer water, sediment, and any nutrients that they carry down catchment.

The process zones were characterized, to the degree possible, for basic hydrologic functions including 1) magnitude, and spatial and temporal continuity of surface water flow, and 2) surface water interaction with subsurface water. In a manner similar to that described by Lerner (2003), surface water – groundwater interactions were characterized for their degree and type of connection (i.e. gaining or losing), temporal characteristics of connections, and the type(s) of subsurface water body that interacts with the channel (e.g. unsaturated zone recharge, perched water tables, deep groundwater). The hydrologic characterization is based on a combination of field observations, geomorphology, hydrologic monitoring data

from instrumented sites (e.g. flumes, tensiometers, piezometers), and, broadly, sediment source area modeling based on geochemical fingerprinting of sediments.

Inspection of Figure 4 shows that the natural drainage density, calculated at 1.05 km/km^2, is extremely low, and is rivaled by the density of roads within the catchment. The drainage network is characterized by a common downstream sequence of process zones. Headwater areas, particularly within cane fields, typically possess waterways that deliver water and sediment to upland channels. (The drainage density in the sugar cane fields is approximately 2.5km/km^2). The upland channels then feed water, sediment (and associated nutrients) to alluvial valley segments, or axial ditches. Many of the upland channels along the south side of the catchment are short, draining relatively small areas, and are disconnected geomorphically from the axial valley, suggesting that they deliver relatively minor amounts of sediment to the axial channel in comparison to northern and headwater drainages.

Wetlands periodically occur along the axial valley and serve as an important type of process zone in that they represent depositional environments that reduce the transfer to sediment and nutrients to downstream areas. In some instances, axial ditches have been excavated into the wetlands, modifying their transfer abilities (as will be discussed in more detail below). A number of dams (reservoirs) have also been superimposed on the drainage network, most of which are located along axial valley type process zones. These features will also impede the down catchment movement of sediment and nutrients.

Both the frequency and length of waterways and upland channels decrease down catchment as relief and hillslope gradients increase. The extent of wetlands also decreases down catchment until reaching the downstream most section of the basin where the drainage network is dominated by a low-gradient alluvial valley with an extensive riparian wetland. In contrast to waterways, upland channels, and wetlands, the frequency of alluvial and bedrock channels increase down catchment, presumably producing a more efficient system of directly transferring sediment, and any nutrients that they carry, downstream to the alluvial valley possessing riparian wetlands, a process zone that has the ability to store large volumes sediment. In fact, a sediment core collected from this reach shows that more than 2 m of historic sediment has accumulated within the wetlands. At the catchment scale, the capability of the process zones to transfer sediment (Table 1), and their spatial distribution (Figure 4), indicates that the movement of material through the catchment is limited and discontinuous except, perhaps, during high magnitude runoff events. Sediment which is delivered to and transferred through waterways and upland channels on hillslopes will primarily be deposited downstream within wetlands and dams (reservoirs) during low- to moderate-floods.

Thus, the upper catchment areas are characterized by a highly disconnected sediment transport system (Figure 5). The mid-catchment areas are dominated by relatively high gradient alluvial and bedrock channels, with fewer, natural depositional zones (although dams now exist). Thus, the mid-catchment area possesses a greater ability to effectively transport sediment downstream, although a larger percentage of the transported sediment is likely to be stored along the more extensive valley bottoms (floodplains). The lower catchment is dominated by a low gradient, alluvial channel boarded by extensive riparian wetlands. The storage of sediment within this zone is extensive, once again limiting the downstream translation of sediment and nutrients that they may carry (Figure 5).

.

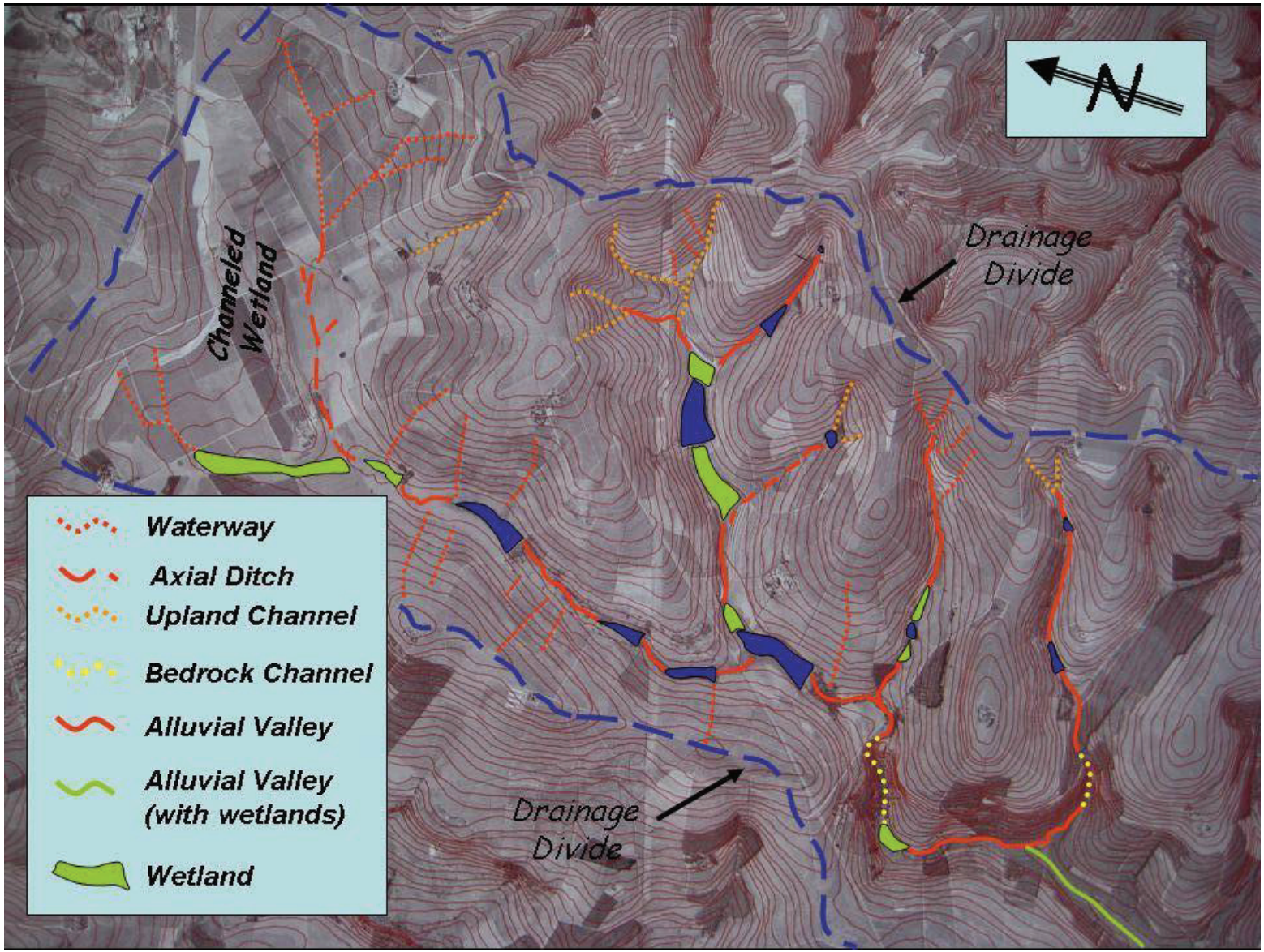

Figure 4. ***Delineation of process zones, connectivity and controls in the Mkabela catchment.***

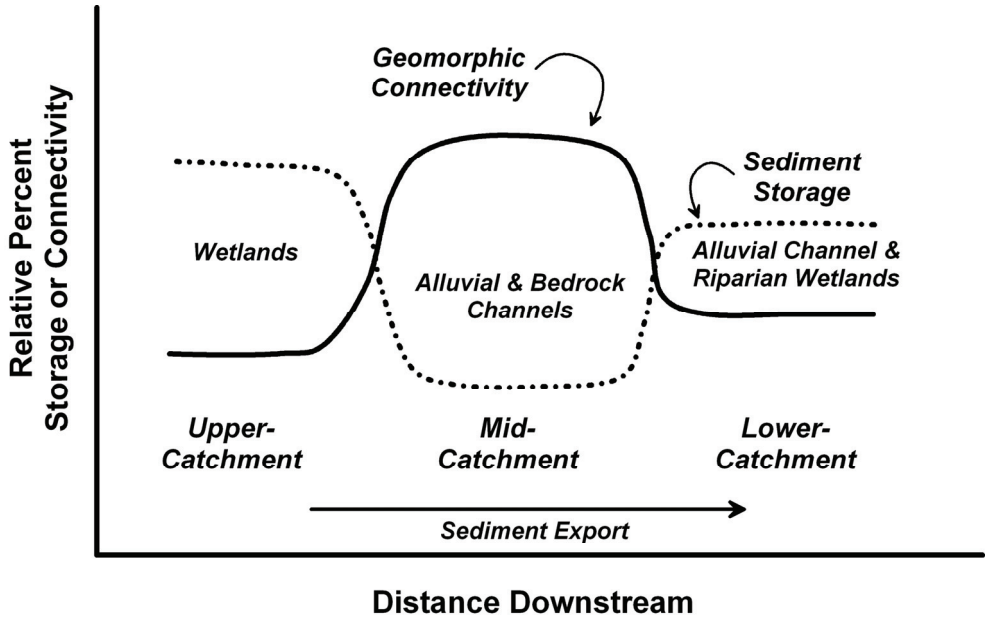

Figure 5. ***Schematic diagram illustrating differences in geomorphic connectivity and sediment storage between subcatchment zones of the Mkabela Basin.***

Sediments and nutrients can reach the stream network, either through overland flow during rainfall events or as subsurface discharge through lateral flow in hillslope profiles or deep fractured aquifers, both during and between events.

The connectivity of water and nutrient delivery from the landscape is primarily dependant on the function of hillslope hydrological processes. These are examined in this study using geophysics and soil hydropedology surveys.

Surface geophysical methods have been used for many decades to investigated, locate, map and characterize subsurface features. In groundwater hydrology investigations, surface geophysical methods represent an extremely important approach to (1) characterize the vadose and water-bearing (or saturated zones), (2) differentiate bedrock from unconsolidated overburden, and (3) locate intrusive dykes, fractured rocks, and weathered zones. The characterization of these features aims to contribute to the understanding of the groundwater flow and pollutants behavior in the catchment.

An Electrical Resistivity Tomography (ERT) survey is one of the geophysical techniques which have proved able to identify soil, geological and hydrogeological features. This technique is used in the Mkabela research catchment to help characterize distribution of water in the subsurface and identify controls afforded by the geological and pedological

structure. These will influence the delivery of nutrients and identify zones of high runoff potential, where sediments are likely to be generated.

2.3.1 Methodology of the Electrical Resistivity Tomography Survey

Hillslope process zone characterization using Electrical Resistivity Tomography was initiated by sourcing previous findings related to the Mkabela catchment, such as geological maps and literature, satellite images and field observations made when visiting the site before geophysical surveying. A geological map was available at a 1:50 000 scale from the Council for Geosciences, Pietermaritzburg. A soil survey report from the Department of Soil, Crop and Climate Sciences, University of the Free State was also available. These data provided a general understanding of soils types and geologic setting in the catchment. Five transects were identified in the headwater subcatchment for ERT surveys as shown in Figure 6.

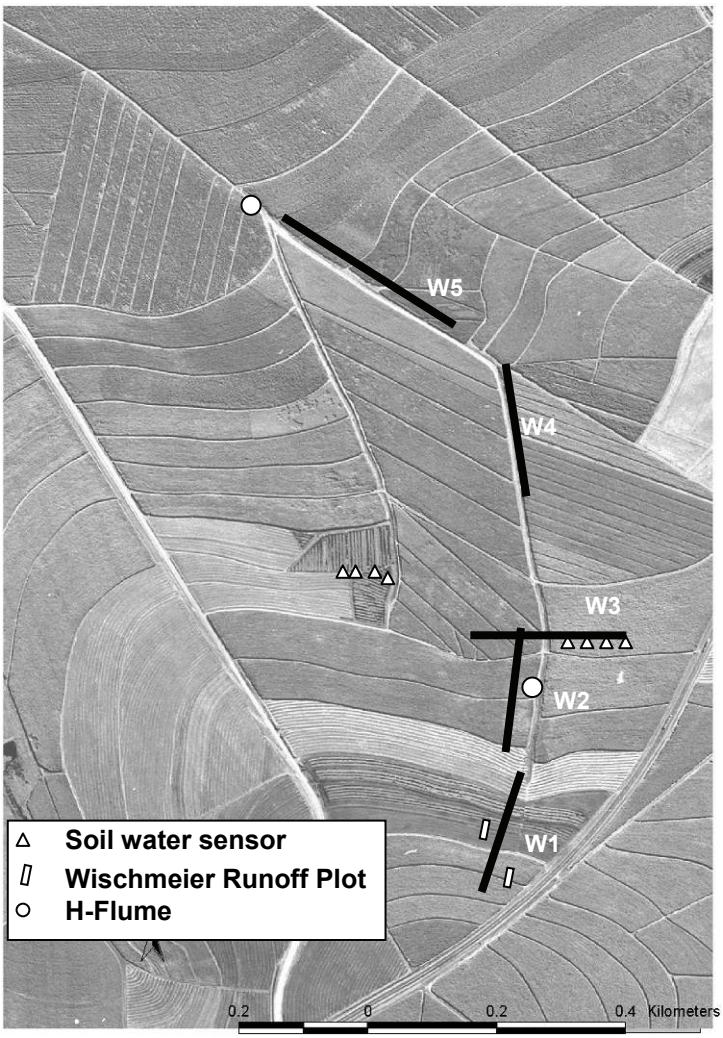

Figure 6. ERT transect locations in the upper Mkabela subcatchment.

The Electrical Resistivity Tomography (ERT) technique is a 2D electrical imaging system which is carried out using a large number of electrodes connected to a multi-core cable (Griffiths and Barker 1996). In order to obtain a 2D electrical image, horizontal and vertical data coverage is achieved by automatic sequential measurements of current and potential locations. The ABEM Lund Imaging System together with a Terrameter SAS 1000 was used on site for data acquisition. The Lund system consists of a basic charging unit, Electrode Selector ES10-64; four Lund spread cables, a suitable quantity of cable joints and cable jumpers, and a supply of electrodes (ABEM 2005). Transect W1 and W5 were extended using a roll-along method. The Electrical resistivity using Wenner alpha array consists of injecting a certain current into the subsurface through two electrodes and measuring the resulting voltage difference at two middle potential electrodes; the four electrodes are equally spaced. The Wenner array has the advantage of resolving horizontal layers more accurately than vertical layers.

2.3.2 Soil and Geologic Setting

2.3.2.1 Soils

The soil survey conducted on the Mkabela catchment indicated that there are a nine soil types including the Avalon (Av), Cartref (Cf), Clovelly (Cv), Glencoe (Gc), Hutton (Hu), Katspruit (Ka), Longlands (Lo), Westleigh (We) (Figure 7), (Le Roux *et al.*, 2006). The soil types Westleigh, Avalon and Longlands are the only ones that can be related to the ERT survey area; they are described in Table 2.

Table 2. Brief description of the primarily soil types found in the study area (after Le Roux et al., 2006)

Soil Type	General Characteristics
Avalon (Av)	The Avalon soil type surveyed to 120 cm depth and consists primarily of soft plinthic B horizons which is a sandy yellow-brown apedal B horizon underlain by hard plinthic horizons.
Cartref (Cf)	Shallow, sandy soils with very little water holding capacity found on steep, short, convex hillslopes.
Clovelly (Cv)	Associated with, and similar to, Longlands soil type.
Glencoe (Gc)	Similar to Avalon soil type, but dominated by hard plinthic subhorizon; found on steeper slopes of higher relief. Parent material is thought to be the Natal Group Sandstone (NGS).
Hutton (Hu)	Found near crest and midslopes of high relief, steep hillslopes. Moderately drained, underlain by NGS.
Katspruit (Ka)	Clayey, strongly gleyed soils found on low-relief (10-15 m) terrain, particular valley bottoms.
Longlands (Lo)	The Longlands soil type was surveyed up to 120 cm depth and consists of soils that are sandier than the Avalon soils with similar profile of soft plinthic B horizons well developed underlain by hard plinthic horizons.
Westleigh (We)	The Westleigh soil type was surveyed up to 110 cm depth and consist a poorly drained hydrosequence dominated by clayey soils with prominent mottling and deep, clayed subsoils.

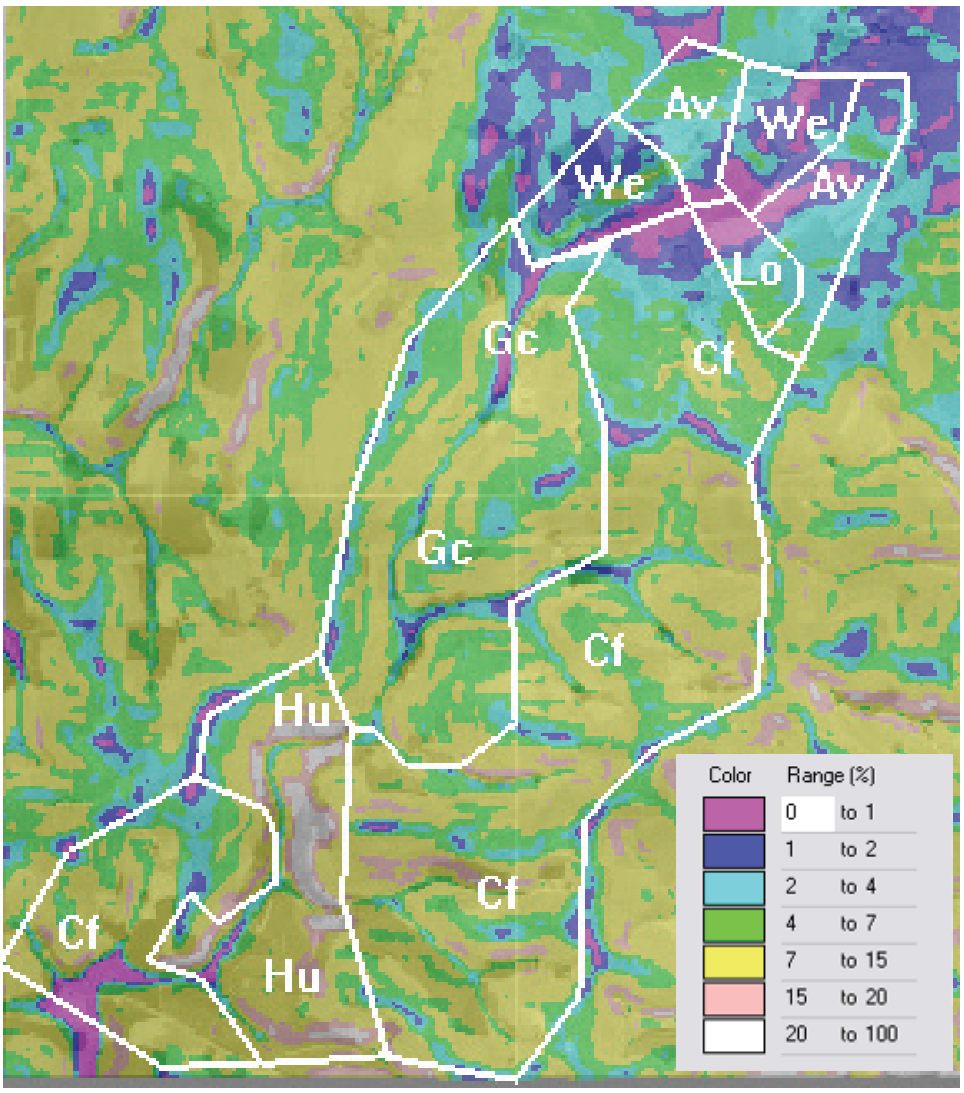

Figure 7. ***Six dominant soil sequence zones (hillslope types) found in the Mkabela catchment. Colours represent the slope range, (after Le Roux et al., 2006).***

2.3.2.2 Geology

According to Le Roux *et al.*, 2006, the Westleigh and Longland soil types are underlain by the Natal Group sandstone while the Avalon soil type is underlain by sedimentary rocks of the Dwyka Group and sandstone of the Natal Group.

A geological map (Figure 8) supports the presence of the Natal sandstone beneath all ERT survey areas. The Dwyka group is also found at the north of the catchment, but out of the ERT survey area.

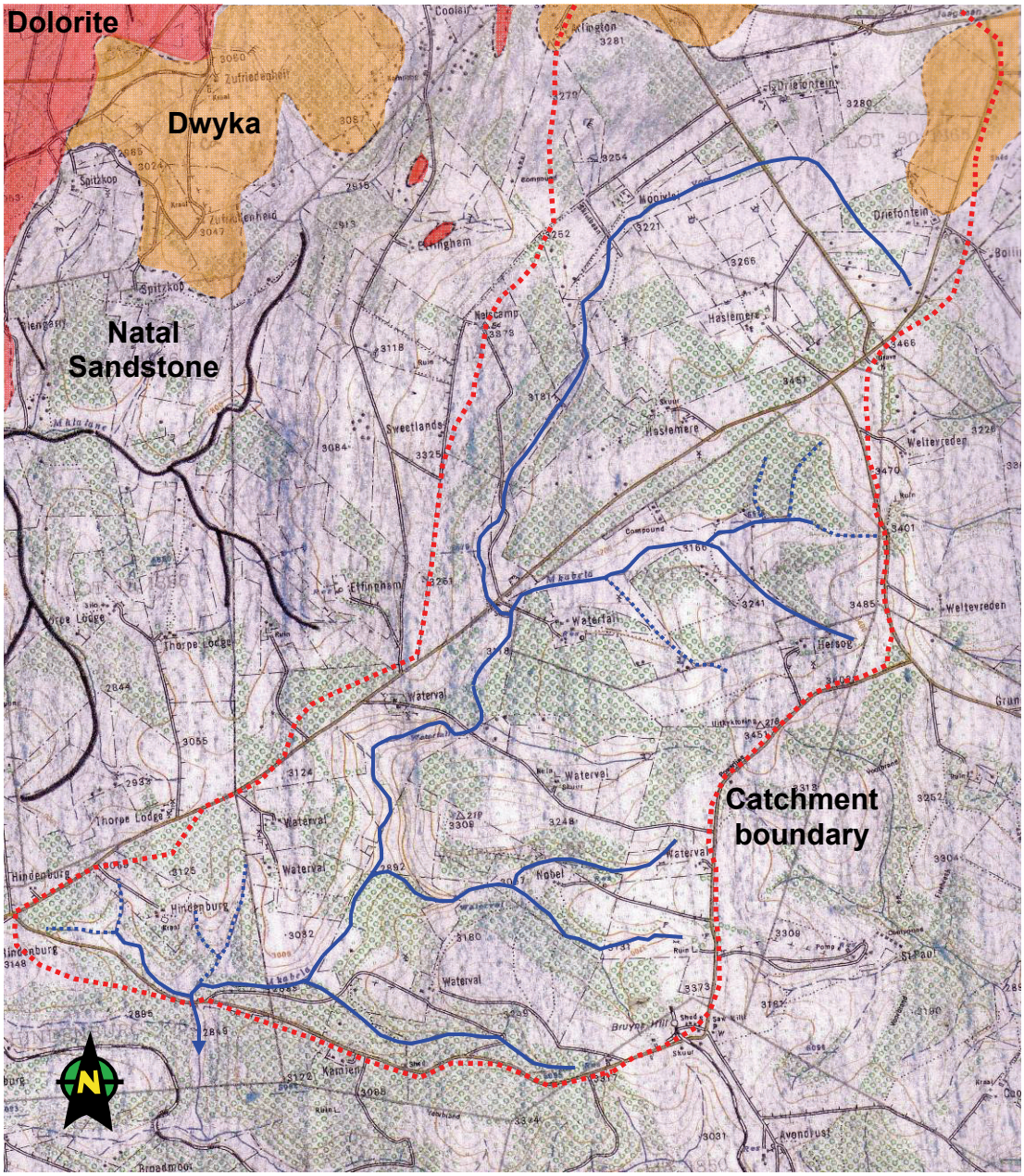

Figure 8. ***Geological map covering the Mkabela catchment (modified from 1:50 000 geological map, Council for Geosciences, Pietermaritzburg).***

Combining the soils survey results and the geologic data a conceptual model can be drawn of the surficial stratigraphy within the study area (Figure 9):

- First a layer: from South East to North West of the ERT survey area, a sandy soil of Avalon type and sandy soil of Longlands type.
- Second layer: sandstone of Natal group.
- An intermediate weathered saprolite zone.

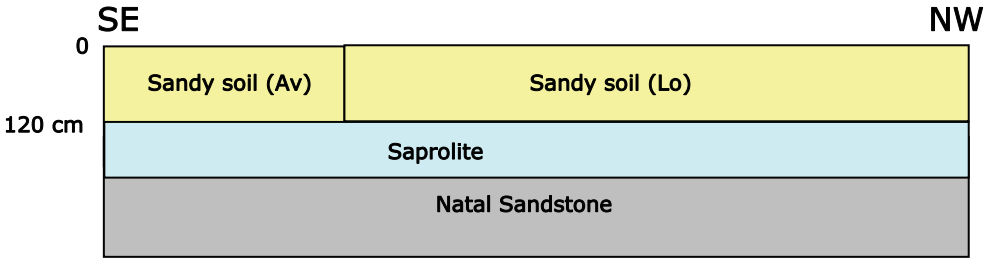

Figure 9. Geological conceptual profile of the ERT survey area.

2.3.2.3 Groundwater Setting

In general there are four modes of groundwater occurrence in KwaZulu-Natal are dictated by the regional geology. The primary water-bearing units include the following:

- An intergranular aquifer which occurs in unconsolidated coastal deposits of the Maputoland Group.
- Fractured aquifers which are associated with cracks, fissures and joints in sandstone of the Natal Group and diamictite (tillite) of the Dwyka Group.
- Karstic aquifers found in weathered carbonate rocks in the Natal metamorphic Province.
- Intergranular and fractured aquifers are found in the Karoo Supergroup rocks, including dolerite and lava of the Drakensberg Group and crystalline rocks of the Natal Metamorphic Province.

In the survey area, groundwater occurrence is also dictated by the lithology of the area. According to Le Roux *et al*., 2006, there is evidence of a phreatic water table fluctuating in the saprolite and underlying rocks with changes of seasons and contributing to the wetting of the different soils profiles in the catchment.

Recent water lever data (Figure 10) collected from one borehole located in the upper headwater catchment, reveals that the groundwater level fluctuates during the rain season depending on the degree of recharge. Water levels vary from a high of 4.7m below ground level (b.g.l), towards the end of the wet season, to a low of 6.6m b.g.l. in the dry season.

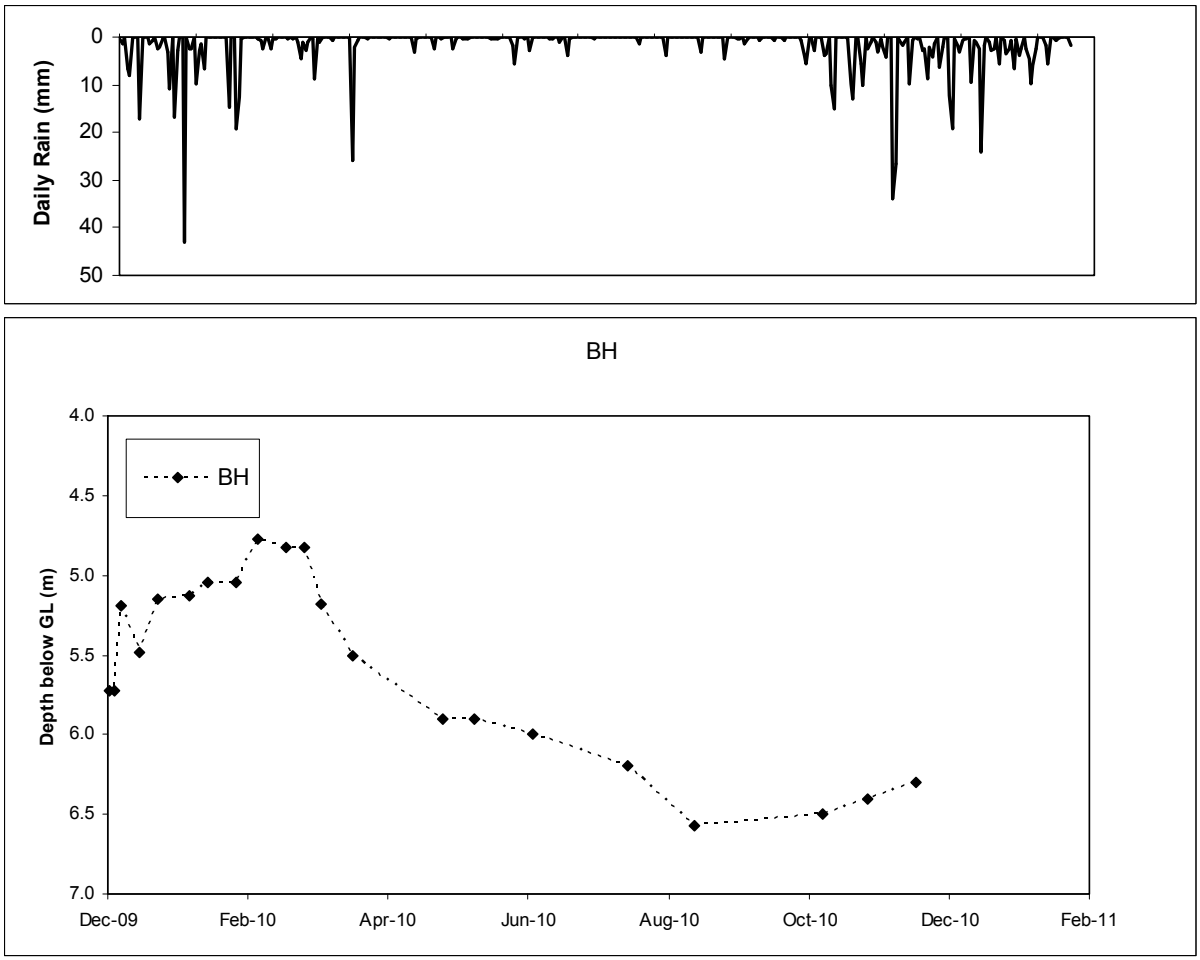

Figure 10. Groundwater level fluctuations December 2009-January 2011.

2.3.3 Electrical Resistivity Results

2.3.3.1 Transect W5

Transect W5, which is located adjacent to Flume 2, exhibits a conductive thin layer of soil (<70 Ωm) followed by a sandy soil horizon which thickens upslope. A perched aquifer (<100 Ωm) is located in the weathered zone as indicated on Figure 11. The bed rock which is fractured sandstone forms a resistive bottom layer (> 200 Ωm). It is located from 2m to 12 m deep, increasing upslope. This ties in with the observation of the water table fluctuations between 4 and 6m below ground level.

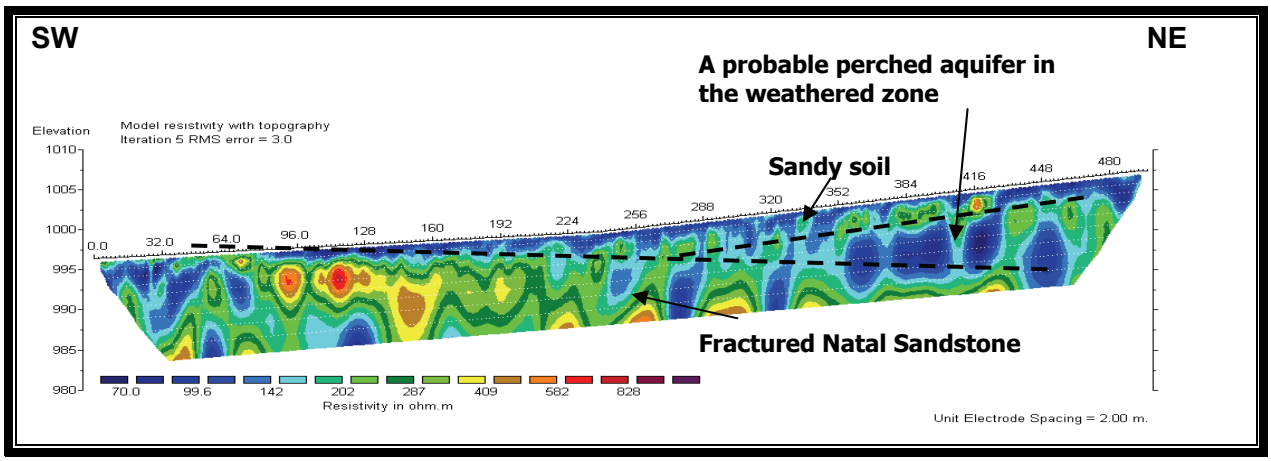

Figure 11. Transect W5 located immediately upstream of Flume 2.

2.3.3.2 Transect W4

The resistivity section obtained along transect W4 exhibits three major layers including 3.7 m of sandy soil (200-600 Ωm), followed by groundwater bearing saprolite (<100 Ωm) with a water table located at approximately 4 m depth. Sandstone is located at 20 m depth (Figure 12). This transect reveals the extent of the perched aquifer described for the transect W5.

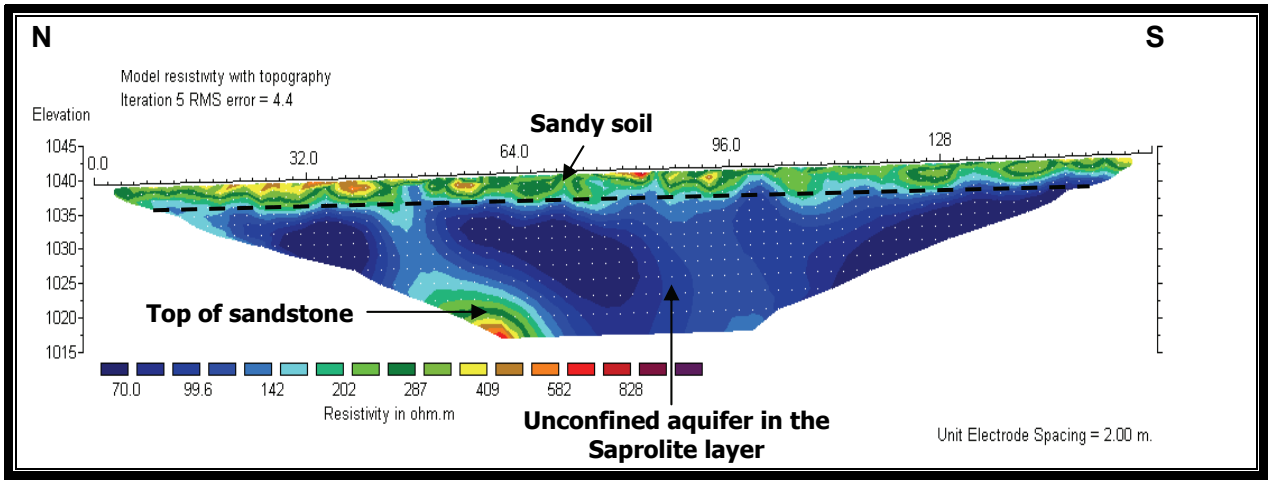

Figure 12. Transect W4 located between W5 and the upstream Flume 1.

2.3.3.3 Transect W2

Transect W2 is located adjacent to the upstream Flume 1. The resistivity section indicates a 3m sandy and resistive layer overlies a weathered zone comprising two shallow perched water bodies, one along the northern side that is about 36 m long and 10 m thick and another in the south of the transect, (Figure 13). These may be connected through transverse water bodies, running in NW and NE directions.

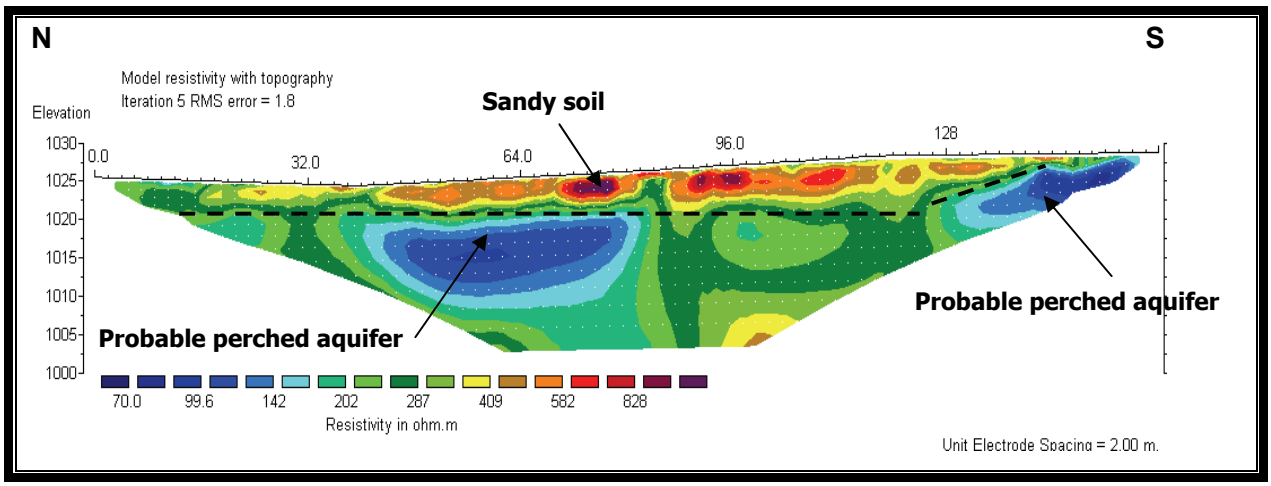

Figure 13. Transect W2 located adjacent to upstream Flume 1.

2.3.3.4 Transect W1

Transect W1 is located upslope of Flume 1 to between the two runoff plots. The northern edge of the transect is characterized by high soil moisture in the top layer that probably communicates with a perched aquifer (<100 Ωm) at 6 m below ground level, (Figure 14). In the field, water seepage can be seen on the ground surface. There appears to be a near surface supply to the water way as well as a deeper water body, which is likely the same as that observed in the borehole.

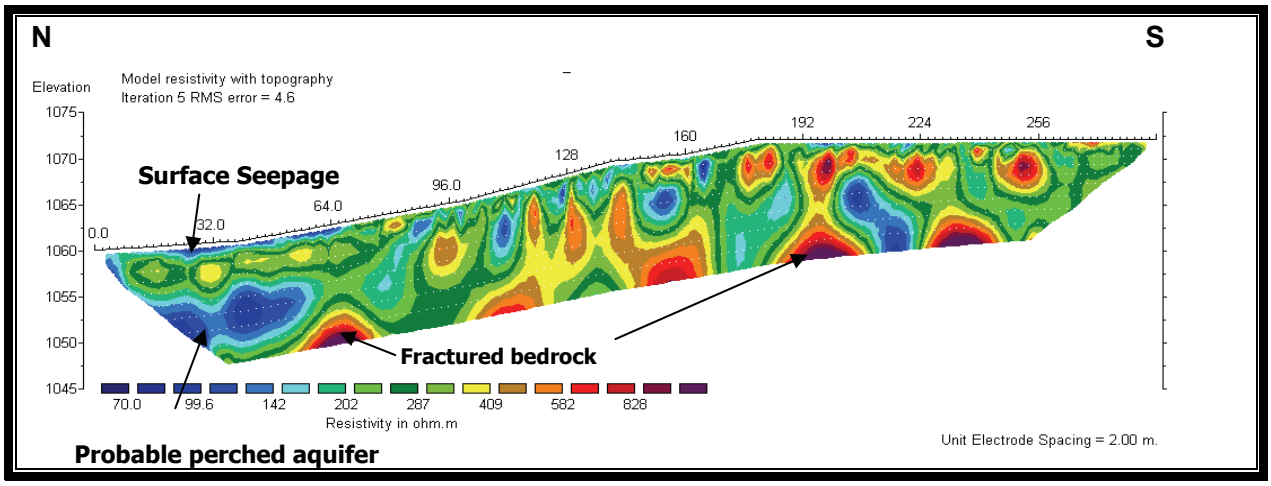

Figure 14. Transect W1 located between the Runoff Plots and Flume 1.

2.3.3.5 Transect W3

Transect W3 is located along the four nests of tensiometers and watermarks in the upper catchment (Figure 6). The section traverses the waterway as indicated in Figure 15. A sandy

layer (200-800 Ωm) covers both sides of the stream. It is underlain toward the west by a perched aquifer (<100 Ωm) at about 4 m depth.

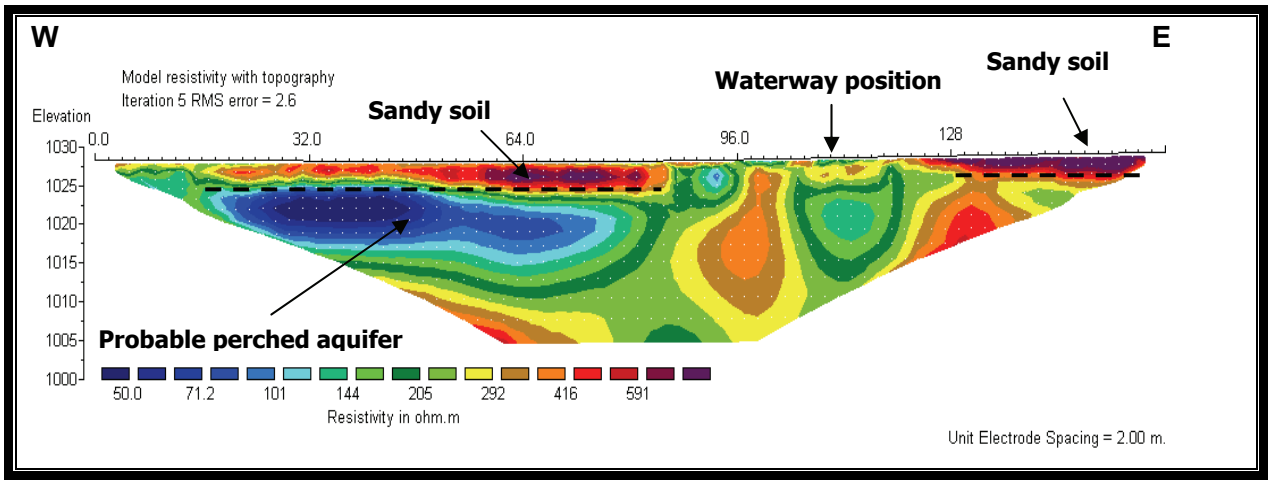

Figure 15. Transect W3 adjacent to the nests of soil moisture sensors.

2.3.4 Hillslope Hydropedology Transects

Cross-sectional and longitudinal transects were derived from topographical and soil descriptions for various hillslope sections in order to identify the likely water generating mechanisms based on hydropedological evidence. The sections chosen for cross-sectional transects were from different hillslope types. The longitudinal transects were extracted for the two main river reaches that meet at a junction and continue as an outlet reach. Table 3 shows the criteria for choosing the transect locations and Figure 16 shows their locations on a topographic map.

Table 3: Criteria for choosing cross- sectional and longitudinal transect points.

Transects	Hillslope Soil Type	Remarks
A1 – A2	Avalon	Runoff plots/Flume1water way
B1-B2	Avalon	Flume 2 water way
C1-C2	Glencoe	Alluvial valley
D1-D2	Cartref	Wetland
E1-E2	Hutton	Bedrock channel
River Reach 1	Glencoe, Hutton	Longitudinal profile
River Reach 2	Cartref , Hutton	Longitudinal profile

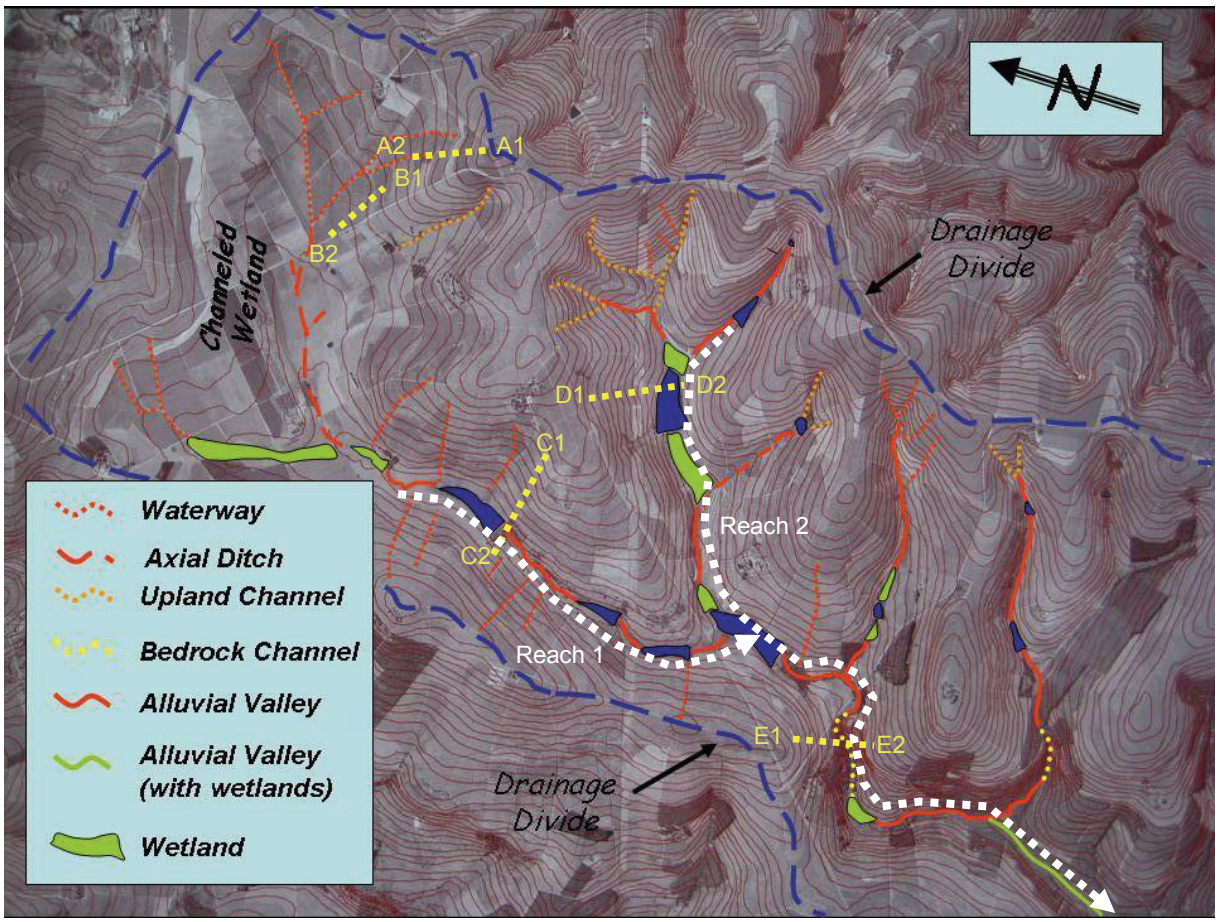

Figure 16. Mkabela catchment showing the location of hillslope and stream transects.

2.3.4.1 Transects on Avalon hillslopes (A_1-A_2 and B_1-B_2)

Within these transects, the most common soil form within the hillslope was the Avalon soil form, which is characterised by an orthic A horizon over a yellow-brown apedal B horizon over a soft plinthic B horizon (Figure 17). The sandy nature of the soils allows the easy infiltration of rain water, while the soft plinthic horizon acts as the aquitard supporting the perched water table. The soft plinthic B horizons are underlain by hard plinthic horizons and the hard plinthic horizons have large pipes of soil material connecting the solum with the saprolite (Le Roux *et al*., 2006).

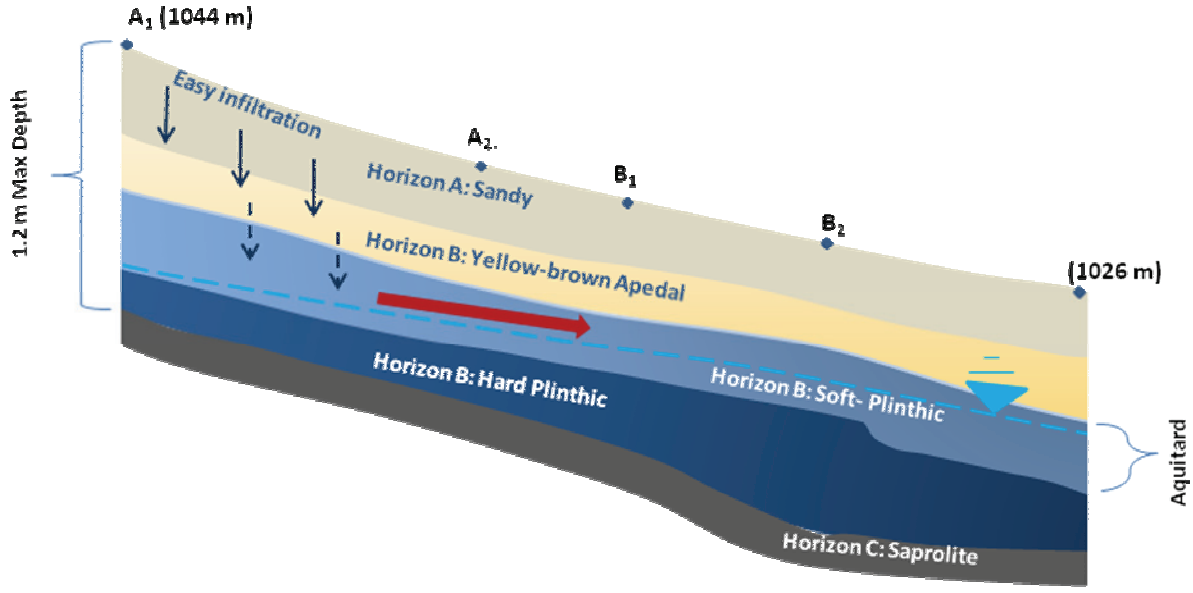

Figure 17. Upper sub-catchment transects A1-B2 showing the soil profile in the Avalon hillslope.

According to Le Roux et al. (2006) the morphological character of these soils implies that the material underlying this hillslope is impermeable. Water tables form in the subsoil when the rainfall exceeds evapotranspiration on a daily basis. Drainage is therefore dependent on lateral movement only. The hydrological behaviour of this hillslope is expected to result in accumulation of water during the rainy season and lateral drainage in the saprolite and soft plinthic horizons. During very wet spells lateral drainage is also expected to occur in the sandy yellow-brown apedal B horizon. The water table of the Avalon soils may drop below the solum in the rainy season. The time it takes to form a water table will depends on the rainfall. The soil profile can hold a large amount of water before water tables will form. The water table periodically rises into the yellow-brown apedal B horizon and may occur there for one to four months on average in the rainy season. The water draining from the Avalon soils feeds the water table of the Katspruit soils lying down slope.

2.3.4.2 Transects on Glencoe hillslopes (C_1-C_2)

This hillslope is steeper than the Avalon hillslope. Transect C1- C2 (Figure 18) has a slope ranging from 4 -15 %. Its soil horizons can go up to maximum depths of 0.9 m. The hydrological behaviour of the Glencoe hillslope is expected to be similar to that of the Avalon hillslope except for the effect of the steeper slope and higher relief (Le Roux et al., 2006). The hard plinthic subsoils are matured plinthic horizons and may be an indication that the redox process is more intense compared to the Avalon hillslope. Water tables may occur in and under the plinthic layer most of the rainy season and several months after.

The Cartef area probably serves as a source of water to the Avalon area (A). The hydrology of the Avalon A hillslope therefore is dominated by more water in the soils than received by vertical drainage from rainfall. Some of the water may originate by overland flow as the Cartef soils are shallow with an E horizon and saturation access is possible. The Cartref soils also lie on steep slopes. After saturation the shallow profile will drain laterally for a short period as the soils are shallow. Although some water may enter the orthic A, yellow brown apedal B and soft plinthic B horizons by lateral flow, the water probably moves in the intermediate vadose zone under the soft plinthic B horizon. Indications are that a water table sits below and in the soft plinthic B horizon of the Avalon soils for significant periods during the peak rainy season. The relative flat slope support a low interflow component of which most moves in the intermediate vadose zone.

The same is true of the Avalon area (B1-B2) except that an increase in wetness is expected.

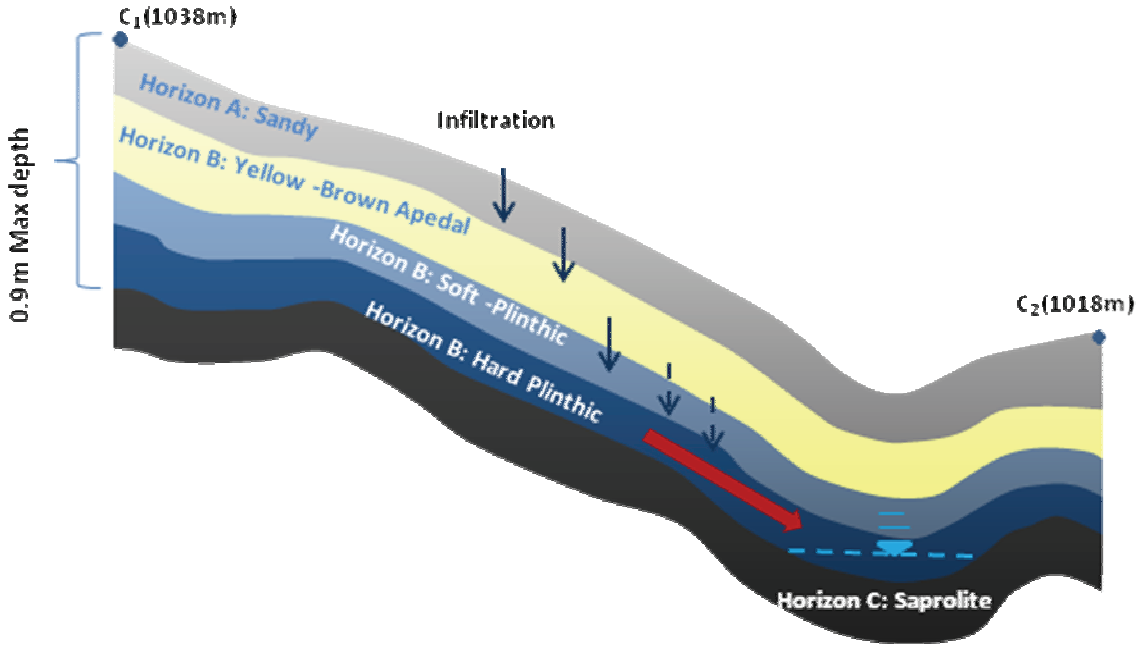

Figure 18. Middle sub-catchment transects C1-C2 showing the soil profile in the Glencoe hillslope.

The occurrence of hard plinthic horizon on steep slopes requires a special environmental setup. Iron rich parent material or a special hydrology can explain it. The hydrology of the Glencoe area (C1-C2) can only be explained by significant water supply by the crest feeding the Glencoe soils in the hillslopes to create a water table under the hard plinthic B horizon (Figure 18) of some significant duration in the rainy season.

2.3.4.3 Transects on Cartref hillslopes (D_1-D_2)

The steep, short, convex slopes of the ridges combined with undulating planform shape, is typical of this hillslope. Transects D1 – D2 (Fig 22) has slope ranging from 4 – 15 %. The underlying material is Natal Group sandstone while the soils under this transects are shallow and sandy with very low water holding capacity (Le Roux et al., 2006). It has a relief of 60 m.

The hydrology of the Cartref area (D1-D2) is characterized by an infiltration excess component as the shallow soils saturate quickly (Figure 19). The E horizon indicates a significant interflow component although for relative short periods.

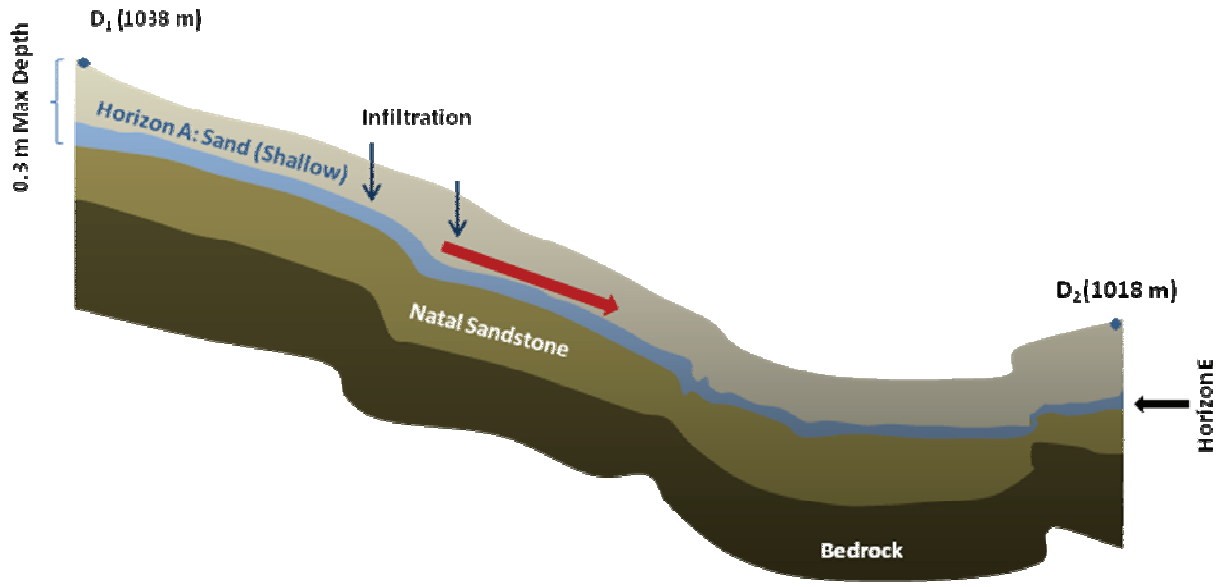

Figure 19. Middle sub-catchment transects D1-D2 showing the soil profile in Cartref hillslope.

2.3.4.4 Transects on Hutton hillslopes (E_1-E_2)

The Hutton hillslope has the highest relief (120 m) and occurs in the steepest sloping area with some slope exceeding 20 %. Transect E1 –E2 (Figure 20) has slope ranging between 7 – 20 %. Shallow Glenrosa soils occur on the steep slopes and deep well drained Hutton soils on the more gentle slopes of the crest and midslope (Le Roux *et al*., 2006). The underlying material is Natal Group sandstone. The Hutton soils are deep and well drained with moderate water holding capacity while Glenrosa soils have very low water holding capacity.

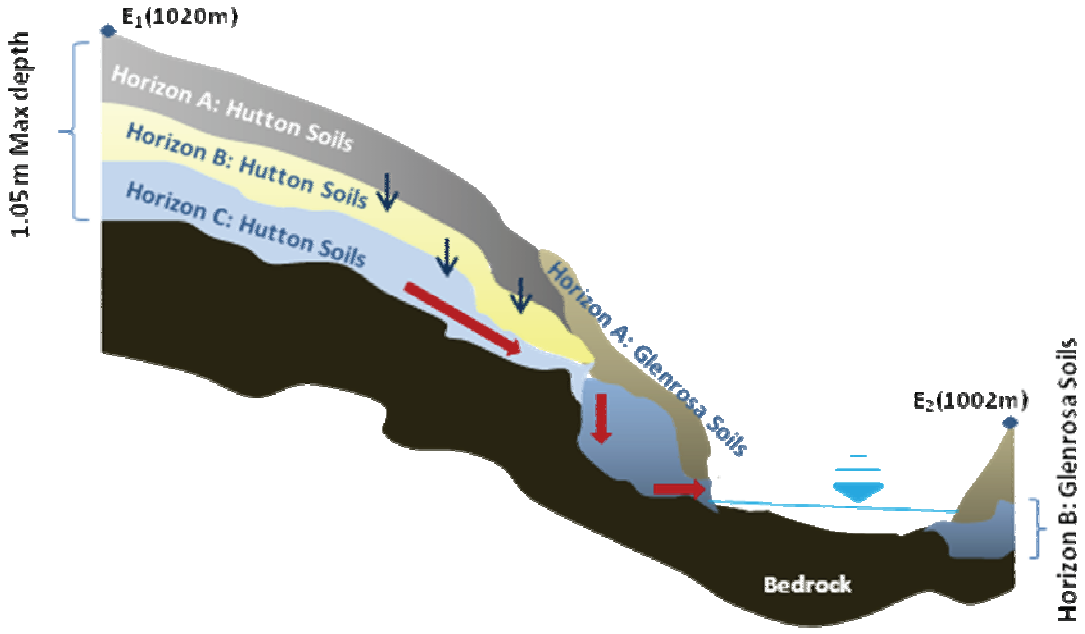

Figure 20. Lower Sub- catchment transects E1-E2 showing soil profile in Hutton hillslope.

The Hutton area (E) has deep recharge soils. Although some water will run overland the ET excess water draining through the soils probably drain into the lower vadose zone as an impermeable intermediate layer is absent in these soils. From the intermediate vadose zone the water may split into a lower vadose zone interflow (that supplies the wetland and/or feeds the river) and a vertical drainage that recharges the ground water.

2.3.4.5 Longitudinal transects along the river reaches

Longitudinal profiles record the downstream changes in elevation, and hence slope, along a river course. Overlaying longitudinal profiles from different sub-catchments can be used to assess the area draining into each section of the river course and compare downstream changes in slope and discharge. It also defines the relative contributions of area from different parts of the catchment, and provides a quick, visual overview of changes in catchment area (and hence discharge) at tributary confluences. From the longitudinal transect performed in the catchment it can be seen that river Reach 1 is longer and steeper than river Reach 2 (Figures 21 and 22).

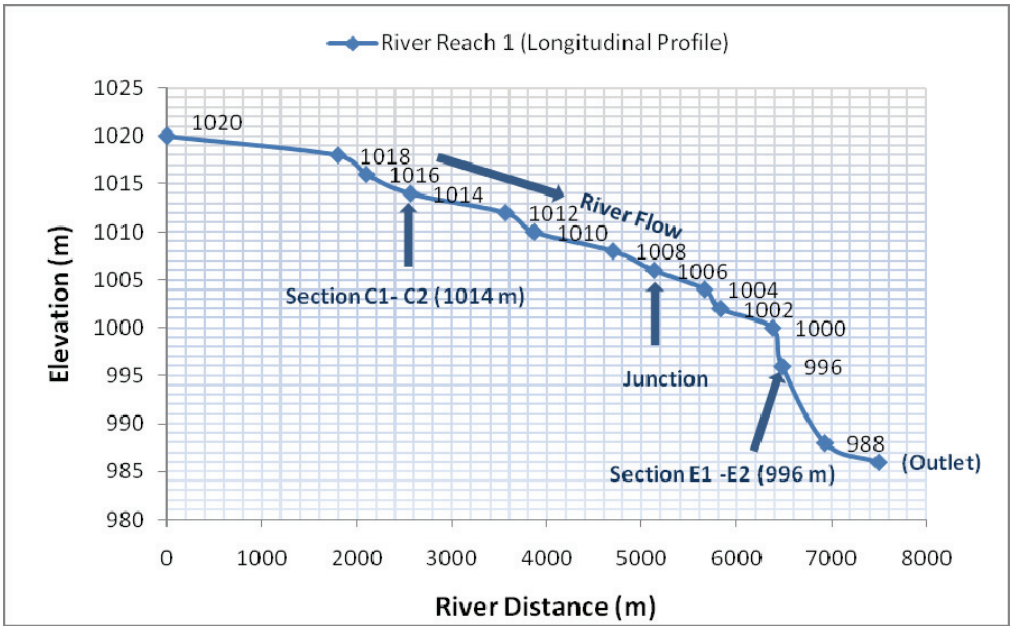

Figure 21. River Reach 1 longitudinal profile

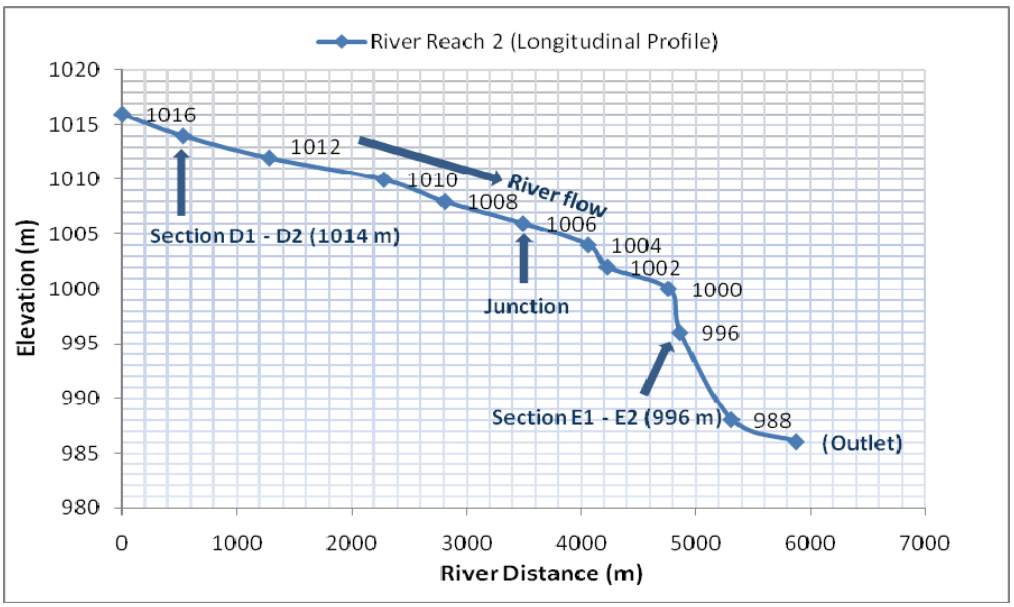

Figure 22. River Reach 2 longitudinal profile

2.4 Process Deductions from Water Isotope Analyses

Water quality and stable isotopes of water, ^{18}O and ^{2}H, have been determined for samples collected from the catchment headwaters to the outlet, some 12km downstream. Samples were collected from overland flow Runoff Plots, from the Flumes in the water ways of the sugar cane and at the grab sample sites named, Road Crossing, Dam in, Dam 1 Out, Dam 2 Out, Bridge 1 and Bridge 2 as shown in Figure 23.

The isotope data have been plotted in three ways:

- As a time series for each station from January 2009 to January 2011,
- For specific events, showing the responses to rainfall and runoff,
- As snap-shot profiles from the headwaters to the catchment outlet for specific wet and dry periods (10 January, 28 February and 15 December 2009, 7 June 2010 and 11 January 2011).

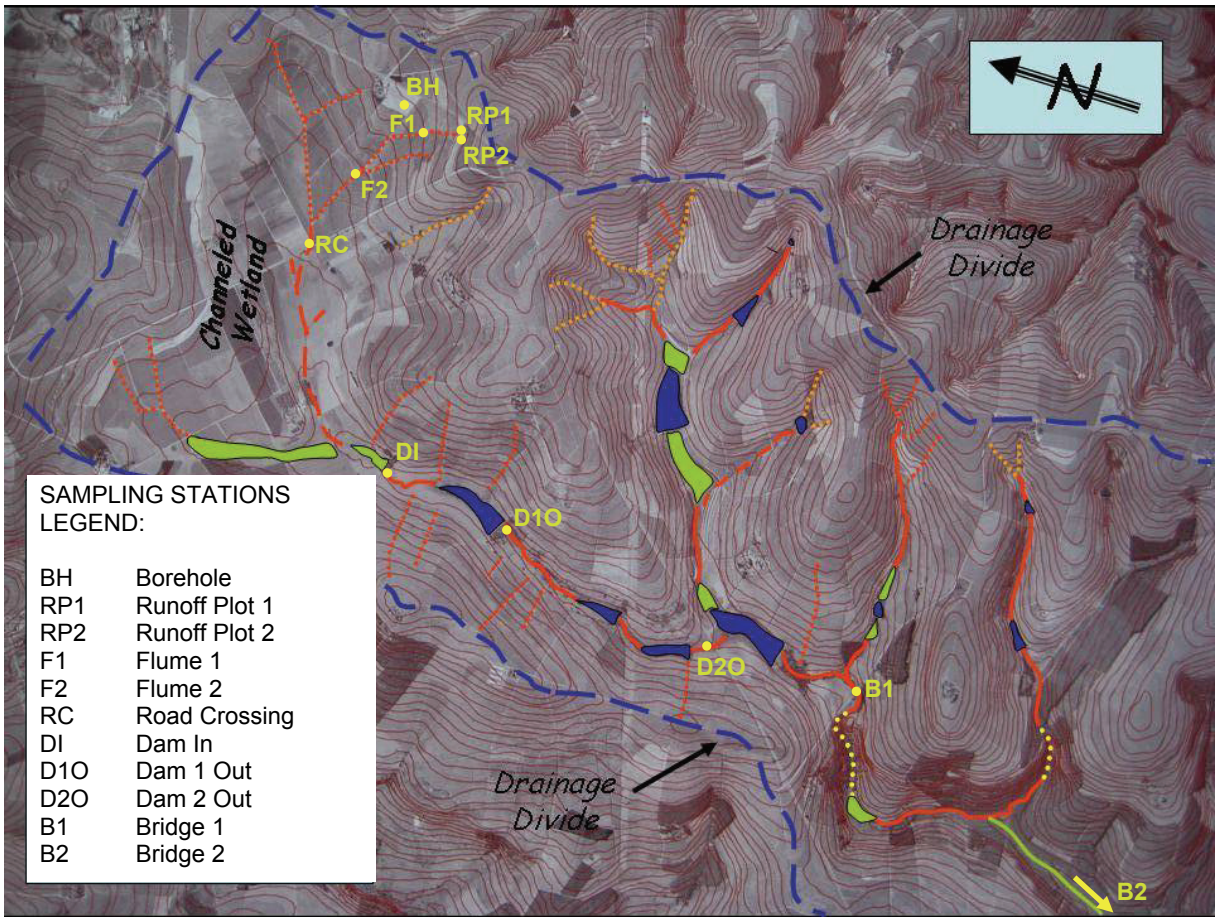

Figure 23. The Mkabela catchment showing the sampling stations.

2.4.1 Isotope Time Series

The time series of ^{2}H and ^{18}O isotope results for 2009 are presented in Figures 27 to 29 for individual monitoring stations, starting at the outlet of the catchment, Bridge 2, (Figure 27) and ending at the runoff plots in the headwaters, (Figure 29). Distinct behaviours are identified from these results:

- In the downstream stations (Bridge 2, Bridge 1 and Dam Out), the isotope ratios become lighter during the dry period between April and October, except during rainfall events (Figure 24);

- All isotope ^{2}H and ^{18}O comparisons (right, Figure 24), reveal an evaporated source of water with regression slopes lower than the Global Meteoric Water Line (GMWL). This reflects the retardation impact of the many farm dames between the Flumes (Figure 25, middle and bottom, right) and the catchment outlet, Bridge 2 (Figure 24, top right);

- Comparison of the evaporation signal from the Dam Out station to the catchment outlet, Bridge 2, shows a decreasing influence of evaporation (Figure 24, right) in the downstream direction as the contribution from adjacent land sources increases relative to upstream reservoir discharges (this is analysed further in 2.4.3);

- The isotope signals during the dry period do not reach the values determined for the groundwater borehole values (Approximately ^{2}H -14$^{o}/_{oo}$ and ^{18}O -3.5 $^{o}/_{oo}$) (Figure 26 bottom) indicating that reservoir storage and local hillslope contributions both contribute to the low flows.

- The isotope comparisons for Flume 2 and Flume 1 (Figure 25, right) show little evidence of evaporation and generally reflect the rainfall patterns represented by the runoff plot samples (Figure 26, right). This indicates a significant contribution from event rainfall to the two flumes. Nevertheless, large changes in isotope ratios occur during events (this is analysed further in 2.4.2);

- The groundwater borehole signal remains constant during dry and wet conditions for the two years of monitoring.

Similar observations can be made for the time series of 2010 (Appendix B3.2). A unique sampling sequence during a rainfall event of 35mm on 10 November 2010 shows that the isotope values vary widely within an event and reflect relative contributions of event and pre-event water, even at the large scale sampling stations (Appendix D3.2.1). These contributions are evaluated in the following section.

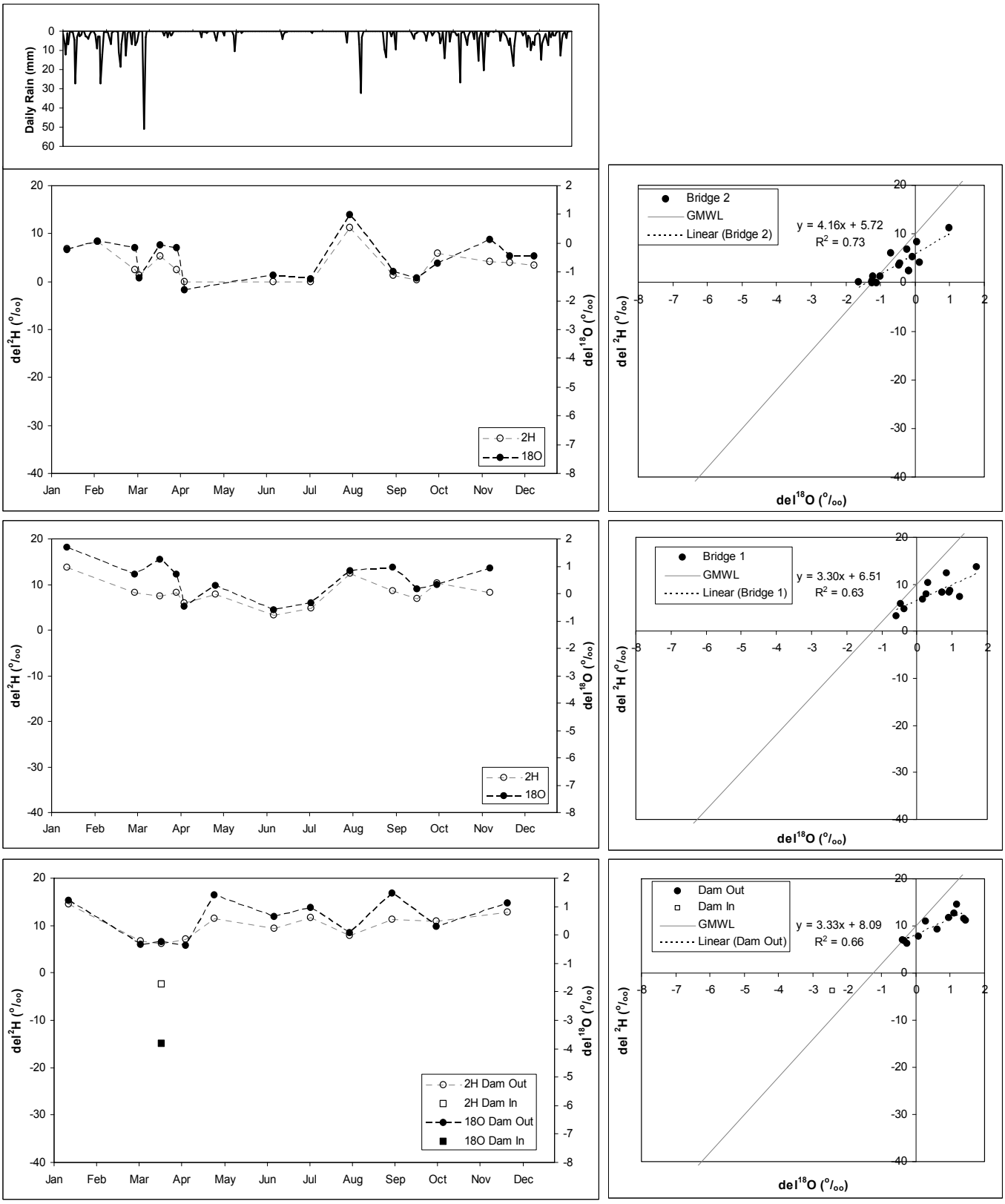

Figure 24. Rainfall and isotope responses for 2009 at the monitoring stations: Bridge 1, Bridge 2 and Dam Out and Dam In.

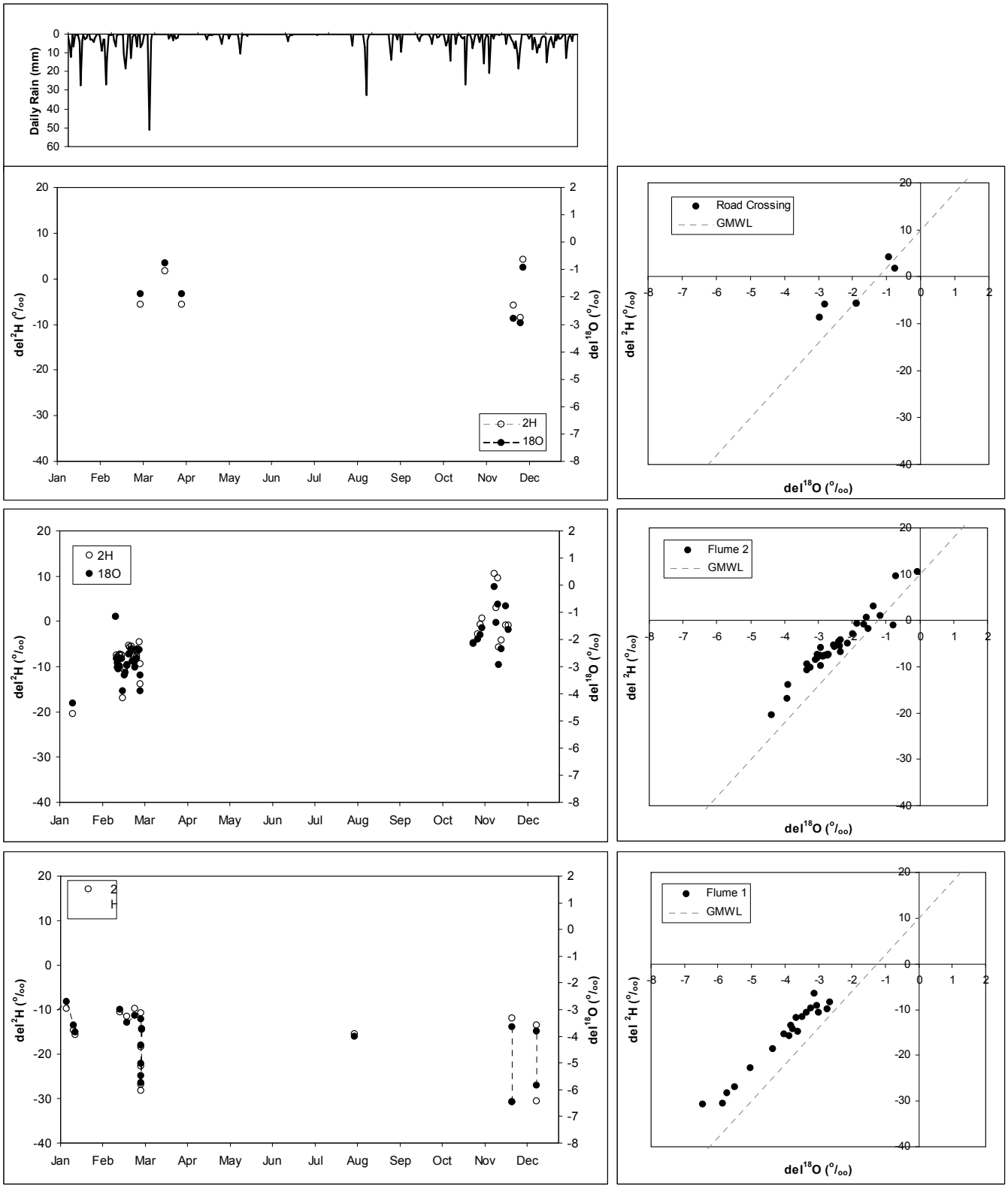

Figure 25. Rainfall and isotope responses for 2009 at the monitoring stations: Road Crossing, Flume 2 and Flume 1.

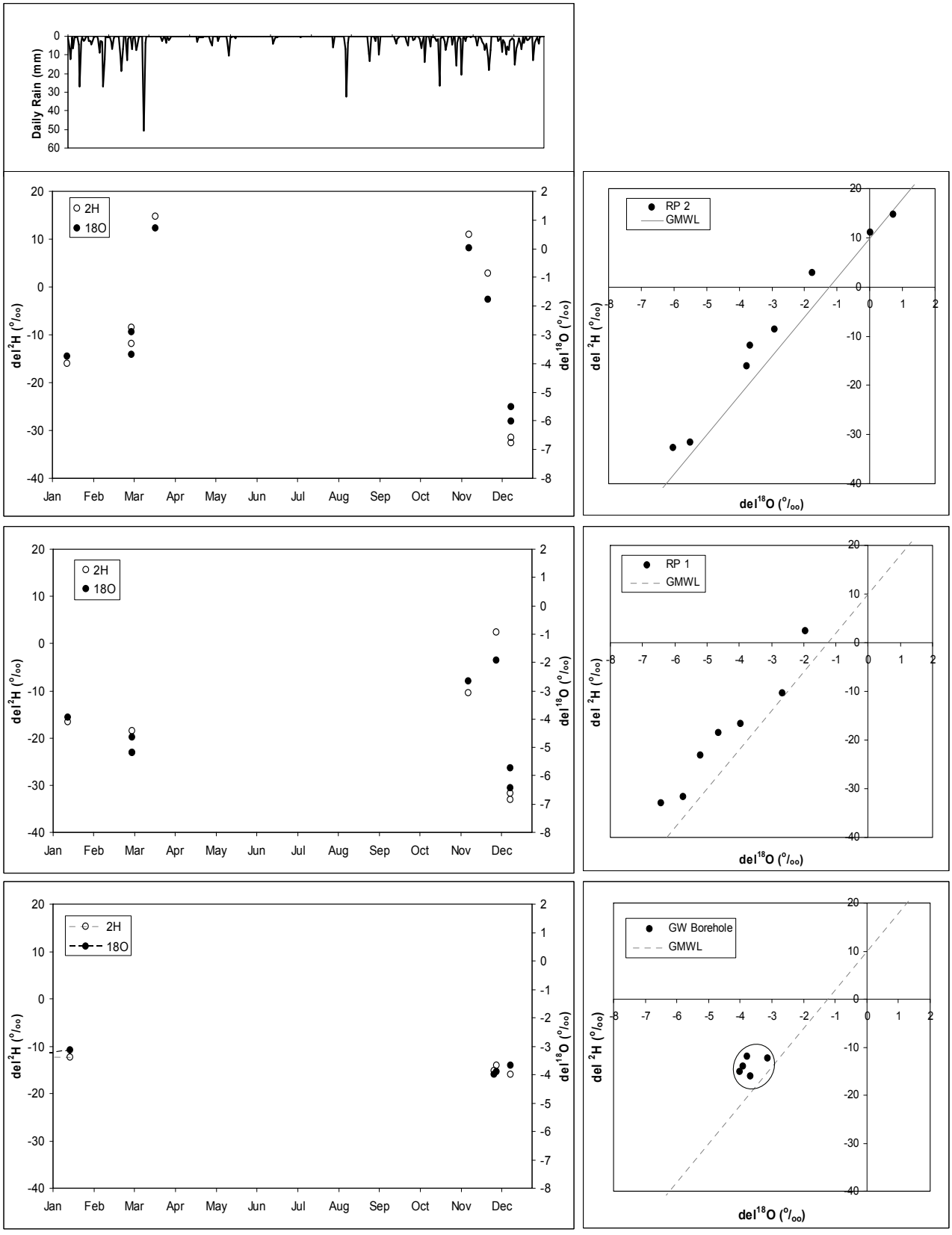

Figure 26. Rainfall and isotope responses for 2009 at the monitoring stations: Runoff Plot 2, Runoff Plot 1 and Groundwater Borehole, BH .

2.4.2 Isotope Event Results

The isotope ratios for selected precipitation events have been analysed for rainfall and runoff at the headwater flume stations. These include events on 10 January 2009, (27mm), 28 February 2009, (51mm), 27 January 2010 (43mm) and 10 November 2010. In addition, samples were collected periodically throughout the catchment during the event of 10 November 2010. Details of these four events are presented in Appendix C.

The 28 February 2009 results show a distinct drop in isotope ratio during the event (Figure 27). The runoff at Flume 1 has an increasing contribution from the event water, indicated by the progressive change in the isotope ratios, from the initial value close to the groundwater signal, towards the isotope ratio of the event water. (The event water isotope signal is reflected by that for the runoff plots collected on 2 March 2009, although this sample will be an average of the rainfall contributing to overland flow during the event). The contribution from event water (rainfall) peaks about 2 hours after the peak of the discharge event, at which time most of the discharge is contributed by event water. Following this peak, the runoff contributions are increasingly dominated by the subsurface water (Figure 27). The discharge isotope signal has returned to values representative of the groundwater within 24 hours of the cessation of the rainfall.

During less intense events, such as the one on 27 January 2010, the isotope ratios do not decrease significantly, although the sample representation is small (Figure C3.2 in Appendix C). Thus, there appears to be a threshold of event magnitude and intensity which controls the connectivity of overland flow and subsurface event water discharge to the lower slopes in the sugar cane fields.

Three isotope samples were collected from the flumes during the event of 10 November 2010 (Figure 28). The resultant isotope values have been used, together with end member values for the groundwater and average rain water, to render the fractional contribution of the subsurface or pre-event water to the total discharge at Flume 2. This pre-event contribution comprises 19% of the total discharge at the peak of the event and typically returns to 100% of the contribution within 24 hours of the cessation of rain (Figure 28).

Also sampled during this event was the network of stations downstream of the flumes. The Road Crossing and Dam-In stations both show significant response to the event water (Figure C4.6), but, with discharge from the first dam consisting only of the over flow, no evidence of event water is discernable (Figure C4.7, left). The rainfall event has

thus only displaced resident water from the dam. At the outlet of the second dam, however, event contributions are evident again (Dam 2 Out Figure C4.7). This indicates effective retention of event water in the upper wetland and first dam, but discernable contributions from event water through the following two, smaller impoundments. It is interesting to note, however, that the NO_3-N and P concentrations in the outlet from the large upper dam (Dam 1) increase dramatically during the event, (Figure C4.3), indicative of possible disturbance of the impounded water in Dam 1, yielding a peak in nutrient load from the reservoir, despite the absence of event water. This rise in NO_3-N and P concentrations is not present in the outflow from the second two impoundments, where the discharge is diluted by event water.

Further downstream, event water comprises 34.5% and 29.2% of the total discharge at the peak of the event at Bridge 1 and Bridge 2 respectively (Figure 28).

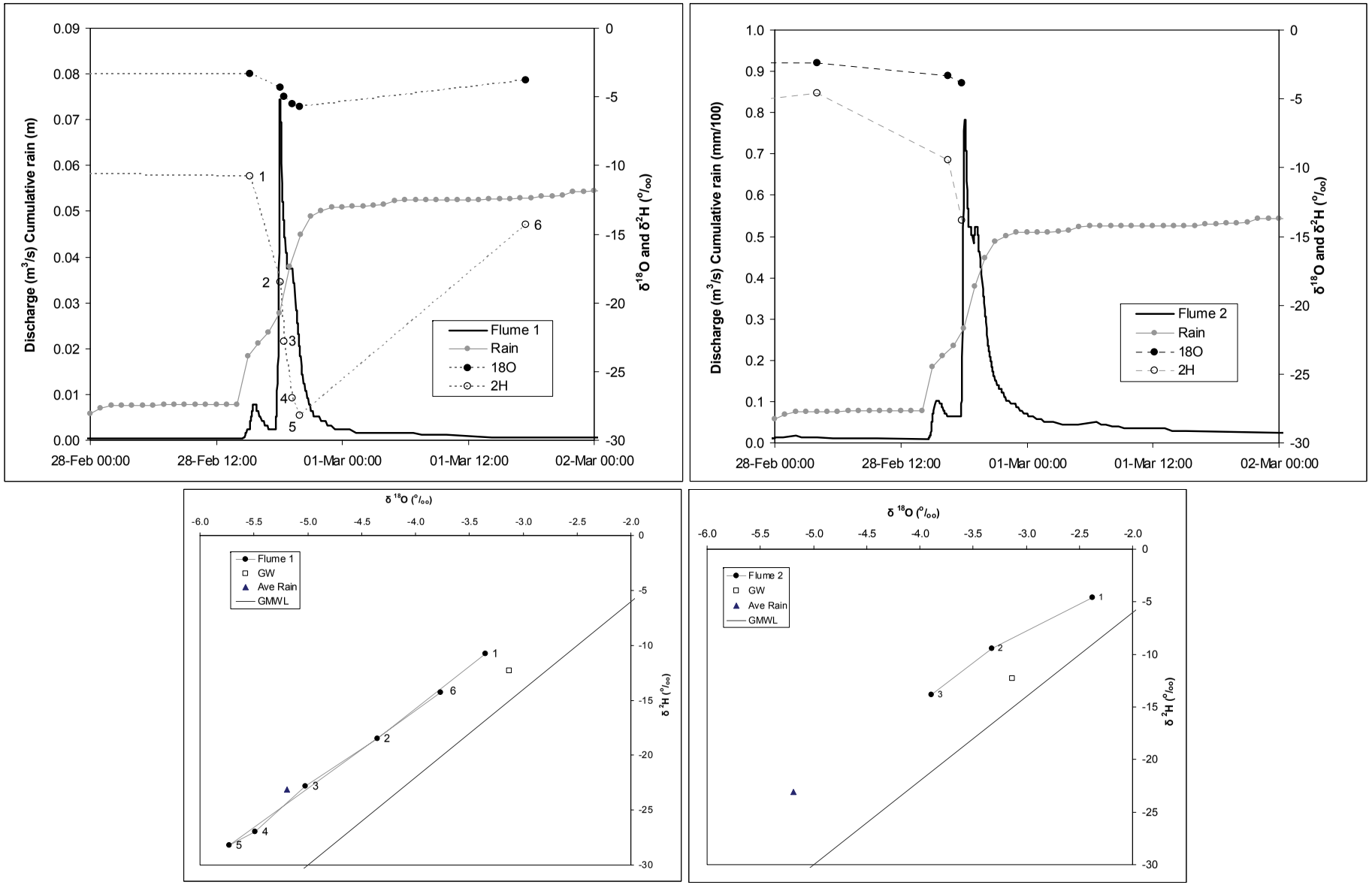

Figure 27. Rainfall, discharge and isotope responses at Flume 1 (left) and Flume 2 (right) for the event of 28 February 2009.

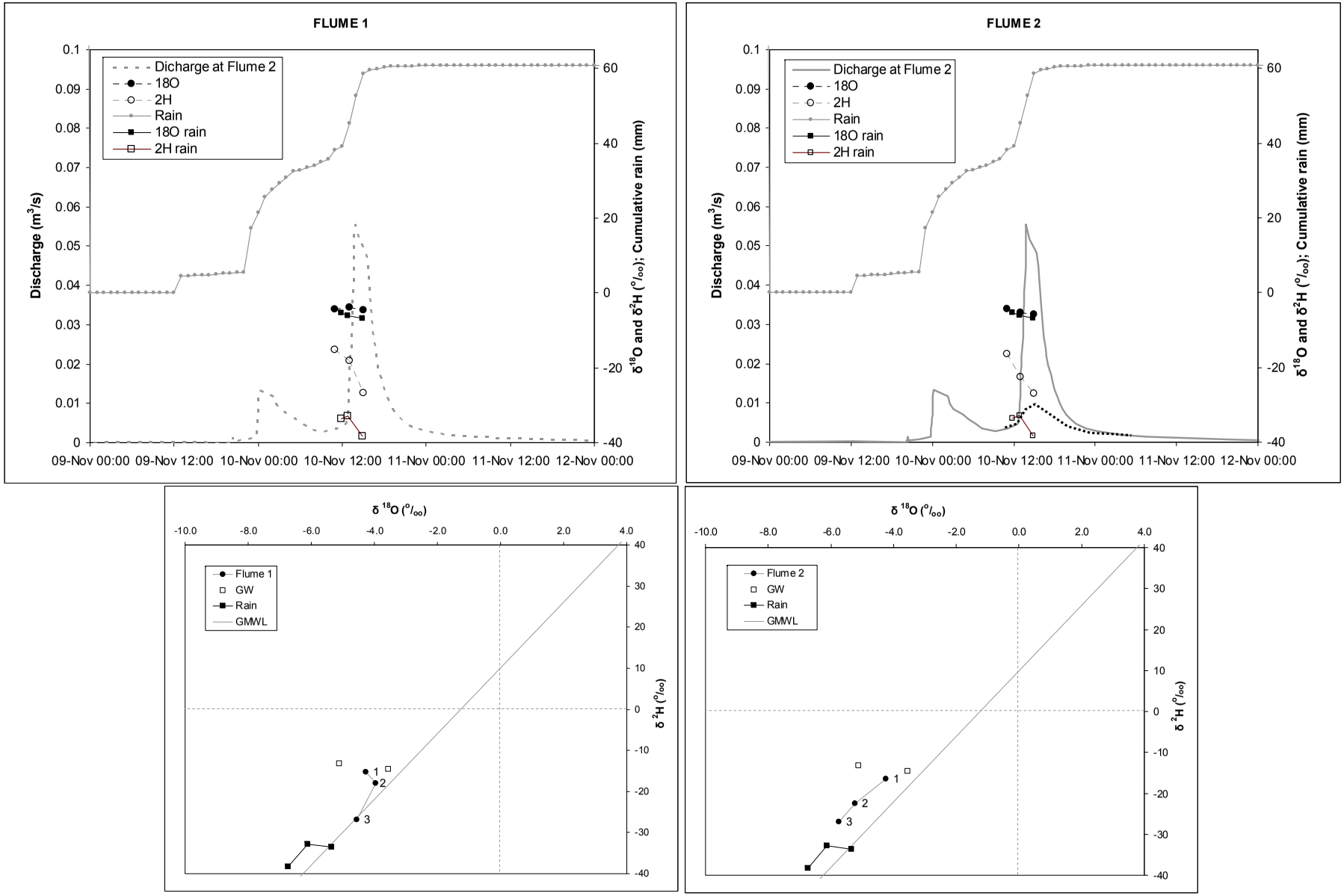

Figure 28. Rainfall, discharge and isotope responses at Flume 1 (left) and Flume 2 (right) for event of 10 November 2010.

2.4.3 Isotope Transects

In order to get an indication of the sources of water, sediments and nutrients from the headwaters to the catchment outlet, sampling events were conducted in which the complete stream network was sampled within a 2 hour period. Selected events have been analysed for 10 January, 28 February, 15 December 2009, 7 June 2010 and 11 January 2011 as detailed in Appendix D. The 11 January 2011 sampling campaign comprised comprehensive sampling throughout the catchment with negligible precipitation in the preceding four days.

The stable isotope signals at the two flumes differ slightly on 7 January 2011 (Figure 29), reflecting different mixes of water. The recorded isotope delta values at Flume 1 are similar to that in the groundwater as reflected in the borehole sample, BH. This is not surprising as there is a spring upslope of the first flume. The isotope delta values at Flume 2 reflect a mixture of groundwater and possibly hillslope water from preceding rain (a total of 20mm precipitation occurred during the preceding 7 days). The isotope values at the Road Crossing and the Dam In sampling stations are similar to those at Flume 2. However, further downstream, samples at the Dam 1 Out and Dam 2 Out stations reflect the evaporation from the reservoirs which occur between the Dam In and Dam Out stations. These isotope values are highly enriched and are similar for Dam 1 and Dam 2 outlets.

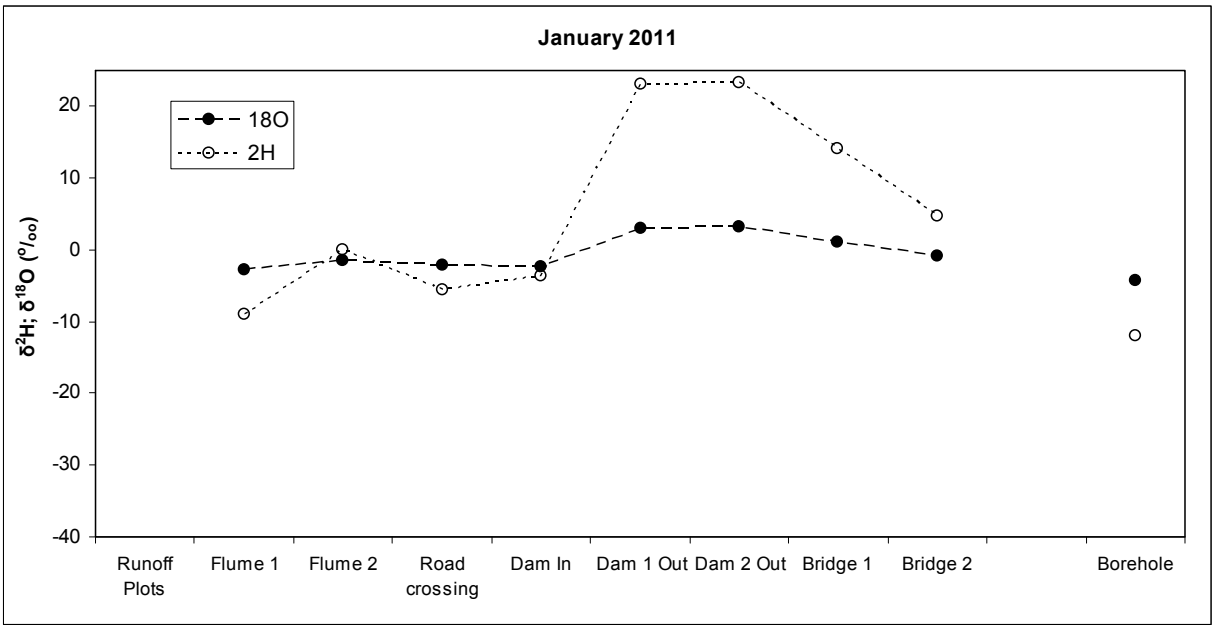

Figure 29. Isotope transect results from the headwater Flumes to the outlet at Bridge 2 for the event of 7 January 2011

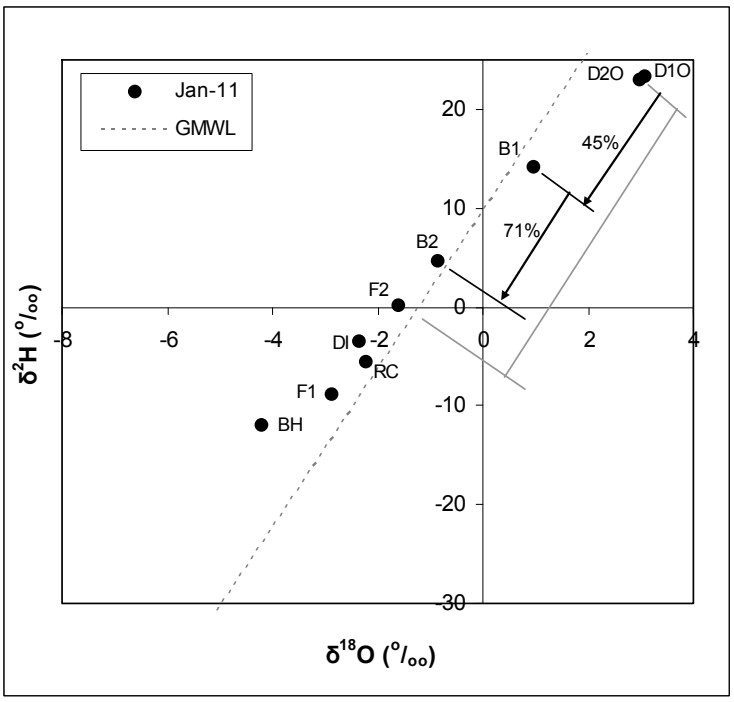

Figure 30. Isotope $\delta^2H/\delta^{18}O$ ratios for the transect results for the event of 7 January 2011.

Downstream of the reservoir outlets, the isotope values at the Bridge 1 and Bridge 2 stations reflect a mixture of upstream inflow from the impounded tributaries as well as contributions from the land units between the reservoirs and the Bridge sampling stations. The isotope ratios (Figure 30), can be used to estimate the proportion of the discharge, at each of the Bridge stations, emanating from local land units, downstream of the reservoirs.

First, it is assumed that the eastern, impounded tributary, upstream of Bridge 1 (Figure 23), will yield a similar evaporated isotope signal as that in the discharge from the Dam Out stations (D1O and D2O in Figure 30). Next, the isotope values of the contributing land units between the reservoir outlets and the Bridge stations are assumed to be similar to the Flume 2 values.

Using the $\delta^{18}O$ values a simple mass balance mixing model can be developed with the end members as the combined discharge from the impounded tributaries (Q_{DO}); the contribution to stream flow of the land unit between the impoundments and the Bridge stations (Q_{LUi}) and the Bridge station discharge (Q_{B1} and Q_{B2}). For the discharge at the first bridge station, this takes the form of:

$$Q_{B1}.\delta_{B1} = Q_{DO}.\delta_{DO} + Q_{LU1}\,\delta_{LU1}$$

Where: δ_{B1} = $\delta^{18}O$ value at the Bridge 1 station,

δ_{DO} = $\delta^{18}O$ value for discharge from both impounded tributaries and

δ_{LU1} = $\delta^{18}O$ value for discharge from the sub-catchment (3.6km^2) between the most downstream reservoir and the Bridge 1 station.

Recognizing that $Q_{B1} = Q_{DO} + Q_{LU1}$, the ratio of discharge from the contributing sub-catchment to the total discharge at the Bridge station, can be expressed as a function of the isotope ratios as in:

$$\frac{Q_{LU1}}{Q_{B1}} = \frac{\delta_{B1} - \delta_{DO}}{\delta_{LU1} - \delta_{DO}}$$

For the sampling event of 11 January 2011, this ratio is 45%, which implies that just less than half the discharge at Bridge 1 is generated from the 3.6km^2 sub-catchment between the most downstream reservoir and the Bridge 1 station. Similar estimates can be performed for the Bridge 2 station. These show that for the 11 January 2011 sampling event, the contribution from the 13km^2 sub-catchment between the Bridge 1 and Bridge 2 stations, comprises 71% of the total discharge at Bridge 2 (Figure 30). Analysis of the remaining selected sampling events yields the contributions listed in Table 4.

Table 4. Percent contribution of the sub-catchment between the impounded tributaries and the Bridge stations to total discharge.

Station	Jan-09	Feb-09	Dec-09	Jun-10	Jan-11
Bridge 1	0.0	0.0	47	49	45
Bridge 2	36	53	22	34	71

The isotope values consistently show decreased evaporated signals at the Bridge 1 and Bridge 2 stations, reflecting the significant contribution from non-impounded sources between the dams and the downstream reaches. This progressive return of the isotope signal to the MWL indicates complete connection between the contributing hillslopes and stream in the landscape between the Dam Out and Bridge stations. This connectivity continues through the base flow period, as reflected by the analyses for June 2010 where 49% of the discharge at Bridge 1 and 34% of that at Bridge 2 are contributed by the relatively small connected sub-catchments immediately upstream of the Bridge stations (Table 4).

3 SEDIMENT SOURCE DETERMINATION

3.1 Upland Sediment Sampling and Analysis

Sediment sources have been defined in geochemical fingerprinting studies in different ways (e.g. by land-use category, geological unit, or tributary basin) depending on the primary intent of the analysis. For this investigation, the sampling strategy was developed to allow the data to be stratified (categorized) in different ways to determine the relative contribution of sediment from six land-use categories and seven soil types, thereby allowing an assessment of how each influence sediment production and availability (Table 5). A total of 73 samples were collected from upland areas in May, 2008 in order to characterize sediment sources (Figure 31). The number of randomly collected samples in each land-use category roughly corresponds to the area that it covers within the catchment. Road samples were not use to calculate statistical properties of specific soil types because of the degree to which the soils were disturbed. All of the sampled upland sediments were obtained from approximately the upper 2 cm of the ground surface. The sediments therefore represent the material most likely to be eroded during a runoff event. In order to reduce field variance, subsamples were collected from about 10 locations within a 5 m radius of the site and composited to create a single sample.

Table 5: Summary of samples collected in May, 2008.

Land-Use Category	**# samples**	**Soil Type**	**# Samples**
Pasture	10	Avalon	10
Pine Forest	2	Cartref	12
Roads	10	Clovelly	3
Sugar Cane	35	Glencoe	18
Vegetables	10	Katspruit	6
Wattles	6	Longlands	5
		Westleigh	9
Total	**73**	**Total**	**63**

All of the upland samples were loaded into pre-cleaned sampling containers, which were subsequently placed in plastic sampling bags, and shipped to the Nevada Bureau of Mines and Geology in the U.S. for analysis. The samples were analyzed using a Micromass Platform ICP-HEX-MS for major elements (e.g. Si, Al, Fe, Ca, Mg, Mn, Na, K, Ti, and P), total acid-soluble trace metals and metalloids (e.g. Pb, Zn, Cd, Cu, Au, Ag, Se, As), selected rare earth elements (e.g. Ga, Nb, La, Lu, Hf), and selected isotopes (e.g. ^{204}Pb,

^{206}Pb, ^{207}Pb, ^{208}Pb). Analysis involved the digestion of 200 mg of dried and homogenized sediment, < 2 mm in size, in 125 mL polypropylene screw-top bottles containing 4 mL of aqua regia. These were sealed and held in a 100ºC oven for 60 min. As the bottles heated up, they were re-tightened every 5 minutes until they remain tight (2 or 3 times total). The leaches were then transferred to 200 mL volumetric flasks, brought up to volume and stored until analyzed by ICP-MS. With respect to total elemental concentrations, the Platform was calibrated using USGS, NIST, and in-house standard reference materials (SRMs). Reagent blanks and the analyte concentrations for the SRMs were plotted against blank-subtracted integrated peak areas. A regression line was fitted to this array of calibration points and the equation of the line was used to quantify unknown sample concentrations. Deviation of standards from the regression line was used to estimate analytical accuracy, which was generally +/- 3 to 5 % of the amount present when determining total concentrations. Replicate analyses were used to determine analytical precision, which was generally < +/- 5 % for most elements. With respect to Pb isotopic analyses, precision when comparing data from individual digestions was 0.2 to 0.3 %

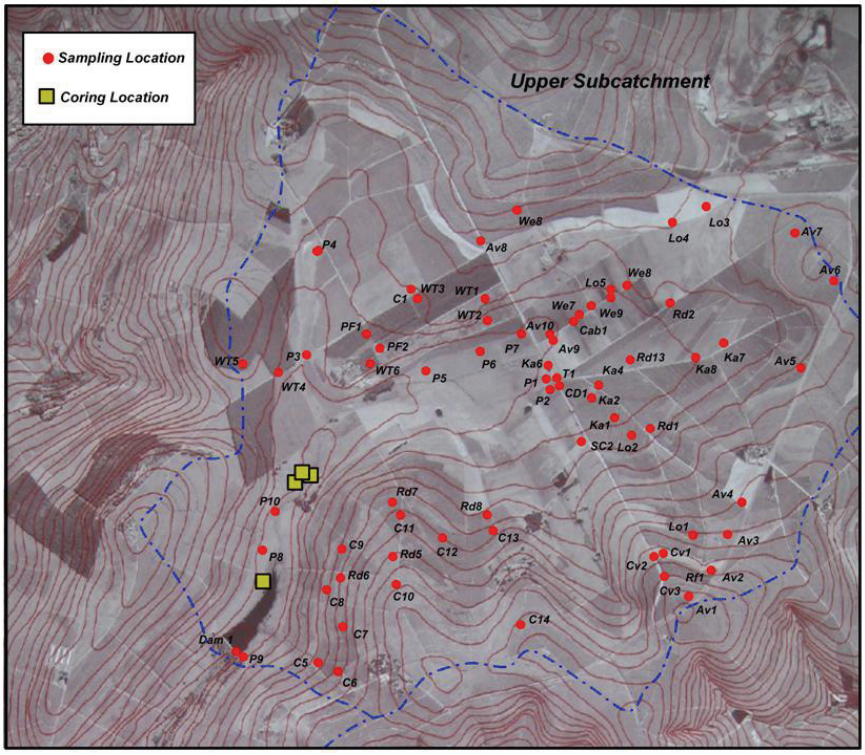

Figure 31. Upland surface soil (circles) and profile (squares) sampling locations.

relative deviation (one sigma) for ^{206}Pb, ^{207}Pb, and ^{208}Pb. Instrumental precision was better. Accuracy of isotopic measurements was assessed with the NIST 981 lead

isotope standard. Accuracy was typically better than +/- 0.5%, and systematic instrumental bias was corrected.

3.2 Delineation of Geochemical Fingerprints

An inherent assumption in the use of sediment mixing models is that the utilized elemental fingerprints are conserved during transport. A comparison of the average concentrations within the upland samples to the maximum concentrations in sediments collected from cores in the downstream wetland and reservoir revealed that the upland averages were often much higher for a number of elements (e.g. Ca, Mn, P, Cu, and Zn). The lower concentrations within the wetland and reservoir sediments, observed even for silt- and clay-dominated units, suggest that these elements were not conserved (i.e., elemental mass was being lost from the system, presumably in the aqueous phase). Thus, not all of the elements for which the samples were analyzed could be utilized as geochemical fingerprints. Operationally, elements were removed from consideration as a fingerprint when the average upland concentration was 10 % higher than the maximum concentration observed within stratigraphic units of the wetland and reservoir cores. The remaining elements were then utilized in a stepwise discriminate analysis to determine which elements were effective at differentiating sediment sources. The results suggest that effective fingerprints can be developed for sediment sources when defined according to either soil type or land-use category (Table 46).

With respect to the soil type, eight elements were identified as fingerprints, including Ti, Cr, Ga, Nb, La, Ce, Lu, and Hf. The majority of these are rare Earth elements which are known to be highly immobile in freshwater systems with normal Eh and pH conditions. The eight elements correctly classified 79 % of the samples (Table 5). The most incorrectly classified samples were obtained from Cartref and Glencoe soils. Interestingly, these soil types primarily resided within areas where the soils had been mapped at only a 1:100,000 scale. Thus, it is possible that some of the samples were incorrectly classified in the field with regards to soil type.

The stepwise discriminate analysis was also carried out for sediment sources defined by land-use. The selected parameters were the same as those used to differentiate soil types (Ti, Cr, Ga, Nb, La, Ce, Lu, and Hf) (Table 6). Sediments collected from specific land-use categories were incorrectly classified about a third of the time. The difficulty of correctly identifying a particular land-cover may be related to two factors. First, once planted, cane fields remain the dominate crop for several years at that location, some crop rotations do

occur through time, particularly with corn. Crop rotations may potentially produce a mixed geochemical signal with regards to land-use. Second, a given land-use category may be underlain by several soil types, complicating its geochemical signature. In fact, when soil type is added to the discriminate analysis as numeric values the ability to correctly classify land-cover increases significantly (to 86 %).

Table 6: *Discriminate Analysis Classification Matrix;(A) Soil Type; (B) Land-Use*

(A)	***Number of Samples Classified per Soil Type***							**%**
Soil Type	**Av**	**Cf**	**Cv**	**Ka**	**Gc**	**Lo**	**We**	**Correct**
Av	9	0	0	1	0	0	0	***90***
Cf	0	9	3	0	3	0	0	***75***
Cv	0	0	3	0	0	0	0	***100***
Ka	0	0	1	5	0	0	0	***83***
Gc	3	0	1	0	11	1	2	***61***
Lo	0	0	0	0	0	5	0	***100***
We	0	0	0	0	1	0	8	***89***
Totals	12	9	8	6	12	6	10	***79***
Av – Avalon; Cf – Cartref; Cv – Clovelly; Ka – Katspruit; Gc – Glencoe; Lo – Longlands; We – Westleigh								
Totals	9	9	5	0	3	6	12	3	***96***
(B)	***Number of Samples Classified per Land Use Type***						**%**
Land-Use	**Sc**	**Veg**	**Wt**	**Pine**	**Rds**	**Past**	**Correct**
Sc	22	3	9	0	1	0	***63***
Veg	0	8	2	0	0	0	***80***
Wt	0	0	5	1	0	0	***83***
Pine	1	0	0	1	0	0	***50***
Rds	0	0	2	0	6	2	***60***
Past	0	0	2	0	1	7	***70***
Totals	23	11	20	2	8	9	***67***
Sc – Sugar Cane; Veg. – Vegetables; Wt – Wattles; Pine – Pine Grove; Rds – Roads; Past – Pasture							

3.3 Source Modeling Procedures

The complex processes involved in the erosion, transport, and deposition of sediment ultimately result in a deposit that represents a mixture of material derived from multiple source areas within the catchment. If the physical and geochemical properties of the source area sediments are conserved during transport and deposition, then it is possible to determine the relative contributions that each source contributed to the resulting mixture. Total conservation of parameter values is rarely achieved in nature. Nonetheless, some properties are generally conserved. This led to the development and subsequent

modification of an empirically based, sediment mixing models that estimated the relative contributions of material from different source areas (Yu and Oldfield, 1989, 1993; Foster and Walling, 1994; Collins et al., 1997a, 1998; Kelley and Nater, 2000; Miller et al., 2005). Recent studies, however, have questioned the validity of these mixing model results because of the problem of equifinality, whereby similar goodness-of-fit values on which the models are based can be generated by different combinations of parameter (source) contributions (Beven, 1996; Rowan et al., 2000). In other words, the derived solution of source contributions is only one of a subset of possible statistically equivalent outcomes, in terms of relative error. During this investigation, the original models were modified by Gail Mackin using MATLB to estimate sediment source contributions while more fully characterizing the uncertainty in the models.

Constraints on the mixing model require that (1) each source type, (x_j, *j*=1, 2,…*n*), contributes some sediment to the mixture, and thus the proportions derived from *n* individual source areas must be non-negative ($0 \leq x_j \leq 1$), and (2) the contributions from all of the source areas must equal unity, i.e.:

$$\sum_{j=1}^{n} x_j = 1. \qquad (1)$$

In addition, some differences (error) between the values of the *m* measured parameters, b_i (*i* = 1, 2, 3…..*m*), in the source area and the mixture must be allowed. The residual error corresponding to the i^{th} parameter can be determined as follows:

$$\varepsilon_i = b_i - \sum_{j=1}^{n} a_{ij} x_j \qquad (2)$$

for *i*=1,2,…*m*, where a_{ij} (*i* = 1, 2, 3….*m*, *j*=1,2,…*n*) are the measurement on the corresponding i^{th} parameter within the j^{th} source area and x_j is the proportion of the j^{th} source component in the sediment mixture. When the number of measured parameters is greater than the number of source areas ($m \geq n$), the system of equations is over-determined, and a "solution" is typically obtained using an iterative computational method that minimizes an objective function using a gradient search, thereby obtaining a best fit solution to the entire data set (Yu and Oldfield 1989). There are several ways to obtain a best fit, but in previous studies, the objective function, f, has taken the form of the sum of the relative errors where $f(x_1,...,x_m) = \sum_{i=1}^{m} \left| \varepsilon_i / b_i \right|$ (Yu and Oldfield 1989) or $f(x_1,...,x_m) = \sum_{i=1}^{m} (\varepsilon_i / b_i)^2$ (Collins

et al., 1997a). However, in the case where f is relatively "flat", the gradient near zero may halt an iterative search method prematurely.

We take an alternative route, following Rowan et al. [2000], and Nach and Sutcliffe [1970], whereby we create the efficiency function

$$E(x_1,...,x_n) = 1 - \frac{\sum_{i=1}^{m}(\varepsilon_i)^2}{\sum_{i=1}^{m}(b_i - d_i)^2}$$

where d_i (i = 1, 2, 3…..m), is the means of the i^{th} parameter over all source regions. An ideal solution would result in $E = 1$ or 100% efficiency. We then create a partition of all possible combinations of non-negative n-tuples $(x_1,...,x_n)$ satisfying the unity constraint (1), by increments of Δx =0.05. By evaluating E at each of the n-tuples, we are able to determine the specific combination of $\hat{x} = (x_1,...,x_n)$ yielding the maximum efficiency on the partition.

As Rowan et al. [2000] pointed out, the efficiency function E, has a maximum value at $\hat{x}$, but there may be a range of n-tuples having an efficiency within a specified tolerance of the maximum efficiency. That is, there are a number of solutions that are statistically equivalent. For example, using the data from WT-C1-1, the optimal efficiency value was 0.9963 with the 50% of the contribution from cane, 25% from corn and vegetable, and 25% from wattle groves. Yet we see that there is a range for the proportion for each source that yields efficiency levels at the 0.95 level or above.

3.4 Collection, Sedimentology and Analysis of Sediment Cores

Five cores were collected in 2008 from the Mkabela basin, including one core from the margin of the upstream most reservoir (R1-C1); three cores from the wetland (WT-C1, WT-C2, and WET), and one core from the hillslope (HS-1). Two additional cores were collected in 2009 from sites along the axial drainage system (TB1, PB1). All of the cores were shipped to the Nevada Bureau of Mines and Geology and subsequently described, photographed, and sampled for geochemical analyses. The samples were then analyzed for the same elements that were analyzed in the surface soil samples.

3.4.1 WT1-C1

3.4.1.1 Core Location and Characteristics

Core WT1-C1 was obtained from approximately 40 m upstream of the wetlands downstream terminus. The area is dominated by a relatively flat surface about 1 m above a small channel that traverses the wetland. At the time of coring, the water table was about 20 cm below the surface, but based on the vegetation, periodically rises to ground level.

The core exhibits a total length of 122 cm. Stratigraphic relationships (Figure 32), including the presence of a buried paleosols consisting of a light brown, very sticky, gravelly clay loam, suggests that historic age sediment is 107 cm thick. A total of 17 samples, collected at 7 cm increments were obtained from the core for geochemical analyses. Sixteen of the samples were taken with the historic deposits. No sample was collected across stratigraphic a unit boundary; thus, the lower sample in each unit is often slightly less than 7 cm.

3.4.1.2 Source Modeling by Soil Type

The soil source modeling shows that three distinct intervals are present in WT-C1 (Figure 33). Samples 10-16 (69.5-107 cm) are composed exclusively of Clovelly (CV) and Katspruit (Ka) soil types. The relative contributions of Clovelly range from 10 to 70 %, and average 4.1 %; Katspruit ranges from 40 to 90 %.

Samples 7-9 (41.5-69.5 cm) are dominated by Katspruit (>60 %), with minor contributions of Westleigh (We), Avalon (Av), Catref (Cf), and Longlands (Lo), in three of the samples. The upper part of the core (samples 1-4) primarily consist of Avalon, Katspruit, and Longlands soil types, with minor contributions of Glencoe (Gc) and Westleigh.

Boundaries between the two of the major source intervals within the core roughly correspond to stratigraphic unit boundaries. The boundary between mid-interval (samples 7-9) and the lower interval (samples 10-16) imprecisely correlates with a gradational stratigraphic boundary within the core. Moreover, source contributions vary as a function of sediment grain size. Loamy sediments exhibit relatively high proportions of Katspruit and Avalon soil materials, as would be expected from the

fine-grained nature of these soil types. Sandy loams possess larger contributions of Longlands and Clovelly, which tend to be sandier soils.

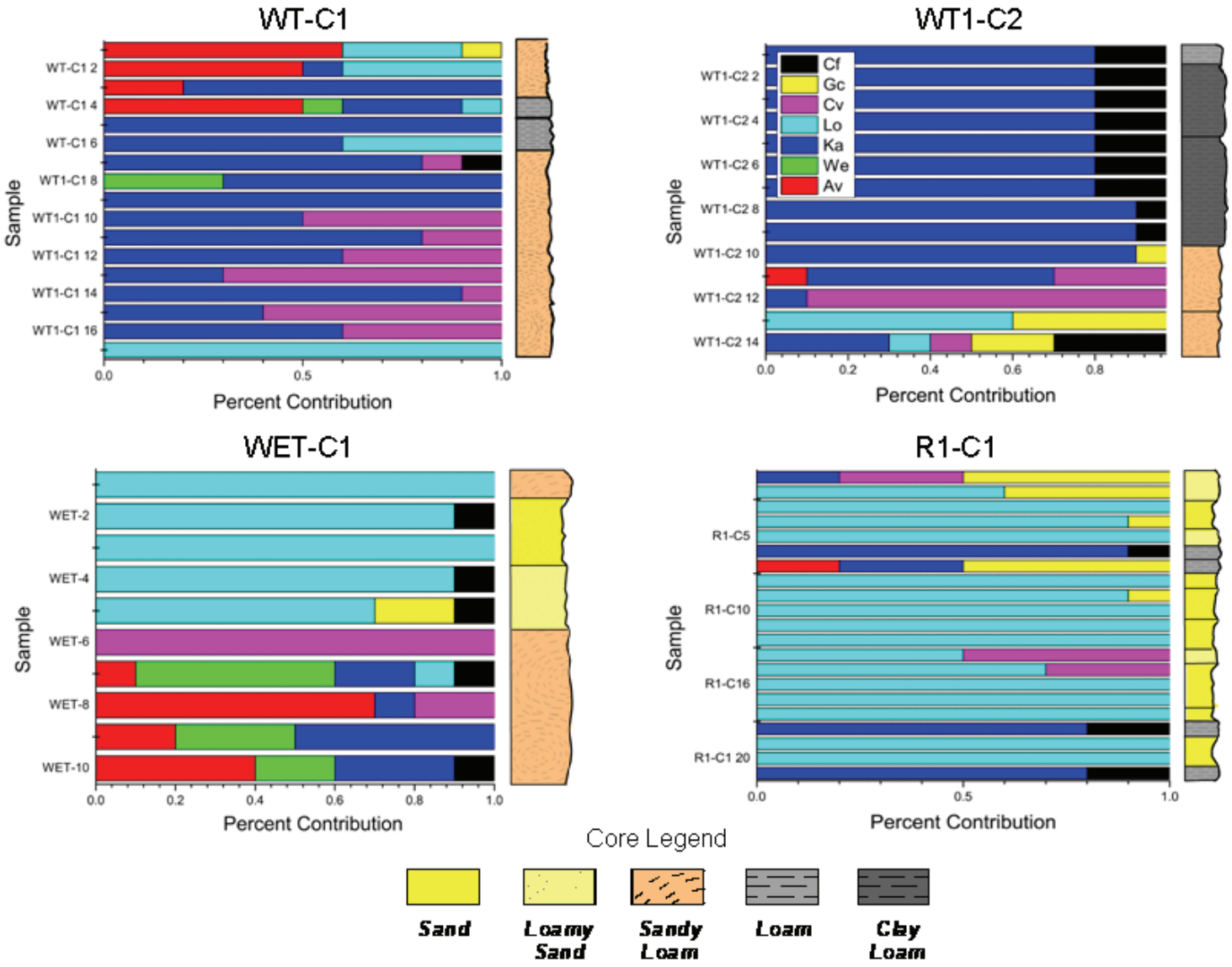

Figure 32. Relative percent of sediment derived from specific soil types within the catchment.

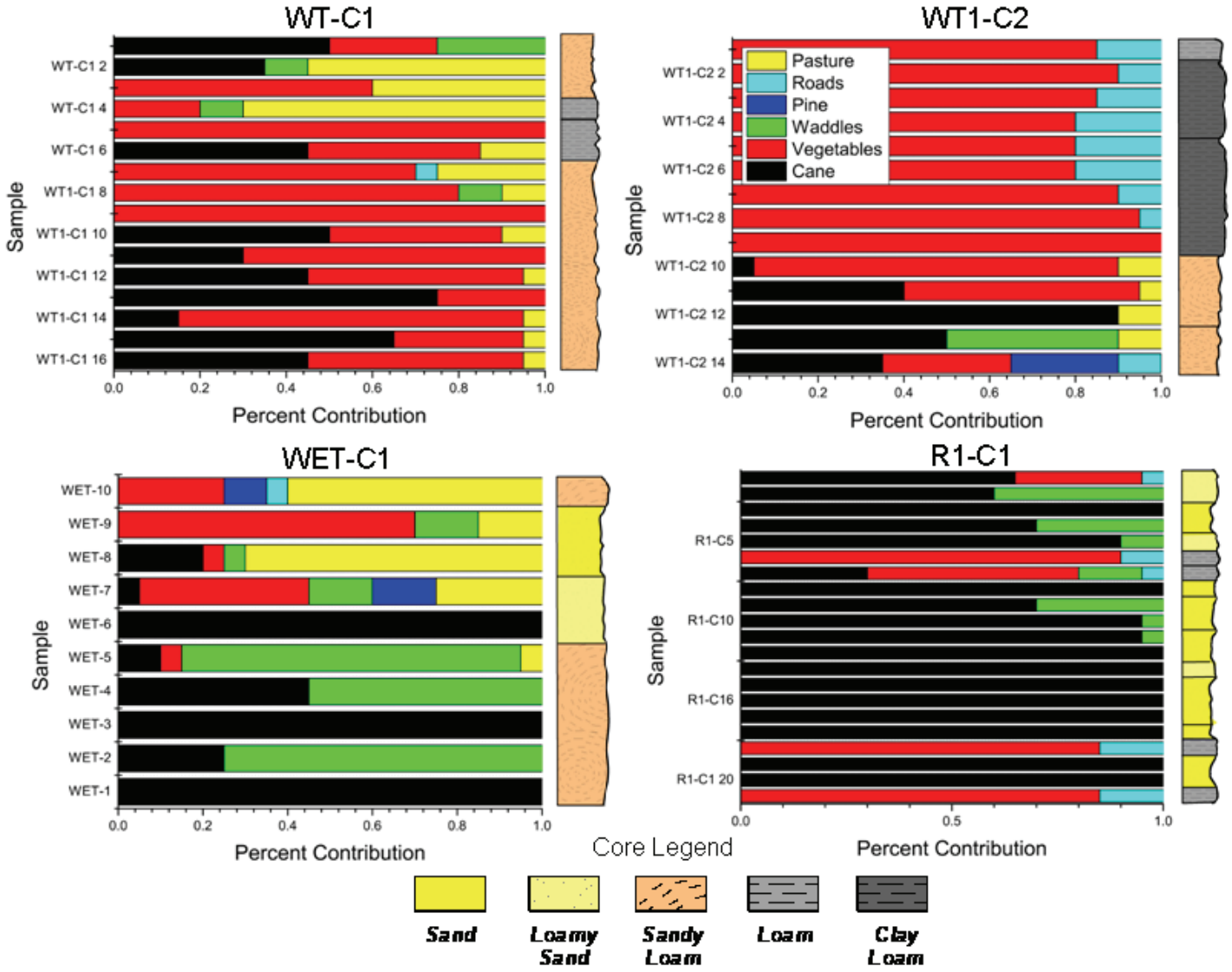

Figure 33. Relative percent of sediment derived from specific land-use types within the catchment.

3.4.1.3 Source Modeling by Land-Use Type

Core WT1-C1 can also be subdivided into three distinct intervals with respect to source contributions modeled according to land-use (Figure 33). The three intervals correlate precisely with the intervals denoted for soil type. Samples 10-16 are composed predominantly of materials from cane (15-75 %) and vegetable (30-80 %) fields. The samples also contain minor amounts of sediment from pastures (<10%). The intermediate interval (samples 7-9) are dominated by sediment from vegetable fields (generally > 70%). The interval also exhibits a notable increase in sediment from pastures (~10-25%), and localized, minor amounts of material from roads and wattle-covered terrain. The upper 6 samples contain a wider range of source inputs, containing significant quantities of sediment from vegetable fields, pastures, and cane fields, with lesser amounts of sediment from wattle-covered terrain (Figure 33).

3.4.2 WT1-C2

3.4.2.1 Core Location and Characteristics

Core WT1-C2 was obtained from a flat surface about 1 m above the wetland channel, approximately 250 upstream of the wetland's downstream terminus. The location was located about 15 m from the channel edge. The water table was about 20 cm below the surface at the time of coring.

The core exhibits a total length of 112.5 cm. Sediments below 90 cm in depth have been interpreted to pre-date historic deposition as they are heavily weathered, and exhibit significant accumulations of clay (Figure 32). A total of 16 samples were collected from the core at 7 cm increments. As was the case for the other cores, samples did not cross stratigraphic boundaries.

3.4.2.2 Source Modeling by Soil Type

Core WT1-C2 can be subdivided into three intervals on the basis of sediment provenance with respect to soil types (Figure 32). The lower most interval ranges from 78-90 cm (samples 13-14), consists of a medium sandy loam, and possesses sediment from a variety of soil types including Longlands (10-60 %), Glencoe (20-40 %), Cartref (0-30 %), Katspruit (0-30 %), and Clovelly (0-10 %). The lower most interval of historic sediment is overlain by a unit ranging from 62-78 cm (samples 11-12). This interval is dominated by sediment from Clovelly (30-90%) and Katspruit (10-60 %) soils, with minor contributions from Avalon soils (0-10 %). The majority of the core, ranging from 0-62 cm in depth), is dominated by

sediment from Katspruit (80-90 %), with <20 % coming from Catref soils, expect in the lower most sample. This latter sample contains sediment from Glencoe rather than Catref soils.

Changes in sediment source contributions correspond to stratigraphic unit boundaries. In addition, the lower most units, containing larger quantities of Clovelly and Longlands soils exhibit larger percentages of medium-sized sand, as might be expected from the sandy nature of these soil types.

3.4.2.3 Source Modeling by Land-Use Type

The provenance of sediment within core WT1-C2 can be subdivided into two intervals which closely, but not precisely, match the boundaries denoted for soils. The lower most historic deposits (below 55.5 cm, sample 10) contain relative large percentages of sediment from cane fields (Figure 33), whereas the overlying sediments are predominantly derived from vegetable fields (>80 %) with lesser contributions from roads. Sample 10, located along the boundary between the two intervals appears transitional in terms of source, consisting of large amounts of sediment from vegetable fields (as is the case for the overlying deposits, as well as minor amounts of sediment from cane fields and pastures (as is the case for the lower deposits). Sample 10 also appears somewhat anomalous in-terms of the soil types with which it is composed.

3.4.3 WET

3.4.3.1 Core Location and Characteristics

Core WET was collected from the lower end of the channeled wetland, some 600m upstream of the reservoir (Figure 32).

The total length of Core WET is 130 cm, the upper 69.5 cm of which is thought to be of historic age based on stratigraphic and geochemical data. A total of 18 samples were collected at 7 cm increments, with the exception of the last stratigraphic unit, which was sampled at 11 cm increments. None of the samples cross stratigraphic boundaries; thus, the samples were obtained from a single stratigraphic layer.

3.4.3.2 Source Modeling by Soil Type

The historic sediments in Core WET can be subdivided into two predominate intervals in terms of the soil types from which the sediments were derived (Figure 33). The lower most sediments (37-69 cm, samples 7-10) are composed primarily of sediment from Avalon,

Westleigh, and Katspruit soils, with minor amounts (10 %) of Catref and Longlands in sample 7. The upper most part of the core (from 0-30 cm) consists primarily of sediment from Longsland soils, with lesser (~10 %) from Catref soils. Sample 6, which separates the two intervals and which is found at the top of a stratigraphic unit, is highly anomalous, consisting exclusively of sediment from Clovelly soils.

Interestingly, sampling intervals dominated by Longlands sediment generally consists of fine sand (as might be expected), whereas those composed of Avalon derived sediment tend to finer-grained, consisting of sandy loams.

3.4.3.3 Source Modeling by Land-Use Type

Changes in sediment provenance modeled by land-use sources closely parallel noted changes in provenance assessed by soil type. The lower most sediments (37-69 cm, samples 7-10) are composed primarily of sediment from pastures (15-70), and in decreasing order, vegetable fields (5-70%), wattles groves (5-15 %), pine groves (0-15 %), cane (5-20) and roads (0-10). The upper most part of the core (from 0-30 cm) consists primarily of sediment primarily from cane fields (10-100 %) and wattles (45-85 %), with small amounts (5 %) from vegetable fields and pastures in sample 5. Sample 6, which separates the two intervals and which is found at the top of a stratigraphic unit, consists exclusively of sediment from cane fields.

3.4.4 R1-C1

3.4.4.1 Sample Location and Characteristics

Core R1-C1 was collected approximately 3 m from the edge of the first reservoir along the main drainage in a low-lying area that is likely to be inundated during flood events. The length of the core is 140 cm. The core was sampled at 7 cm increments for Pb-210 dating, generating a total of 20 samples. For geochemical analysis, two samples of similar thickness were collected for units more than 5 cm thick. A total of 21 samples were collected for geochemical analyses. All of the sediment appears to be of historic age.

3.4.4.2 Source Modeling by Soil Type

Source modeling with respect to soil types suggests that the majority of the sediment within the reservoir environment is derived from Longlands soil, with the exception of five, notable, but thin horizons. Sampling intervals 18 and 21 at the bottom of the core is composed exclusively of sediment from Katspruit type soils. The sampling interval from 60-73 cm

(samples 13-14) contains 30-50 % Covelly soils material, in addition to Longlands. Thin loamy fine sand to loam layers between 29.5 and 39 cm contain no definable sediment from Longslands soils, but are dominated by Katspruit (sample 6) or a mixture of Katspruit, Glencoe, and Clovelly (sampling interval 7). The upper most sediments also contain significant amounts of Clovelly material, as well as Glencoe and Katspruit in the case of sampling interval 1.

Intervals dominated by sediment from Longlands soils are dominated by fine to medium sands. Layers consisting of loam or loamy sands contain less material from the sandy Longsland soils, and more from the typically fine-grained Katspruit, Avalon, Glencoe, and Clovelly soils.

3.4.4.3 Source Modeling by Land-Use

The majority of the sand dominated sediment within Core R1-C1 appears to have been derived from cane fields. Fine-grained, loamy sediments (e.g. found in sampling intervals 1, 6, 7, 18, and 19) appear to have been derived primarily from vegetable plots. Figure 33 also shows that there is a notable increase in the contribution of sediment from wattle groves above 55.5 cm, as well as vegetables and roads, above 39 cm following a period of input primarily from cane fields between 55.5 and 106 cm.

4 SEDIMENT DATING

Based on their stratigraphy and location, two cores (WT-C1 and R1-C1) were dated using ^{210}Pb. The analysis of ^{210}Pb was carried out by Dr. Robert Flett (Flett Research Ltd.) located in Winnipeg, Canada. Dr. Flett was also contracted to use the raw ^{210}Pb data model to age-depth relationships within the cores. The results were then used to determine sedimentation rates at the site.

^{210}Pb in the relatively fine-grained sediment of core WT-C1 was measurable and could be used to determine both sediment age and sedimentation rates (Figure 34). However, the ^{210}Pb content of the sediment from R1-C1 was very low and irregular, showing no consistent pattern. The chemical recovery of the ^{209}Po isotope spike, needed to separated the amount of supported and unsupported ^{210}Pb in the sample, was unusually poor, indicating that the sediment contain elements or compounds that are interfering with the distillation and/or plating processes. However, the ^{226}Ra content of the deepest sediment samples (from 133-140 cm) was 3.05 DPM/g, very close to the ^{210}Pb activity of 3.15 DPM/g. This indicates

that the deep sediments are probably older than 100 yr. It is possible that all the sediments are older than 100 yr (which we believe is very unlikely), or, they contain very limited quantities of organic and fine sediment that typically sequester atmospheric ^{210}Pb. The latter is consistent with core descriptions (Appendix A), and the high dry bulk density measured for the samples. In summary, then, it was not possible to confidently determine the date of deposition of any of the sediments within the core from the reservoir's margin (R1-C1), other than to suggest that the lower most materials are likely to be more than 100 years old.

In core WT-C1, ^{210}Pb were also low. The single ^{226}Ra measurement of 0.82 DPM/g in the deepest section (at 112-122 cm depth), which based on stratigraphic data represent pre-historic sediment, is similar to the ^{210}Pb measurement of 0.60 DPM/g in the same section. This suggests that background levels of ^{210}Pb have been attained at 105 cm, and perhaps at the shallower depth of 70 cm in the core. Depth-age relations were modeled using the constant rate of supply (CRS) method for background values at both depths.

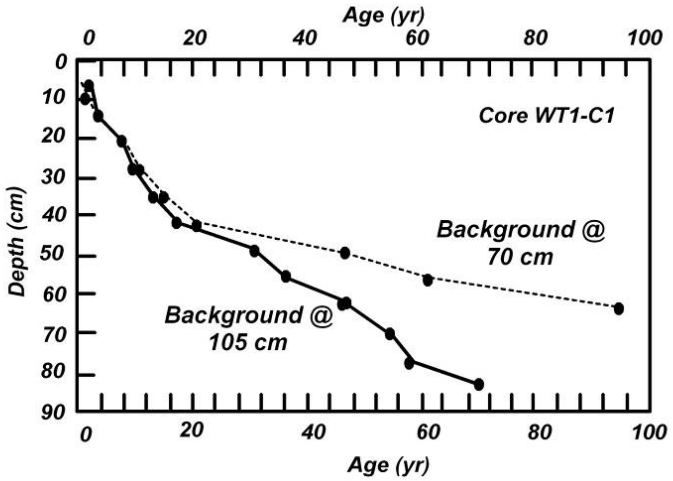

Figure 34. Estimated age of the sediments in Core WT-C1 as determined by ^{210}Pb analysis. The slope of the line in age-depth plot represents the sedimentation rate. Sedimentation rates/slope increase at above 41.2 cm, or after about 1992.

Age-depth relations for both models are similar for the upper 6 samples (last 20 years), but progressively diverge after that (Figure 34). Data from both models indicate that sedimentation rates within the wetland are relatively uniform until the end of the 1980s, at which point sedimentation rates begin to increase significantly to the present.

5. DISCUSSION: CONNECTIVITY AND CONTROLS OF SEDIMENT

A difficult question in the use of geochemical fingerprinting methods to determine sediment provenance is the grain-size of the material that should be analyzed. Many investigators focus only on the <63 um fraction because (1) it comprises a significant portion of the suspended sediment load in rivers, (2) it generally represents the chemically active phase, and (3) it is less effected by the dilution of chemical concentrations by relatively inert, particles composed of quartz, feldspars, and, perhaps, carbonates. Analysis of only fine-grained sediment is not, however, without its problems. Sand, in some cases, can comprise a significant part of the suspended sediment load, and may dominate alluvial and/or reservoir deposits. Such is the case in the Wartburg Catchment where the reservoir deposits are composed almost exclusively of sand-sized particles. Some wetland deposits, such as those found near the top of Core WET, are also composed of sand-sized materials. As a result, documentation of sediment provenance within the catchment required an analysis of both the silt- and clay-sized sediment and the sand-sized fraction.

Two approaches have been utilized when attempting to determine the provenance of both fine- and course (sand-sized) sediment using geochemical tracers. First, the sediment may be subdivided into a coarse- and fine-grained fraction, and analyzed separately. This approach is rarely used because of its considerable effort and cost. Second, the bulk sample is analyzed, and if necessary, a grain-size correction factor is included in the mathematical mixing model to account for the possible effects of dilution. During this study, we utilized this latter approach.

An examination of the core data collected from the wetland and reservoir shows that the deposits exhibit significant spatial (depth, areal) variations in grain size. These variations between process zones are dramatic. The upstream most reservoir within the catchment is dominated by sand, as was mentioned earlier. The wetland, however, consists primarily of loamy or sandy loam deposits. The observed variations in deposit grain size presumable reflect changes in sediment source and the nature of the source materials, hydraulic sorting of the sediment during transport and deposition, or a combination of the two.

The utilized sediment mixing model suggests that the nearly all of the sand-sized sediment within the reservoir is derived from Longlands and, to a much lesser degree, Clovelly soils. Both of these soil types exhibit sandy textures within the catchment (Le Roux *et al.,* 2006). They tend to be sandier than the clay-rich Westleigh or Avalon hillslope soils, and much sandier than valley bottom soils such as clayey Katspruit soil (Le Roux *et al.,* 2006). The geographic distribution of Longlands and Clovelly soils has been mapped in detail for only

the headwaters of the Wartburg Catchment. Here Longlands and Clovelly soils are located along the eastern corner of the Catchment, and are shown to abut Cartref soils on the 1:100,000 soils map (Figure 7). It is likely, however, that Longlands and Clovelly soils extend further south beyond the region mapped in detail, and therefore underlay a majority of the eastern hillslopes which drain into both the wetland and the reservoir. It appears reasonable, then, that Longlands and Clovelly soils could in fact serve as the primary source of sand-sized sediment within the reservoir, particularly given the relatively steep slopes (4-7 %) upon which they occur. It is perhaps reassuring to note that near surface sediment from a soil core (HS1) obtained from a hillslope underlain by Longlands was modeled to consist of predominantly of Longlands derived sediment.

The hillslopes underlain by Longlands and Clovelly soils are primarily covered by sugar cane fields. This is also consistent with the land-used based mixing model results which indicate that the majority of the sand-sized sediment was derived from cane fields.

Several loam textured layers occur within the reservoir core (R1-C1). These finer-grained units were modeled to consist of sediment primarily derived from Katspruit, and to a much lesser degree, Cartref, Glencoe, and Avalon soils. As would be expected, Katspruit soils are rich in clay as are Avalon and Glencoe soils (although not to the degree of Katspruit soils), (Le Roux *et al.,* 2006).

The Katspruit soils are primarily covered by vegetable fields on relatively flat sections of the valley bottom, and the land-used based modeling suggests that the loamy deposits within the reservoir are primarily derived from vegetable fields, with minor contributions from roads (with a clay-plinthic base) and cane fields (presumably underlain by Avalon or other clayey hillslope soil).

Similar texture, soil type, land-use associations occur with all three of the cores obtained from the wetland. These are particularly apparent for the lower portions of the historic deposits. For example, core WT-C1 sediments below approximately 69.5 cm (sample 10 and below) exhibit a fine sandy loam texture. Modeling suggests the sediments were derived from Katspruit soil (fine component) and Clovelly soils (sand component), covered primarily by vegetables and cane, respectively (Figures 32 and 33). Finer grained deposits (loam textured) between 41.5 and 62.5 cm (samples 7-9) Katspruit and Westleigh soils (both fine grained) overlain by vegetables (including corn, which can be found on Westleigh hillslopes).

A detailed examination of the modeling results indicates that a significant change in sediment source near the middle to top of the wetland and reservoir cores is superimposed on the texture, soil type, land-use association. In Core WT-C1, the change in source begins at

approximately 55 cm depth (sample 8) with a progressive increase in the contribution of sediment from pastures, wattles, and, to a much lesser degree, roads. Avalon and Longlands soil contributions also become more prevalent. The top of Core WET (above sample 6) also exhibits an increase in the contribution of sediment from wattle groves, and an increase in Longlands and Cartref (the latter of which underlies wattle groves). In Core WT-C2, sediment above 62 cm (sample 10), the sediment is derived almost exclusively from areas composed of Katspruit soils and vegetable fields, with a rather abrupt input of material from roads. Further downstream in the reservoir, the change in source is characterized by an increase in sediment from wattle groves, and an increase in sediment from Glencoe soils.

Interestingly, changes in sediment source coincide with a notable increase in sedimentation rates in Core WT-C1, from approximately 0.67 cm/yr to 2.21 cm/yr. The ^{210}Pb data suggest that the change occurred between approximately 1988-1992.

The noted changes in sediment source may be related to (1) changes in land-use and crop type through time, both in terms of the absolute area covered and their position on the landscape, and (2) changes in management strategies. More likely, however, is that the alterations are associated with a major alteration in the geomorphic connectivity of headwater drainages to the wetland and reservoir further downstream in the catchment. Discussions with a local sugar cane farmer stated that in the early 1990s, the lower half of his fields were changed from maize to sugar cane (Zone A, Figure 35). This would have involved contouring and water way development associated with cane, in order to limit sediment yield off-site. In addition, the valley bottle upstream of the cored wetland consistently flooded, resulting in the deposition of sediment in an area which he was attempting to pasture. Thus, it appears that drainage across a road that limited flow into the wetland was altered. More significantly, a ditch was excavated within the valley immediately south of the road to downstream of the confluence of a tributary entering from the west and which drains the wattle grove. The net result of the change was an increase in geomorphic and hydrologic connectivity that allowed drainage from the fields within the headwater areas of the catchment to be transported further downstream. The change appears as an increase in sedimentation rates in Core WT-C1 as well as an increase in sediment from the wattles and cartfer soils from the tributary, as well as road material that previously limited downstream drainage. The increased contribution of sediment from pastures, present in Core WT-C1, is probably due to bank erosion along the excavated ditch.

Core WT1-C2 exhibits a significant increase in sediment from vegetable fields underlain by Katspruit soils, at the expense of sediment from cane fields. Given the conversion of corn fields to sugar cane around 1990, the change in sediment provenance is surprising. However, it may be related to better sediment control practices on the cane fields which

Figure 35. Zones affecting sediment delivery to the wetland.

allowed a larger proportion of the sediment to be derived from the vegetable plots. It is also important to remember that sediment source is texture dependent, so that the contribution of sand-sized sediment from the cane fields was shown to increase as a result of the drainage alteration within Cores WET and WT-C1.

6. DISCUSSION: CONNECTIVITY AND CONTROLS ON NUTRIENTS

6.1 Nutrient and Suspended Solids Observations

The nutrient and suspended solids responses have been analysed in three ways:

- As a time series from January 2009 to January 2011,
- On a rainfall event basis and
- As transects from headwater to outlet for selected sampling events.

6.1.1 Nutrient Time Series Results

The time sequence of nutrient and suspended solids concentrations during 2009 and 2010 are shown for all stations from the catchment outlet (Bridge 2) to the headwaters (Runoff Plots) in Appendix B1-2. Of note in these sequences is the significant drop in concentrations of nutrients and suspended solids between the Flume 2 and Road Crossing or Dam 1 Out stations, reflecting the barrier to nutrient and sediment flux afforded by the wetland and first farm dam. Beyond the Dam 2 Out station, however, nutrient loads increase downstream as reflected by the higher concentrations and the Bridge 1 and Bridge 2 stations in Figure 36. The analysis of isotopes in Chapter 2 verifies that the source of this increase in nutrient load originates from the sugar cane hillslopes between the reservoirs and the Bridge stations and the lack of load reduction in the predominantly bedrock channel. The wetland upstream of Bridge 2 also, does not seem effective in reducing loads.

Also of significance is the apparent lack of relationship between suspended solids and P concentrations (Figure 37). This gives credence to the notion that much of the P load may be organic and that P appears to have a significant subsurface pathway. Examination of the instantaneous profiles of nutrient and suspended solids concentrations from headwater to outlet (Appendix D1 and D2), however, show some correlation between the suspended solids and P concentrations. This suggests that the suspended solids-P relationship may depend on event intensity and thus transported particle size fraction.

In general, the concentrations of NO_3 and P are lower in the dry season than in the wet, although concentrations vary greatly during rainfall events. However, the range of NO_3 concentrations in the groundwater, 5-25 mg/l, (Appendix B2.2.3), is similar to that observed in the time series at Bridge 2, 5-16 mg/l, (Appendix 2.2.1), suggesting that the dominant contributions to stream flow NO_3 are subsurface.

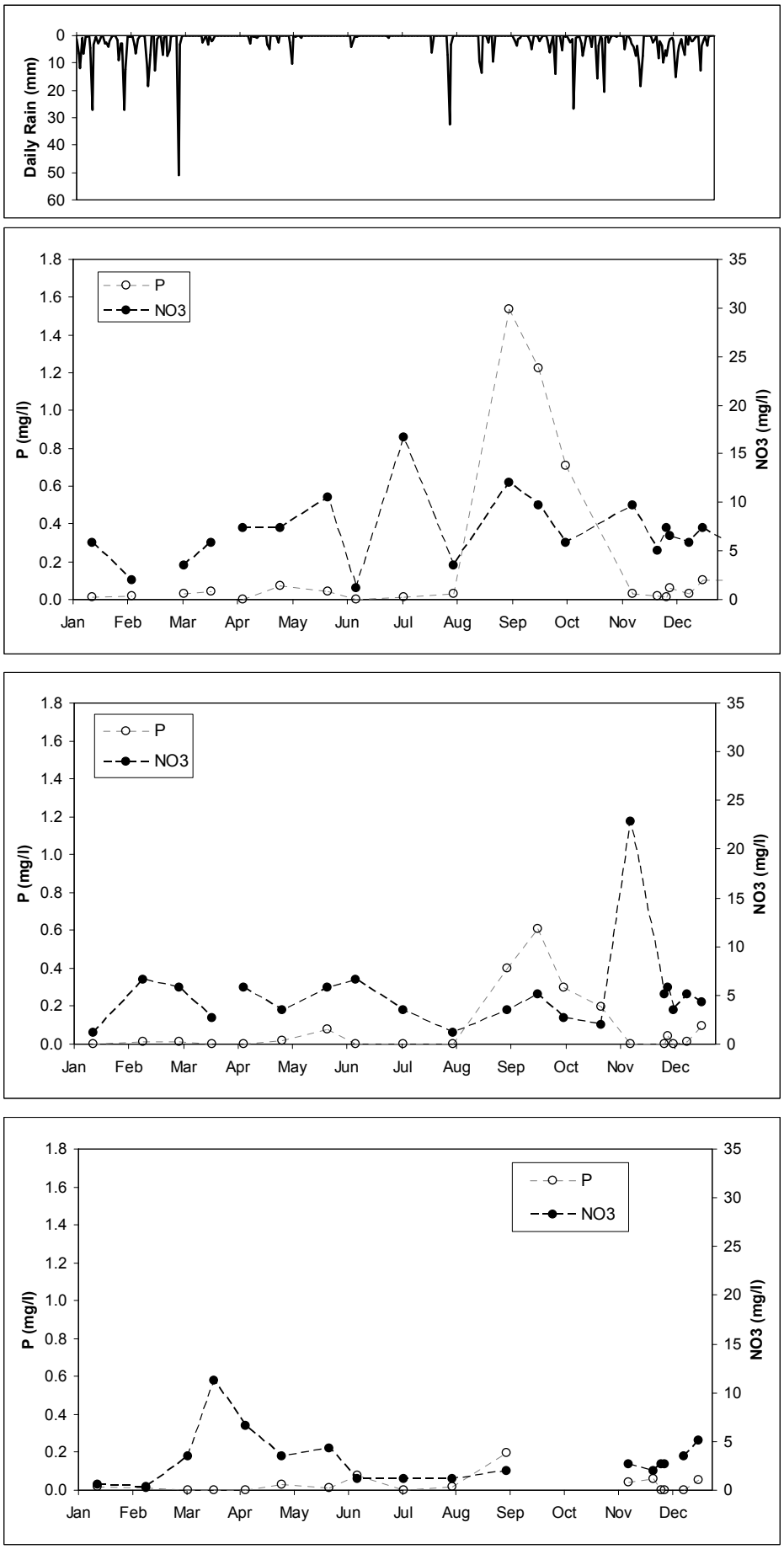

Figure 36. Rainfall, Nitrate and P responses for Bridge 2 (top), Bridge 1 (middle) and Dam Out (bottom) for 2009.

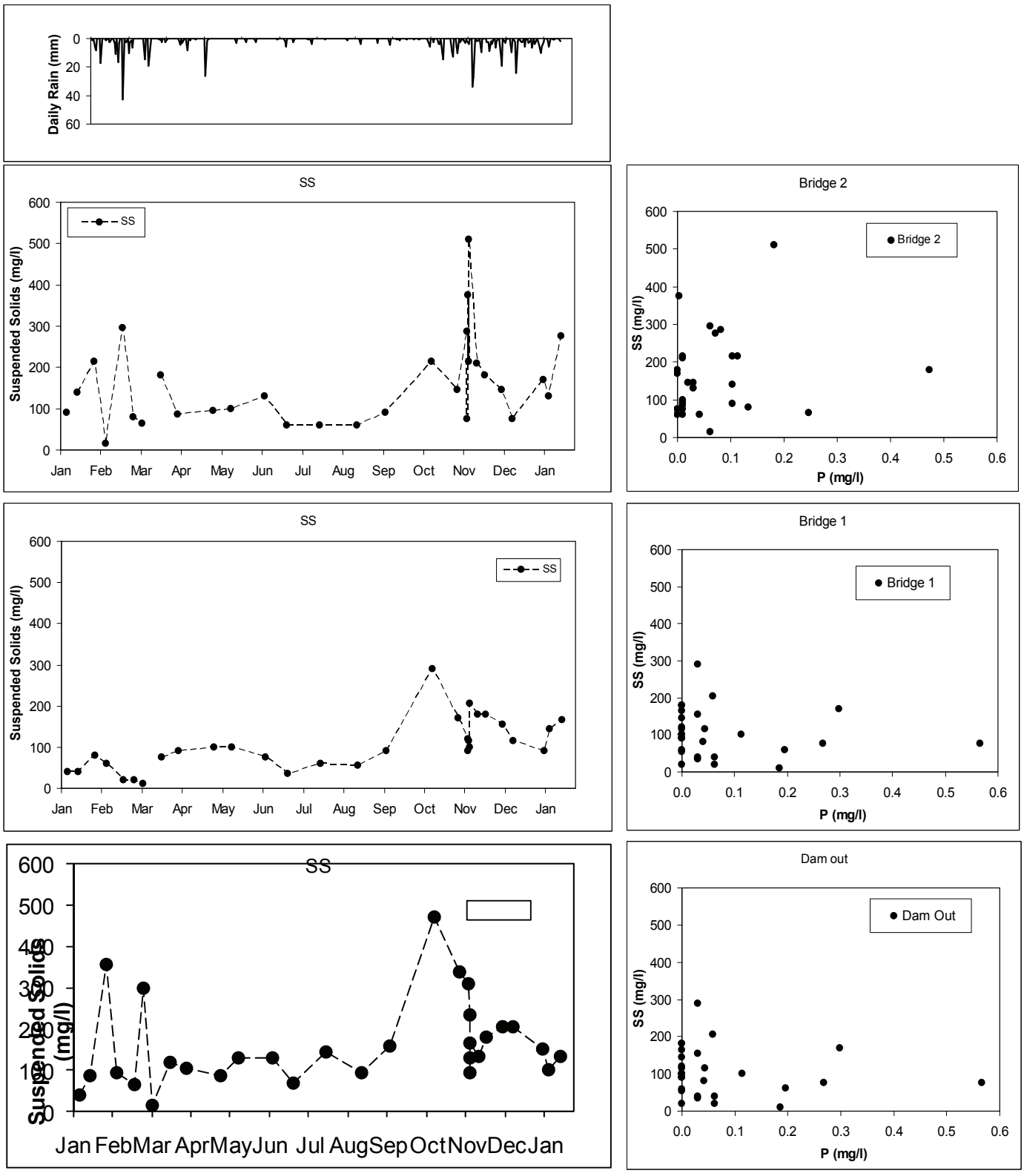

*Figure 37. Rainfall and suspended solids responses for Bridge 2 (top), Bridge 1 **(middle) and Dam 2 Out (bottom) for 2009, showing the relationship between P and Suspended Solids (right).***

6.1.2 Nutrient Event Results

Results of the nutrient (NO_3 and P) and suspended solids responses to the 28 February 2009 high intensity rainfall (51mm) and the 10 January 2009 low intensity rainfall (27mm) events are shown in Figures 38 and 39 respectively.

It is clear that the 51mm event results in a significant contribution of nutrients and sediments, with concentrations increasing during the event. Unfortunately the automatic sampler at the Flume 2 station had not been serviced for four weeks and the last sample in the container (24^{th} sample) was taken at the peak of the runoff event (Figure 38 left). Nevertheless, the increase in concentrations is similar to those observed at Flume 1. Of note, in the event observed at Flume 1, is the double peak of the nutrient and suspended solids during the event, which mimics the double discharge peak. However, the nutrient and suspended solids concentration peaks lag the runoff peaks by about one hour.

No significant increase in either nutrients or sediment concentration is observed during the moderate event of 10 January 2009 (Figure 39). Again, there is only one sample at both flumes during the event, but concentrations are similar to background values and are much lower (almost 10 fold) than during the 28 February 2009 event. These results, again, reflect connectivity thresholds for sediments and nutrient delivery which are dependant on event depth and intensity.

The nutrient and sediment concentrations are diluted by event water between Dam 1 Out and Dam 2 Out stations during the 10 November 2010 event, (Appendix C4.3), but beyond this, local sub-catchment contributions are evident at the Bridge stations (Appendix C4.4).

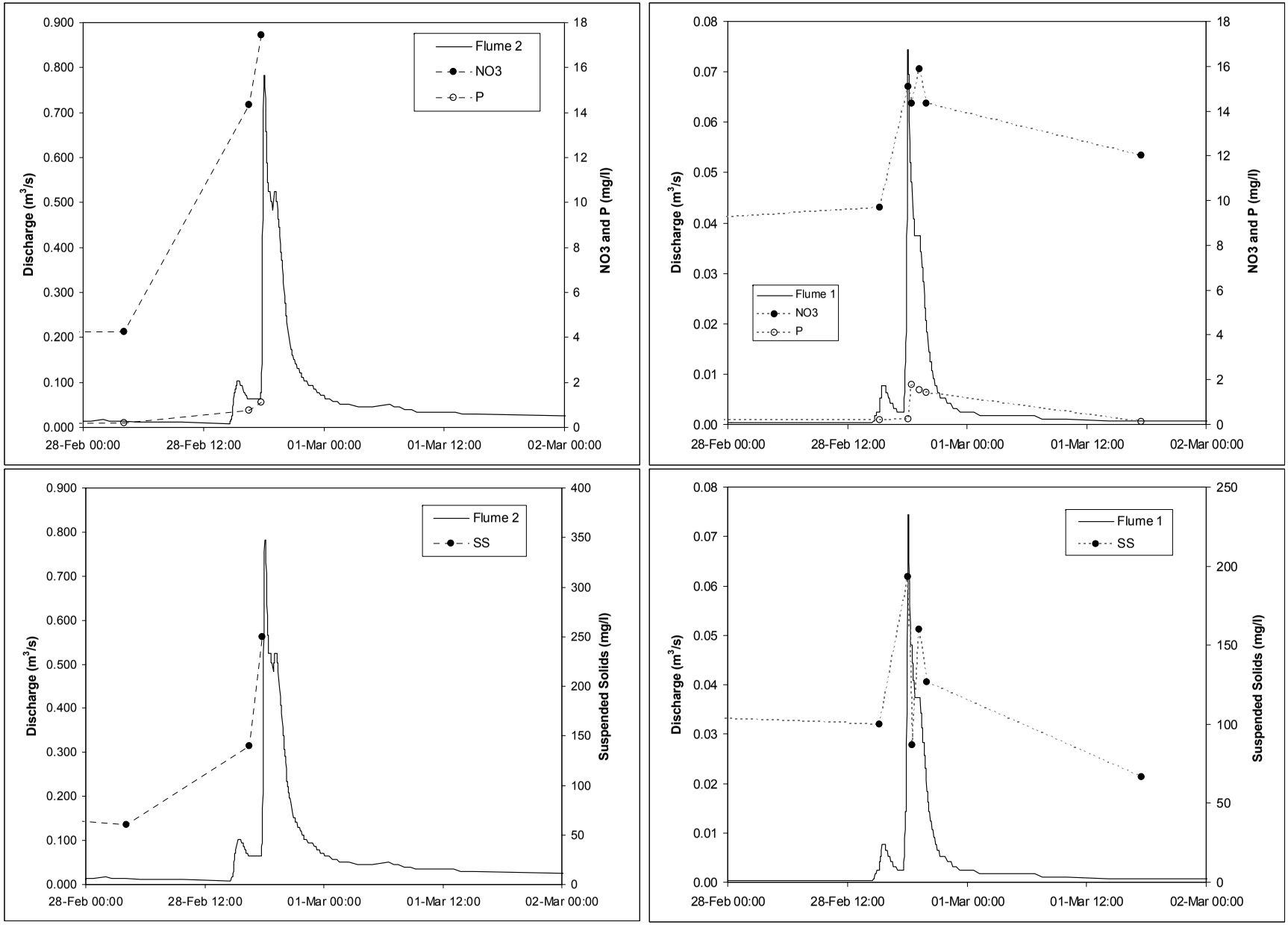

Figure 38. Rainfall, discharge Nitrate and P (above) and Suspended Solids (below) responses for event of 28 February 2009.

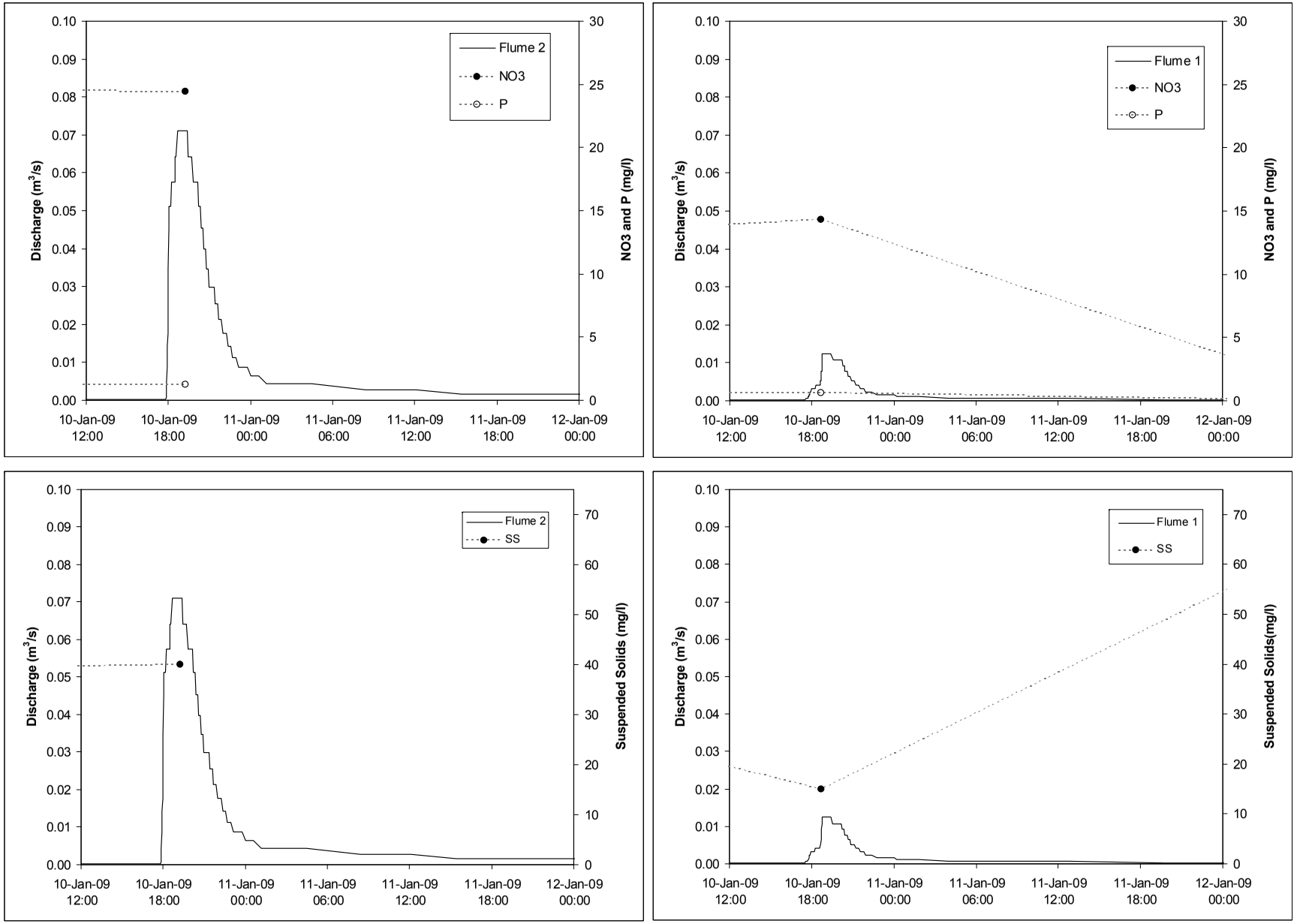

Figure 39. Rainfall, discharge Nitrate and P (above) and Suspended Solids (below) responses for event of 10 January 2009.

6.1.3 Nutrient Transect Results

The water quality data show an interesting drop in sediment and associated P concentrations between the runoff plot, RP1 and the first flume, Flume 1 for an event of 7 January 20111 (Figure 40).

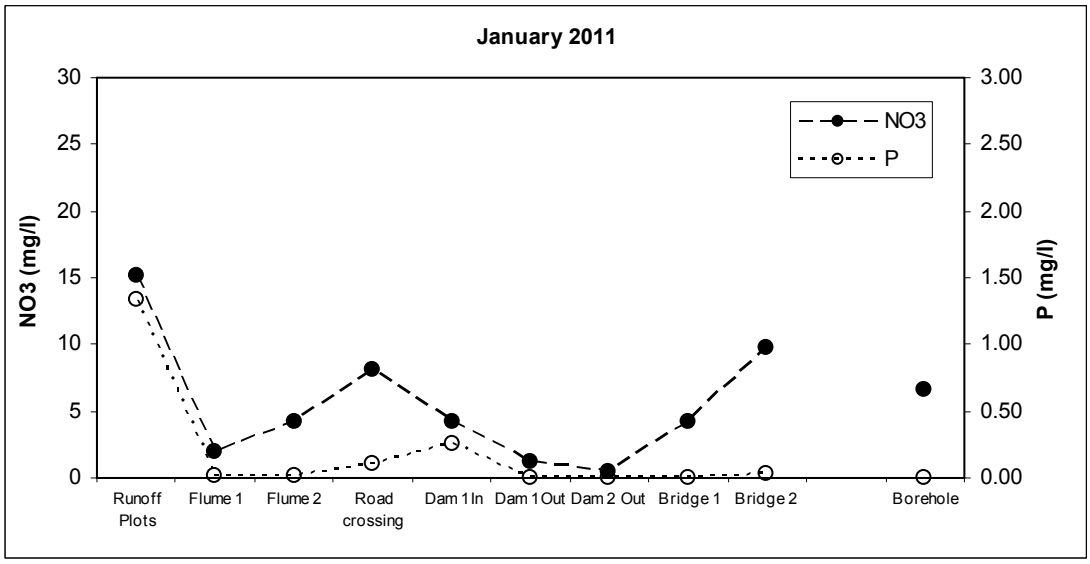

Figure 40. Concentrations of nutrients from headwater to outlet for the event of, 7 January 2011.

This is associated with the dilution of the runoff with subsurface water between the runoff plots on the upper slopes and the flume, down slope of the emergence of a subsurface seepage zone. Interestingly, however, the sediment concentration continues to drop between the first and second flume, while the P (and NO_3) concentration increases. This could be due to further subsurface sources contributing nitrate and phosphate (Deasy *et al*., 2007). Sediments and NO_3 are clearly retarded in the wetland and reservoir between the Flume 1 and Dam Out stations. Loading of sediments and nitrates increases beyond Dam Out, reflecting contributions from the sugar cane land use between the Dam Out station and the outlet of the catchment.

A complete set of nutrient responses along the stream network for selected events is presented in Appendix D.

6.2 Nutrient Processes through Trace Element Observations

Several trace elements were excluded as geochemical tracers because of their non-conservative nature, but provide useful information regarding the downvalley transfer of sediment and nutrients within the catchment. The two of most importance are copper (Cu) and Zinc (Zn).

Both elements are contained in fertilizer known to have been used on vegetable fields within the catchment. In fact, the utilized fertilizer is reported (on its bag) to contain 2.5 % Zn. The potential impact of the fertilizer on Zn concentrations in the soil is illustrated by comparing the amount of Zn within pasture and vegetable fields underlain by the same soil type (Katspruit). The pasture samples exhibit a mean Zn concentration of 3.58 µg/g, compared to a concentration of 139 µg/g for the vegetable plots, the latter higher by two orders of magnitude (Figure 41). In addition, Zn concentrations with soils of the vegetable plots are much higher than is typically found in uncontaminated bedrock (16-105 µg/g) or soils (60 µg/g), (Turekian, 1971; Buonicore, 1996; Miller and Orbock Miller, 2007). Similar trends are found for Cu, although differences are between background materials and the vegetable plots are not as significant (Figure 41). Cu and Zn concentrations are also very strongly correlated for the core samples, suggesting that they were derived from the same source (Figure 42).

Cu and Zn concentrations within the wetland cores vary systematically with depth, but the trends are distinctly different (Figure 43). Variations in observed trends can be explained, however, by differences in sediment provenance. In Core WT-C1, for example, both Cu and Zn concentrations increase from the bottom of the core toward the surface (from samples 16 to 7). The concentrations then abruptly decrease by a factor of 5 before remaining relatively constant until reaching the ground surface. The change in concentration is coincident with the observed increase in sedimentation rates (discussed early), and a change in sediment source. More specifically, Zn and Cu concentrations tend to increase as contributions from vegetable fields increase, and decrease as contributions from pastures and cane fields increase (compare Figures 43 and 34). The influence of sediment provenance on Cu and Zn concentrations within the cores is illustrated more directly in Figure 44. Although the trends are weak and numerous outliers exist, there is a clear tendency for Zn and Cu concentrations to increase as the modeled contribution of sediment from vegetable fields increases, whereas indirect relations exist for cane and pasture. The dramatic decrease in concentration above sample 7 in Core WT-C1 can therefore be explained by (1)

increasing contributions of sediment from pasture and cane fields, and (2) higher rates of sedimentation which presumable exacerbated the effects of dilution on Cu and Zn concentrations.

In contrast to Core WT-C1, contributions of sediment from vegetable fields in Core WT1-C2 increase toward the surface (decreasing age) above sample 12 (Figure 43). As expected from the above paragraph, concentrations of Cu and Zn increase as the contributions of sediment from vegetable fields increase. It is also notably that the lowest Cu and Zn concentrations are associated with sample 12 which the source model suggests contain the most sediment from the cane fields.

The indirect relationship between Cu and Zn concentrations and the relative contribution of sediment from pastures is understandable, but it is surprising with regards to cane fields given the relatively high mean concentrations calculated for Cu and Zn for the upland samples (Figure 41). The mean values, however, vary widely across the cane fields, in part, as a function of soil type. High Cu and Zn concentrations in the upland areas are associated with Cartref and, to a less degree, Avalon soil types. They are also high in Katspruit soils which underlie the vegetable plots that were fertilized (Figure 41; Katspuit soils underlying pastures were not included in the calculations). Low Cu and Zn are found in Westleigh, Clovelly, and Glencoe soils. Longlands soils exhibit very high Cu concentrations, but very low Zn concentrations. It is possible, then, that sediment from the cane fields within the wetlands was primarily derived from those soil types (or areas) possessing low Cu and Zn values; specifically, Westleigh, Clovelly, Glencoe, Katspruit (in pastures) and, for Zn, Longlands soils. Outliers on Figure 44 (high Cu and Zn with no significant input of sediment from vegetable fields, and high Cu and Zn with high input from Cane fields and pastures) is presumably related to the influx of sediment to the wetland from cane fields with high Cu and Zn concentrations.

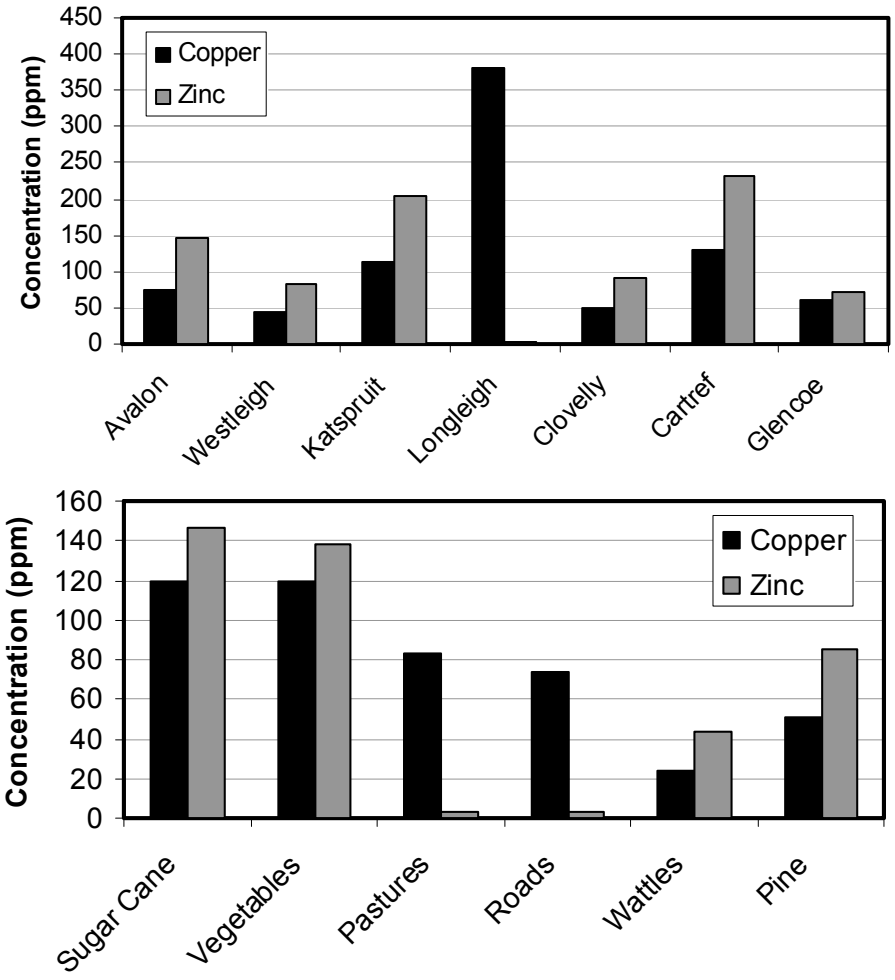

Figure 41. Mean concentrations of Cu and Zn calculated for upland soil (a) and land-use (b) types. Note that the mean shown for Katspruit soils does not include samples from pastured areas.

Cu and Zn concentrations in general tend to be much high within cane fields than within pastured areas where Zn enriched fertilizers presumably were not utilized. Cu and Zn concentrations are also higher within the cane fields than is typically found in bedrock. The data suggest, then, that the fertilizers used on the vegetable plots were also used on cane fields, or alternatively, used on corn fields which were then converted into cane fields.

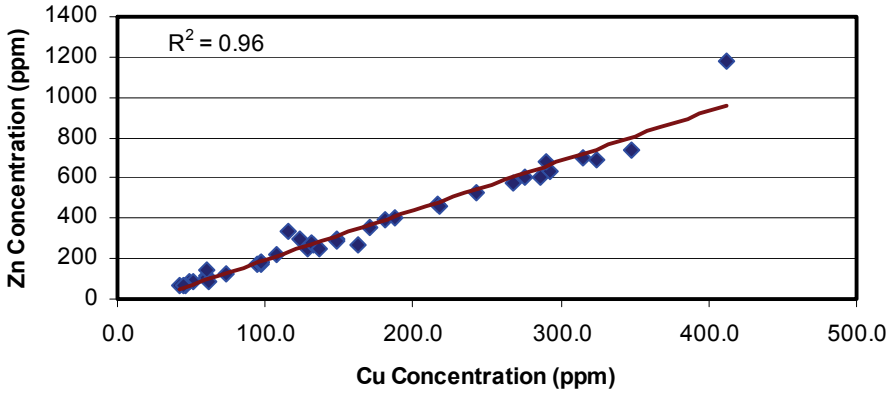

Figure 42. Relationship between Cu and Zn concentration with wetland and dam (reservoir) core samples.

The difference in Cu and Zn concentrations in Longlands soils is interesting as the parent material for it is thought to be the same as that for the other soil types in the catchment (Natal Group Sandstones). Moreover, if the high Cu concentrations consistently observed for Longlands soil samples were related to fertilizer, high Zn concentration would also be expected as shown on Figure 42. It is unclear at this time why such large differences exist, when they do not for the other soil types. It is possible, however, that the sandy nature of Longlands soils, combined with their occurrence on relatively steep slopes, allowed the more mobile Zn to be leached from the sampled surface sediments.

Figure 45 shows that Cu and Zn concentrations are relatively low from the bottom of the core (R1-C1, Sample 21) to Sample 9. Concentrations of both above sample 9 are generally 3 to 5 fold higher. The change in concentrations is roughly coincident with the modeled change in sediment provenance that was attributed earlier to the construction of a drainage ditch through an upstream wetland. In other words, the higher Cu and Zn concentrations appear to result from an increase in system connectivity and the capacity for sediment derived from headwater vegetable fields and other sediment sources to be transported downstream through the wetlands and to the reservoir.

Interestingly, Cores WT1-C2 and B2WTC1 exhibit similar variations in Cu and Zn concentrations to that observed for approximately the top third of R1-C1 (Figures 43, 45). Concentrations are high at the surface and then systematically decrease with depth before increasing further down core. The primary difference is that the abrupt decrease in Cu and Zn concentrations observed at depth within Core R1-C1 is not

present in the other two cores. The zone of relatively low Cu and Zn concentrations corresponds sedimentologically to layers containing significant amounts of sand-sized sediment which the source modeling indicates was derived in part from cane fields. The Cu- and Zn-enriched horizons are finer-grained and derived predominantly from vegetable plots in Cores WT1-C2 and R1-C1 (source modeling was not performed on Core B2WTC1 because it was located well downstream of the sampled upland sediment sources). The similarities in concentration with depth suggest that all three locations, spanning the entire study catchment, received similar contributions of sediment from the various sources. It therefore appears that following the construction of the upstream drainage ditch through the upstream most wetland, the axial drainage network was geomorphically and hydrologically connected.

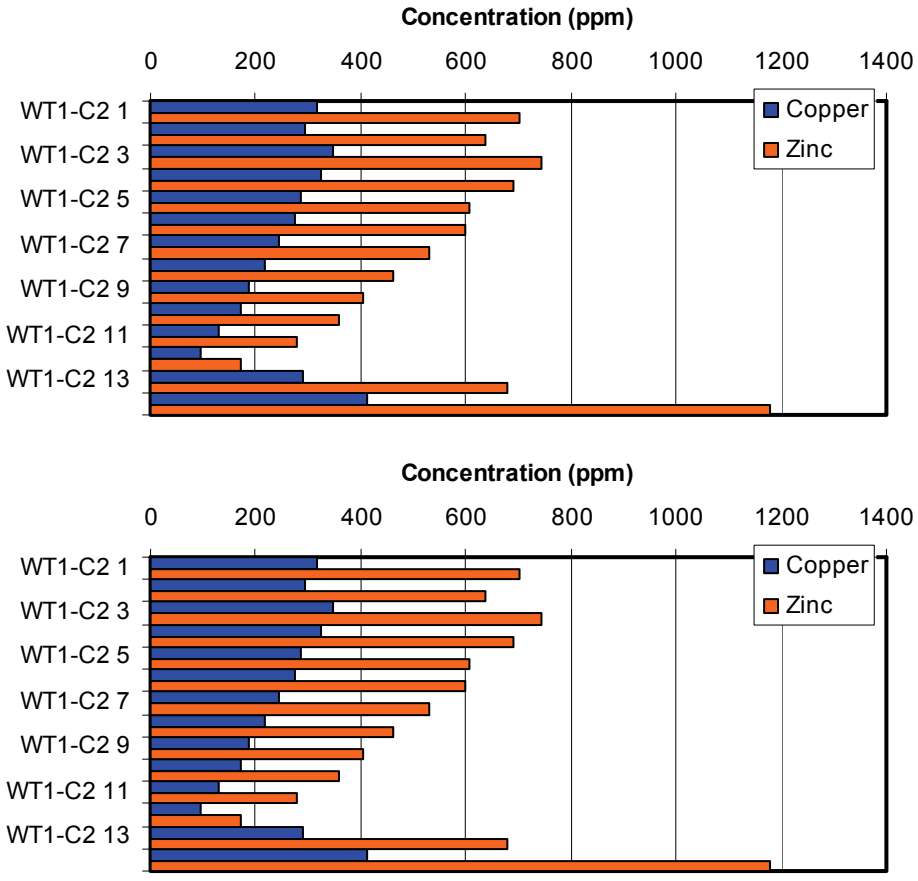

Figure 43. Variations in Cu and Zn concentrations with depth in wetland cores WT1-C1 and WT1-C2.

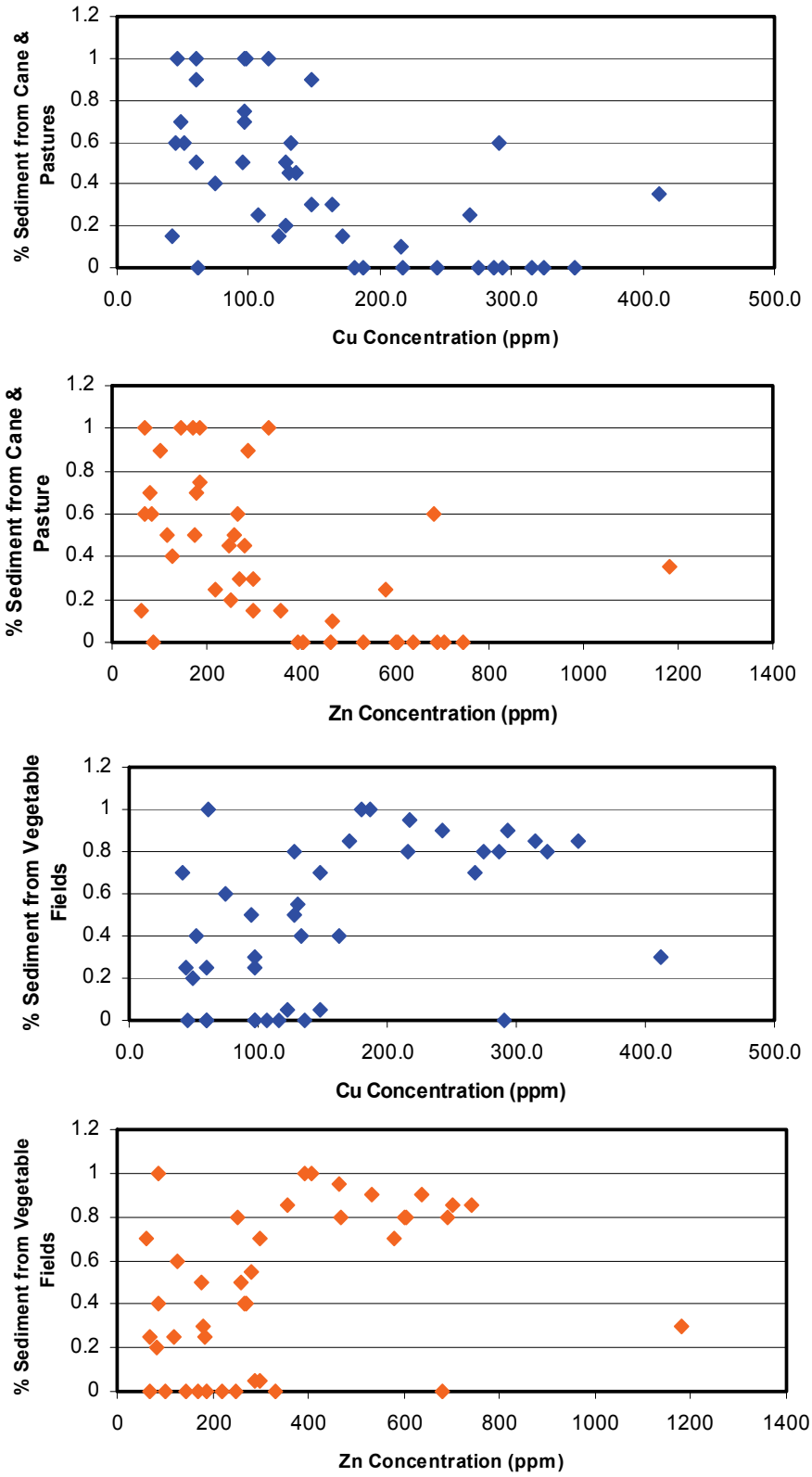

Figure 44. Relationship between Cu and Zn concentrations and % relative contribution from vegetable and pasture + cane fields.

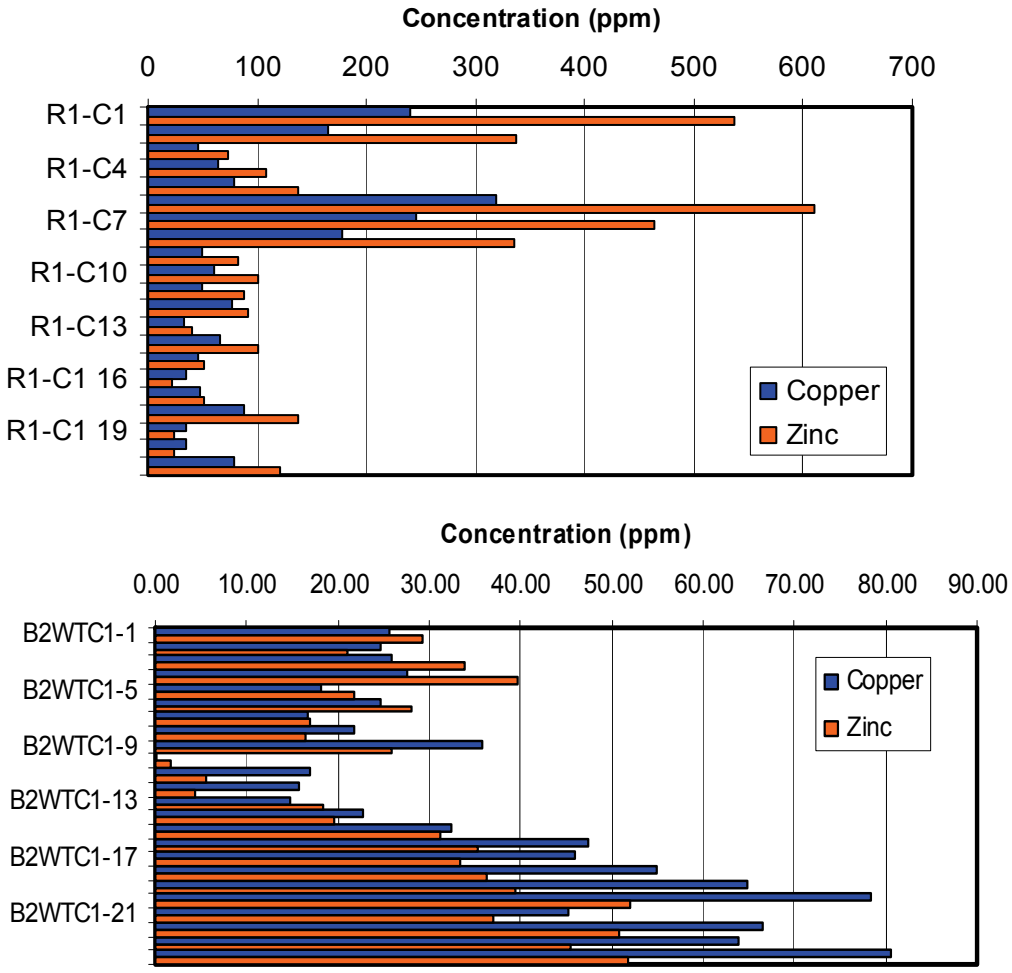

Figure 45. Variations in Cu and Zn concentrations with depth in wetland cores R1-C1 and B2WTC1.

From a process oriented perspective, the combined data set suggests that during periods of low-runoff/discharge, fine-grained sediment eroded from vegetable fields underlain by fine-grained soils (e.g. Katspruit) were delivered to the axial drainage and transported downstream through the catchment (Figure 46). Very little of this fine sediment was deposited and stored with the reservoir, indicating that the dams had little impact on the storage of silt- and clay-sized particles during most events. This is not necessarily surprising given that water overflows the dams during periods of surface runoff. Apparently, cane fields, underlain by sandier materials, are not significantly eroded during these relatively low-magnitude events or, alternatively, what sediment is eroded, is redeposited on the hillslopes as a result of the utilized

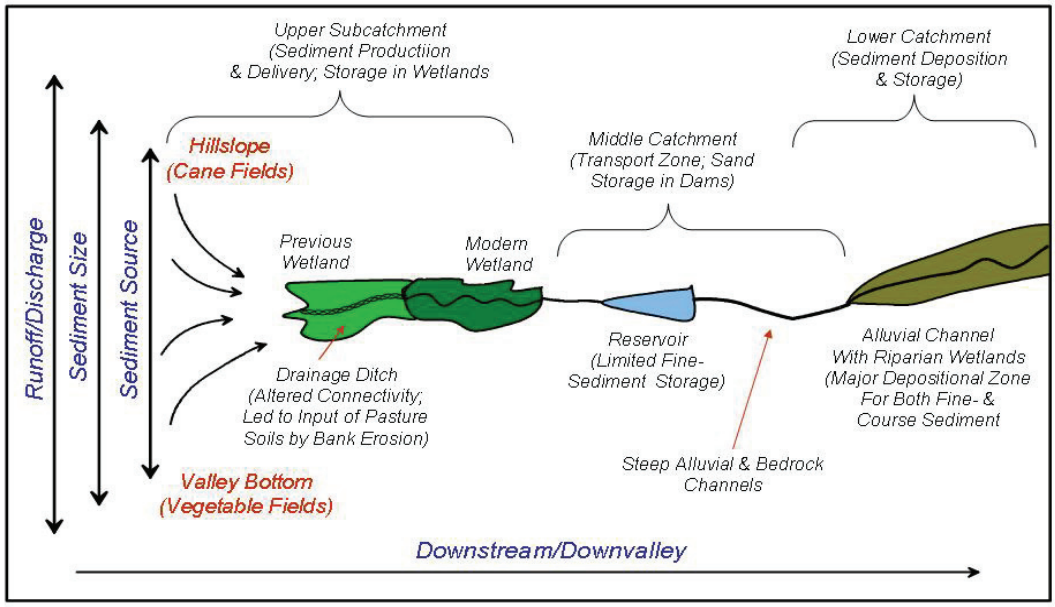

Figure 46. Schematic diagram of the primary processes occurring in each of the three delineated subcatchments, and the variations in sediment size and source from varying runoff magnitudes.

management practices. During larger runoff/discharge events, sediment is not only eroded from the valley bottom sediment sources, but from sandier hillslope soils covered largely by sugar cane. The sandier sediments, exhibiting lower elemental concentrations, tended to dilute the concentrations of Cu and Zn within the wetland and reservoir sediments, and produce relatively coarse-grained wetland and dam (reservoir) deposits. Although a larger quantity of sand-sized material was deposited and stored in the reservoir, the sand-sized fraction also appears to have been transported downstream at least until reaching the riparian wetlands located at coring site B2WTC1.

In spite of the fact that Core B2WTC1 is 1.79 m long, it does not appear that sediments pre-dating the construction of the drainage ditch were reached as Cu and Zn concentrations were not observed to abruptly decrease as in Core R1-C1. Thus, as suggested during the discussion of the various process zones, alluvial reaches characterized by extensive riparian wetlands appear to be a significant site for sediment and nutrient storage. In fact, if it is assumed that the bottom of the core represents the time at which the drainage ditch was constructed, then the average rate of sediment deposition at the site was 9.47 cm/year, an extremely high value.

7. CONCLUSIONS AND RECOMMENDATIONS

The combined process zone NPS delivery analysis resulted in the following conclusions:

(1) The study catchment is composed of a series of distinct process zone types, each characterized by differences in their ability to produce, transfer, and store sediment. The nature and spatial arrangement of the process zones within the basin show that it can be subdivided into three subcatchments, referred to here as upper, mid- and lower subcatchments. The three subcatchments differ in their tendencies to transport and store sediment and nutrients.

(2) The construction of a drainage ditch through the upstream most wetland significantly altered the geomorphic and hydrologic connectivity of the catchment. Prior to its construction, sediments (and the nutrients that they carry) were largely deposited within wetlands which encompassed a majority of the valley floors within the upper catchment. Sediments delivered to the mid-catchment area were generally transported downstream as a result of confined flows and steep channel gradients which often include bedrock reaches. There is very little storage within the reach, except within local dams.

(3) Following construction of the ditch across the upper most wetland, sediments could be transported from the headwaters of the catchment, through downstream wetlands and dams (reservoirs) and to a low-gradient alluvial channel boarded by an extensive riparian zone. Thus, the axial drainage system is geomorphically and hydrologically connected during most events throughout the study basin. However, current rates of sediment deposition within the downstream most riparian wetlands is extremely high, approaching 10 cm/yr, suggesting that this reach limits the further downstream movement of sediment.

(4) The complex interactions between runoff, soil type and characteristics, and land-use (among other factors) appear to create temporal and spatial variations in sediment provenance. Silt- and clay-rich layers found within the wetland and reservoir deposits appear to have been derived from the erosion of fine-grained, valley bottom soils which are frequently utilized as vegetable fields. The deposits tend to exhibit elevated concentrations of Cu and Zn, presumably from the use of fertilizers which contain both

elements. Coarser-grained deposits within the wetland and reservoir presumably result from the erosion of sandier hillslope soils extensively utilized for sugar cane. Erosion of these upland cane fields presumable occurs during relatively high magnitude runoff events that are capable of transporting sand-sized sediment off the slopes, and which create dam (reservoir) deposits lacking significant quantities of silt- and clay-sized particles. Therefore, sediment source, as might be expected, varies as a function of runoff magnitude.

(5) Sediment source determination on multiple cores from the wetland demonstrated that sediment partitioning during transport not only produced deposits of varying sedimentological and chemical characteristics, but deposits consisting of sediment from different source areas. As a result, within highly variable depositional environments, multiple cores should be collected and analyzed to determine sediment provenance.

(6) The nutrient (N and P) transport in the catchment mirrors the sediment migration through the channel system. However, the relationship between sediment and P is poor, suggesting that much of the P transport in contributing hillslopes is in the dissolved phase and likely occurs subsurface during recession and low flow sequences.

(7) The first reservoir in the monitored network (Dam 1) is effective in retaining event water from connecting with the downstream network. However, increased nutrient and sediment loads from the reservoir during these events suggest a disturbance and release of resident nutrients and sediments from the reservoir.

(8) The loads of nutrients between Bridge 1 and Bridge 2 stations reflect the bedrock control, where contributions from sugar cane hillslopes between these stations are not retained, even in the short wetland upstream of Bridge 2.

(9) Stream discharge and consequent NPS-P from the two impounded tributaries is limited by the storage afforded in these impoundments. The contributions of event water from the upper 70% of the catchment often comprise less than 50% of the discharge at the Bridge 1 and Bridge 2 stations.

(10) The dominant contribution mechanism for nutrients in the landscape appears to be in the subsurface, in lateral discharge in the intermediate layer between the sandy soil and bedrock.

(11) Event water, carrying high nutrient loads, dominates the responses at the field scale, while low flows reflect the groundwater concentrations of N and P.

It is recommended that:

(1) Sediment fingerprinting and dating are further developed to determine the connectivity and depositional history of deposits in the lower part of the Mkabela catchment.

(2) Specific indicators of nutrient migration are identified and sampled in the sediments of the wetlands and reservoirs throughout the catchment to determine their sources, pathways and associations with sediments.

(3) Detailed experiments are conducted to determine the mobility of P in the subsurface.

(4) Sampling of nutrients, suspended solids and stable isotopes should continue, but the frequency of sampling increased during rainfall events so that the connectivity from headwaters to outlet can be assessed. Selected geochemical species should be added to the sample analyses to better identify sources, pathways and travel times.

(5) Modifications to the use of simulation models require detailed use of GIS mapping and on-site truthing to identify the types of controls and connectivity features identified in this study. The techniques of hydropedological delineation of typical hillslope response types should be further improved and tested against hillslope monitoring of water and nutrient movement. Algorithms for sediment trapping and nutrient exchange mechanisms in control features have been widely developed and applied and these should be judiciously selected and introduced in new algorithm developments. Modifications to model algorithms will also require features for simulating threshold responses in hillslope and streams to mimic the connectivity features identified.

REFERENCES

Bracken, L.J. and Croke, J. 2007. The concept of hydrological connectivity and its contribution to understanding runoff-dominated geomorphic systems. *Hydrol. Process.* 21:1749-1763.

Brierley G.J., and Fryirs, K.A., 2005. Geomorphology and River Management: Applications of the River Styles Framework. Blackwell Publishers, Oxford.

Brunsden, D., 1993. Barriers to geomorphological change. In: Thomas, D.S.G. and Allison, R.J., (eds), Landscape Sensitivity, pp. 7-12. John Wiley, Chichester,.

Deasy, C.; Brazier, R.; Heathwaite, L.; Hodgkinson, R. 2007. Quantifying agricultural phosphorus transfers at hillslope to catchment scales. Diffuse phosphorus loss: risk assessment, mitigation options and ecological effects in river basins. The 5th International Phosphorus Workshop (IPW5) in Silkeborg, Denmark, 3-7 September 2007 pp. 189-191.

Edwards, A.C., Withers, P.J.A., 2007. Linking phosphorus sources to impacts in different types of waterbody. Soil Use Manage. 23 (Supplement) 133-143.

Frissell, C.A., Liss, W.J., Warren, C.E., and Hurley, M.D., 1986. A hierarchical framework for stream habitat classification: viewing streams in a watershed context. Environmental Management 10:199-214.

Grant, G.E., Swanson, F.J., and Wolman, M.G., 1990. Pattern and origin of stepped-bed morphology in high-gradient streams, western Cascades, Oregon. Geological Society of America Bulletin 102:340-352.

Grant, G.E. and Swanson, F.J., 1995. Morphology and processes of valley floors in mountain streams, western Cascades, Oregon. In: Costa, J.E., Miller, A.J., Potter, K.W., and Wilcock, P.R., eds., Natural and Anthropogenic Influences in Fluvial Geomorphology, The Wolman Volume, pp. 83-101. Geophysical Monograph 99, American Geophysical Union,

Harvey, A.M., 1997. Coupling between hillslope gully systems and stream channels in the Howgill Fells, northwest England: temporal implications. Geomorphologie: Relief, Processes, Environment 1:3-20.

Harvey, A.M., 2001. Coupling between hillslopes and channels in upland fluvial systems: implications for landscape sensitivity, illustrated from the Howgill Fels, northwest England. Catena 42:225-250.

Harvey, A.M., 2002. Effective timescales of coupling within fluvial systems. Geomorphology 44:175-201.

Heathwaite, A.L. 2003. Making process-based knowledge usable at operational level: a framework for modelling diffuse pollution from agricultural land. Environmental Modelling and software Volume 18, Issues 8-9, October-November 2003, Pages 753-760.

Heathwaite A.L., Quinn P.F., and Hewett C.J.M. 2005 .Modelling and managing critical source areas of diffuse pollution from agricultural land using flow connectivity simulation. *J. of Hydrology* 304: 446-461

Hooke, J., 2003. Coarse sediment connectivity in river channel systems: a conceptual framework and methodology. *Geomorphology* 56:79-94.

Kronvang, B., Vagstad, N., Behrendt, H., Bøgestrand, J., Larsen, S.E., 2007. Phosphorus losses at the catchment scale within Europe: an overview. *Soil Use Manage.* 23 (Suppl. 1) 104-116.

Kishi, T., Mori, A., Hasegawa, K., and Kuroki, M., 1987. Bed configurations and sediment transports in mountainous rivers. In: Comparative Hydrology of Rivers of Japan. Final Report, pp. 165-176, Japanese Research Group of Comparative Hydrology, Hokkaido University, Sapporo, Japan.

Lerner, D.N., 2003. Surface water-groundwater interactions in the context of groundwater resources, *in* Xu, Y. and Beekman, H.E., editors, Groundwater recharge estimation in Southern Africa: UNESCO IHP Series no. 64, p. 91-107.

Le Roux P.A.L., Fraenkel, C.H., Bothma, C.B., Gutter, J.H., and Du Preez, C.C. (2006) Soil survey report: Mkabela Catchment. Dept. of Soil, Crop and Climatic Sciences, University of Free State, Bloemfontein. RSA.

Lorentz, S., Bursey, K., Idowu, O., Pretorius, J. and Ngaleka, K. 2008. Definition and upscaling of key hydrological processes for application in models. WRC Report 1320/1/08. Water Research Commission, Pretoria, South Africa.

Meerkerk, A.L., van Weselmael, B., and Bellin, N. 2009. Application of connectivity theory to model the impact of terrace failure on runoff in semi-arid catchments. *Hydrol. Process*. 23:2792-2803.

Montgomery, D.R. and Buffington, J.M., 1993. Channel classification, prediction of channel response, and assessment of channel conditions. Washington State Timber, Fish, and Wildlife, Report TFW-SH10-93-002.

Ocampo C.J., Sivapalan, M. and Oldham, C. 2006. Hydrological connectivity of upland-riparian zones in agricultural catchments: Implications for runoff generation and nitrate transport. *J. of Hydrology* 331:643-658.

Pfister, L., McDonnell, J.J., Wrede, S., Hlúbikovák, D., Matgen, P., Fenicia, F., Ector, L. and Hoffman, L. 2009. The rivers are alive: on the potential for diatoms as a tracer of water source and hydrological connectivity. *Hydrol. Process.* 23:2841-2845.

Payraudeau, S., Junker, P., Imfeld, G. And Gregorie, C. 2009. Characterising hydrological connectivity to identify critical source areas for pesticide losses. 18th World IMACS/MODSIM Congress, Cairns, Australia 13-17 July 2009. http://mssanz.org.au/modsim09

Shepherd, B., Harper, D. and Millington, A. 1999. Modelling catchment- scale nutrient transport to watercourses in the U.K. *Hydrobiologia*, Volumes 395-396, February 1999, pp. 227-238 (12).

Stieglitz, M., Shaman, J., McNamara, J., Engel, V., Shanley, J. and Kling, G.W. 2003. An approach to understanding hydrologic connectivity on the hillslope and the implications for nutrient transport. *Global Biogeochem. Cycles* 17(4):16.1-16.15.

Tromp-van Meerveld H.J. and McDonnell, J.J., 2006. Threshold relations in subsurface stormflow: 2. The fill and spill hypothesis. Water Resour. Res. 42(W02411).

Wenninger, J., Uhlenbrook, S., Lorentz, S. and Leibundgut, C. 2008. Identification of runoff generation processes using combined hydrometric, tracer and geophysical methods in a headwater catchment in South Africa. Hydrological Sciences Journal. 53(1):65-80.

Withers, P.J.A., Ulen, B., Stamm, C., Bechmann, M., 2003. Incidental phosphorus loss – is it significant and can it be predicted. *J. Soil Science and Plant Nutrition* 166, 459-468.

APPENDIX A
SEDIMENT FINGER PRINTING RESULTS

Table A1. Samples collected from cores during the excursion of 28-30 May 2008 and 3 June 2008 (WET samples).

Core samples			
Name	**Depth**		
R1-C1-A	0 -22		
R1-C1-B			
R1-C1-C			
R2-C1-D	87 -117		
R1-C1-E	117 -140		
WT1-C2-A			
WT2-C1-B			
WT1-C2-C	0 -99		
WT1-C2-D	99 -130		
WT1-C1-A	0 -33		
WT1-C1-B			
WT1-C1-C	46 -98		
WT-C1-D			
WET4	0 -340	03-Jun-08	
WET4	340 -660	03-Jun-08	
WET4	660 -1000	03-Jun-08	
WET4	1000 -1300	03-Jun-08	
WET4	1300-1310	03-Jun-08	
HS1	0 -340	03-Jun-08	
HS1	340 -600	03-Jun-08	
HS1	600 -980	03-Jun-08	
HS1	980 -1050	03-Jun-08	
mineralized sandstone from vegetable patch			03-Jun-08

Table A2 Samples collected from the surface during the excursion of 28-30 May 2008.

Bottled Samples					
Name	**Land Use**	**Soil**	**name**	**Land Use**	**Soil**
Av-1	Cane	Avalon	Rd 1	Road	
Av-2	Cane	Avalon	Rd 2	Road	
Av-3	Cane	Avalon	B-1		
Av-4	Cane	Avalon	B-2		
Av-5	Cane	Avalon	B-3		
Av-6	Cane	Avalon	B-4		
Av-7	Cane	Avalon	B-5		
Av-8	Cane	Avalon	B-6		
Av-9	Cabbage	Avalon	B-7		
Av-10	Veg. Bare	Avalon	B-8		
Wt-1	Wattle		B-9		
Wt-2	Wattle		B-10		
Wt-3	Wattle		C-1	Cane	
Wt-4	Wattle		C-2	Cane	
Wt-5	Wattle		C-3	Cane	
Wt-6	Wattle		C-4	Cane	
We-1	Cane	Westleigh	C-5	Cane	
We-2	Cane	Westleigh	C-6	Cane	
We-3	Cane	Westleigh	C-7	Cane	
We-4	Corn	Westleigh	C-8	Cane	
We-5	Cane	Westleigh	C-9	Cane	
We-6	Veg, bare	Westleigh	C-10	Cane	
We-7	Corn	Westleigh	C-11	Cane	
We-8	Corn	Westleigh	C-12	Cane	
We-9	Veg, bare	Westleigh	C-13	Cane	
Lo-1	Cane	Longlands	C-14	Cane	
Lo-2	Cane	Longlands	Ka-1	Corn	Katspruit
Lo-3	Pasture	Longlands	Ka-2	Corn	Katspruit
Lo-4	Cane	Longlands	Ka-3	Corn	Katspruit
Lo-5	Cane	Longlands	Ka-4	Cane	Katspruit
Rd 1 (3-Jun-2008)	Road		Ka-5	Cabbage	Katspruit
Rd 2 (3-Jun-2008)	Road		Ka-6	Cabbage	Katspruit
Rd 3 (3-Jun-2008)	Road		CD-1		
Rd 4 (3-Jun-2008)	Road		CD-2		
Rd 5 (3-Jun-2008)	Road		Cv-1	Cane	Clovelly
Rd 6 (3-Jun-2008)	Road		Cv-2	Cane	Clovelly
Rd 7 (3-Jun-2008)	Road		Cv-3	Cane	Clovelly
Rd 8 (3-Jun-2008)	Road		Bf-1		
T-1	tillite		Bf-2		

Table A3: Results of initial surface sampling: May 2007: Elements.

Lab#	Sample Name	Moistures	Co	*Co(ppm)*	Ni	*Ni(ppm)*	Cu	*Cu(ppm)*	Zn	*Zn(ppm)*	Ga	*Ga(ppm)*
		%	ppm	*(dry basis)*	ppm	*(dry basis)*	ppm	*(dry basis)*	ppm	*(dry basis)*	ppm	*(dry basis)*
SA6	*Gory farm bare soil*	1.73	18.8	*19.1*	43.1	*43.8*	182.1	*185.3*	376.5	*383.1*	9.8	*10.0*
SA7	*Gory farm cabbage*	7.38	15.3	*16.6*	37.4	*40.4*	158.2	*170.8*	340.3	*367.4*	7.5	*8.1*
SA8	*Gory farm cabbage #2*	8.73	11.6	*12.7*	29.1	*31.9*	130.0	*142.5*	304.8	*334.0*	5.5	*6.0*
SA9	*Gory farm cabbage #3*	8.21	9.7	*10.5*	25.4	*27.7*	113.1	*123.2*	245.2	*267.1*	4.3	*4.7*
SA10	*Cane #4*	0.09	1.0	*1.0*	6.1	*6.1*	36.9	*36.9*	70.9	*71.0*	0.7	*0.7*
SA11	*Cane #5*	0.05	1.2	*1.2*	6.4	*6.4*	41.7	*41.7*	64.6	*64.6*	1.6	*1.6*
SA12	*Runoff plot 2-F1*	1.63	3.4	*3.5*	15.4	*15.7*	52.7	*53.6*	80.6	*82.0*	4.2	*4.2*
SA13	*Runoff plot 2-F2*	1.35	6.0	*6.1*	17.7	*17.9*	61.2	*62.1*	104.8	*106.3*	4.8	*4.9*
SA14	*Runoff plot 2-F3*	0.20	2.9	*2.9*	8.8	*8.8*	49.1	*49.2*	76.8	*77.0*	2.6	*2.6*
SA15	*Forest (pines) #1*	0.23	3.2	*3.2*	8.1	*8.2*	53.7	*53.9*	96.0	*96.3*	3.2	*3.2*
SA16	*Forest #2*	1.89	3.3	*3.4*	9.2	*9.4*	53.3	*54.3*	92.5	*94.3*	3.4	*3.5*
SA17	*Wetland downstream channel*	30.71	7.1	*10.3*	15.0	*21.6*	46.7	*67.4*	83.8	*120.9*	4.2	*6.1*
SA18	*Channel wetland*	24.01	8.6	*11.3*	14.7	*19.3*	29.0	*38.2*	56.7	*74.7*	2.5	*3.3*

Lab#	Sample Name	As ppm	*As(ppm) (dry basis)*	Y ppm	*Y(ppm) (dry basis)*	Mo ppm	*Mo(ppm) (dry basis)*	Sn ppm	*Sn(ppm) (dry basis)*	W ppm	*W(ppm) (dry basis)*	Tl ppm	*Tl(ppm) (dry basis)*
SA6	*Gory farm bare soil*	10.7	*10.9*	24.3	*24.8*	4.8	*4.9*	5.4	*5.5*	1.74	*1.8*	0.43	*0.4*
SA7	*Gory farm cabbage*	10.1	*10.9*	17.9	*19.3*	4.7	*5.1*	4.6	*5.0*	1.42	*1.5*	0.40	*0.4*
SA8	*Gory farm cabbage #2*	9.2	*10.1*	19.6	*21.5*	4.0	*4.4*	3.9	*4.2*	1.14	*1.3*	0.33	*0.4*
SA9	*Gory farm cabbage #3*	7.8	*8.5*	18.1	*19.8*	4.0	*4.3*	3.4	*3.7*	1.03	*1.1*	0.30	*0.3*
SA10	*Cane #4*	2.1	*2.1*	7.4	*7.4*	0.9	*0.9*	0.3	*0.3*	0.11	*0.1*	0.08	*0.1*
SA11	*Cane #5*	2.8	*2.8*	7.0	*7.0*	0.8	*0.8*	0.3	*0.3*	0.07	*0.1*	0.09	*0.1*
SA12	*Runoff plot 2-F1*	5.1	*5.2*	10.2	*10.4*	1.6	*1.6*	1.2	*1.2*	0.37	*0.4*	0.26	*0.3*
SA13	*Runoff plot 2-F2*	8.7	*8.8*	13.7	*13.9*	2.5	*2.6*	2.0	*2.0*	0.53	*0.5*	0.24	*0.2*
SA14	*Runoff plot 2-F3*	4.1	*4.1*	8.5	*8.5*	1.3	*1.3*	0.7	*0.7*	0.28	*0.3*	0.16	*0.2*
SA15	*Forest (pines) #1*	5.4	*5.4*	7.4	*7.4*	1.8	*1.9*	3.6	*3.6*	0.30	*0.3*	0.17	*0.2*
SA16	*Forest #2*	6.3	*6.4*	7.1	*7.3*	1.8	*1.9*	0.9	*0.9*	0.32	*0.3*	0.17	*0.2*
SA17	*Wetland downstream channel*	5.7	*8.3*	12.8	*18.5*	2.2	*3.2*	1.6	*2.3*	0.47	*0.7*	0.22	*0.3*
SA18	*Channel wetland*	11.2	*14.7*	19.8	*26.1*	2.2	*2.9*	1.6	*2.1*	0.55	*0.7*	0.22	*0.3*

Lab#	Sample Name	Pb ppm	*Pb(ppm) (dry basis)*	Bi ppm	*Bi(ppm) (dry basis)*	*Pb 206/208*	*Pb 207/208*	*Pb 206/207*	Mo ppm	*Mo(ppm) (dry basis)*	Sn ppm	*Sn(ppm) (dry basis)*
SA6	*Gory farm bare soil*	28.9	*29.4*	0.166	*0.169*	*0.491*	*0.407*	*1.207*	4.8	*5.0*	5.4	*5.6*
SA7	*Gory farm cabbage*	24.5	*26.4*	0.144	*0.155*	*0.469*	*0.400*	*1.174*	4.7	*4.9*	4.6	*4.8*
SA8	*Gory farm cabbage #2*	22.3	*24.4*	0.116	*0.127*	*0.482*	*0.405*	*1.192*	4.0	*4.2*	3.9	*4.0*
SA9	*Gory farm cabbage #3*	19.6	*21.3*	0.098	*0.106*	*0.482*	*0.406*	*1.186*	4.0	*4.1*	3.4	*3.5*
SA10	*Cane #4*	5.6	*5.6*	0.020	*0.020*	*0.476*	*0.387*	*1.229*	0.9	*0.9*	0.3	*0.3*
SA11	*Cane #5*	5.6	*5.6*	0.014	*0.014*	*0.455*	*0.378*	*1.206*	0.8	*0.8*	0.3	*0.3*
SA12	*Runoff plot 2-F1*	10.6	*10.8*	0.041	*0.042*	*0.489*	*0.406*	*1.204*	1.6	*1.6*	1.2	*1.2*
SA13	*Runoff plot 2-F2*	10.8	*11.0*	0.048	*0.049*	*0.483*	*0.404*	*1.197*	2.5	*2.6*	2.0	*2.1*
SA14	*Runoff plot 2-F3*	7.1	*7.2*	0.023	*0.023*	*0.476*	*0.396*	*1.202*	1.3	*1.3*	0.7	*0.7*
SA15	*Forest (pines) #1*	8.7	*8.7*	0.031	*0.031*	*0.476*	*0.409*	*1.164*	1.8	*1.9*	3.6	*3.7*
SA16	*Forest #2*	10.5	*10.7*	0.027	*0.027*	*0.477*	*0.410*	*1.162*	1.8	*1.9*	0.9	*0.9*
SA17	*Wetland downstream channel*	10.5	*15.2*	0.051	*0.073*	*0.479*	*0.398*	*1.203*	2.2	*2.3*	1.6	*1.6*
SA18	*Channel wetland*	12.6	*16.6*	0.059	*0.078*	*0.487*	*0.406*	*1.200*	2.2	*2.3*	1.6	*1.6*

Lab#	Sample Name	W ppm	*W(ppm) (dry basis)*	Tl ppm	*Tl(ppm) (dry basis)*	Pb ppm	*Pb(ppm) (dry basis)*	Bi ppm	*Bi(ppm) (dry basis)*	*Pb 206/208*	*Pb 207/208*	*Pb 206/207*
SA6	*Gory farm bare soil*	1.74	*1.8*	0.43	*0.5*	28.9	*30.4*	0.166	*0.175*	*0.491*	*0.407*	*1.207*
SA7	*Gory farm cabbage*	1.42	*1.5*	0.40	*0.4*	24.5	*25.7*	0.144	*0.151*	*0.469*	*0.400*	*1.174*
SA8	*Gory farm cabbage #2*	1.14	*1.2*	0.33	*0.3*	22.3	*23.2*	0.116	*0.120*	*0.482*	*0.405*	*1.192*
SA9	*Gory farm cabbage #3*	1.03	*1.1*	0.30	*0.3*	19.6	*20.4*	0.098	*0.102*	*0.482*	*0.406*	*1.186*
SA10	*Cane #4*	0.11	*0.1*	0.08	*0.1*	5.6	*5.6*	0.020	*0.020*	*0.476*	*0.387*	*1.229*
SA11	*Cane #5*	0.07	*0.1*	0.09	*0.1*	5.6	*5.6*	0.014	*0.014*	*0.455*	*0.378*	*1.206*
SA12	*Runoff plot 2-F1*	0.37	*0.4*	0.26	*0.3*	10.6	*10.8*	0.041	*0.042*	*0.489*	*0.406*	*1.204*
SA13	*Runoff plot 2-F2*	0.53	*0.5*	0.24	*0.3*	10.8	*11.1*	0.048	*0.049*	*0.483*	*0.404*	*1.197*
SA14	*Runoff plot 2-F3*	0.28	*0.3*	0.16	*0.2*	7.1	*7.2*	0.023	*0.023*	*0.476*	*0.396*	*1.202*
SA15	*Forest (pines) #1*	0.30	*0.3*	0.17	*0.2*	8.7	*8.9*	0.031	*0.032*	*0.476*	*0.409*	*1.164*
SA16	*Forest #2*	0.32	*0.3*	0.17	*0.2*	10.5	*10.7*	0.027	*0.027*	*0.477*	*0.410*	*1.162*
SA17	*Wetland downstream channel*	0.47	*0.5*	0.22	*0.2*	10.5	*10.8*	0.051	*0.052*	*0.479*	*0.398*	*1.203*
SA18	*Channel wetland*	0.55	*0.6*	0.22	*0.2*	12.6	*12.9*	0.059	*0.061*	*0.487*	*0.406*	*1.200*

Table A4: results of initial surface sampling: May 2007. Major species.

(Lab #)	**Sample**	ICP-OES **CaO(%)**	**CaO(%) (Dry basis)**	ICP-OES **Fe_2O_3(%)**	**Fe_2O_3(%) (Dry basis)**	ICP-OES **K_2O(%)**	**K_2O(%) (Dry basis)**	ICP-OES **MgO(%)**	**MgO(%) (Dry basis)**	ICP-OES **Na_2O(%)**	**Na_2O(%) (Dry basis)**	Moisture wt.%
SA-6	*Gory farm bare soil*	0.469	*0.48*	7.75	*7.89*	0.307	*0.31*	0.435	*0.44*	0.135	*0.14*	1.73
SA-7	*Gory farm cabbage*	0.472	*0.51*	7.41	*8.00*	0.403	*0.44*	0.439	*0.47*	0.133	*0.14*	7.38
SA-8	*Gory farm cabbage #2*	0.391	*0.43*	6.34	*6.94*	0.400	*0.44*	0.398	*0.44*	0.098	*0.11*	8.73
SA-9	*Gory farm cabbage #3*	0.343	*0.37*	5.58	*6.07*	0.464	*0.51*	0.345	*0.38*	0.085	*0.09*	8.21
SA-10	*Cane #4*	0.160	*0.16*	0.859	*0.86*	0.114	*0.11*	0.172	*0.17*	0.024	*0.02*	0.09
SA-11	*Cane #5*	0.158	*0.16*	0.884	*0.88*	0.121	*0.12*	0.140	*0.14*	0.001	*0.00*	0.05
SA-12	*Runoff plot 2-F1*	0.295	*0.30*	0.974	*0.99*	0.411	*0.42*	0.277	*0.28*	0.036	*0.04*	1.63
SA-13	*Runoff plot 2-F2*	0.877	*0.89*	2.37	*2.40*	0.306	*0.31*	0.624	*0.63*	0.078	*0.08*	1.35
SA-14	*Runoff plot 2-F3*	0.303	*0.30*	1.07	*1.07*	0.209	*0.21*	0.220	*0.22*	0.042	*0.04*	0.20
SA-15	*Forest (pines) #1*	0.243	*0.24*	1.34	*1.34*	0.212	*0.21*	0.194	*0.19*	0.036	*0.04*	0.23
SA-16	*Forest #2*	0.458	*0.47*	1.26	*1.28*	0.206	*0.21*	0.222	*0.23*	0.034	*0.03*	1.89
SA-17	*Wetland downstream channel*	0.061	*0.09*	3.13	*4.52*	0.175	*0.25*	0.179	*0.26*	0.046	*0.07*	30.71
SA-18	*Channel wetland*	0.159	*0.21*	8.69	*11.43*	0.207	*0.27*	0.231	*0.30*	0.066	*0.09*	24.01

APPENDIX B

Time Series: Suspended solids, Nutrient and Isotope

B1 Suspended solids

B1.1 Suspended solids time series 2009

B1.1.1 Bridge 2, Bridge 1 and Dam Out

B1.1.2 Road crossing, Flume 2 and Flume 1

B1.1.3 Runoff plot 1, Runoff plot 2 and Groundwater

B1.2 Suspended solids time series 2010

B1.2.1 Bridge 2, Bridge 1 and Dam Out

B1.2.2 Road crossing, Flume 2 and Flume 1

B1.2.3 Runoff plot 1, Runoff plot 2 and Groundwater

B2 Nutrients

B2.1 NO_3 and P time series 2009

B2.1.1 Bridge 2, Bridge 1 and Dam Out

B2.1.2 Road crossing, Flume 2 and Flume 1

B2.1.3 Runoff plot 1, Runoff plot 2 and Groundwater

B2.2 NO_3 and P time series 2010

B2.2.1 Bridge 2, Bridge 1 and Dam Out

B2.2.2 Road crossing, Flume 2 and Flume 1

B2.2.3 Runoff plot 1, Runoff plot 2 and Groundwater

B3 Isotopes

B3.1 Isotope time series 2009

B3.1.1 Bridge 2, Bridge 1 and Dam Out

B3.1.2 Road crossing, Flume 2 and Flume 1

B3.1.3 Runoff plot 1, Runoff plot 2 and Groundwater

B3.2 Isotope time series 2010

B3.2.1 Bridge 2, Bridge 1 and Dam Out/Dam In

B3.2.2 Road crossing, Flume 2 and Flume 1

B3.2.3 Runoff plot 1, Runoff plot 2 and Groundwater

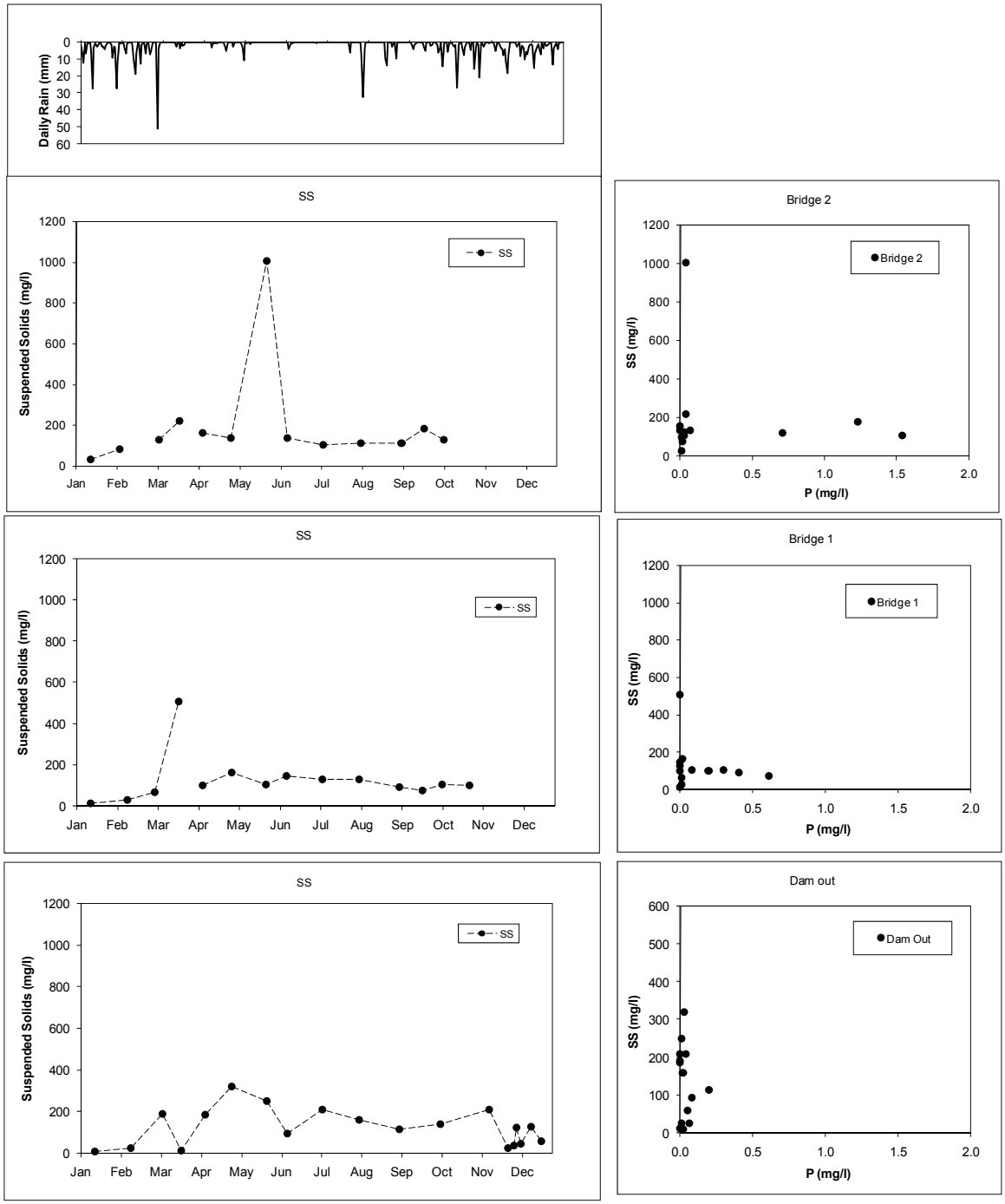

Figure B1.1.1 Rainfall and Suspended solids for 2009 at the monitoring stations: Bridge 2 (top), Bridge 1 (middle) and Dam Out (bottom) showing Suspended solids-P relationship (right).

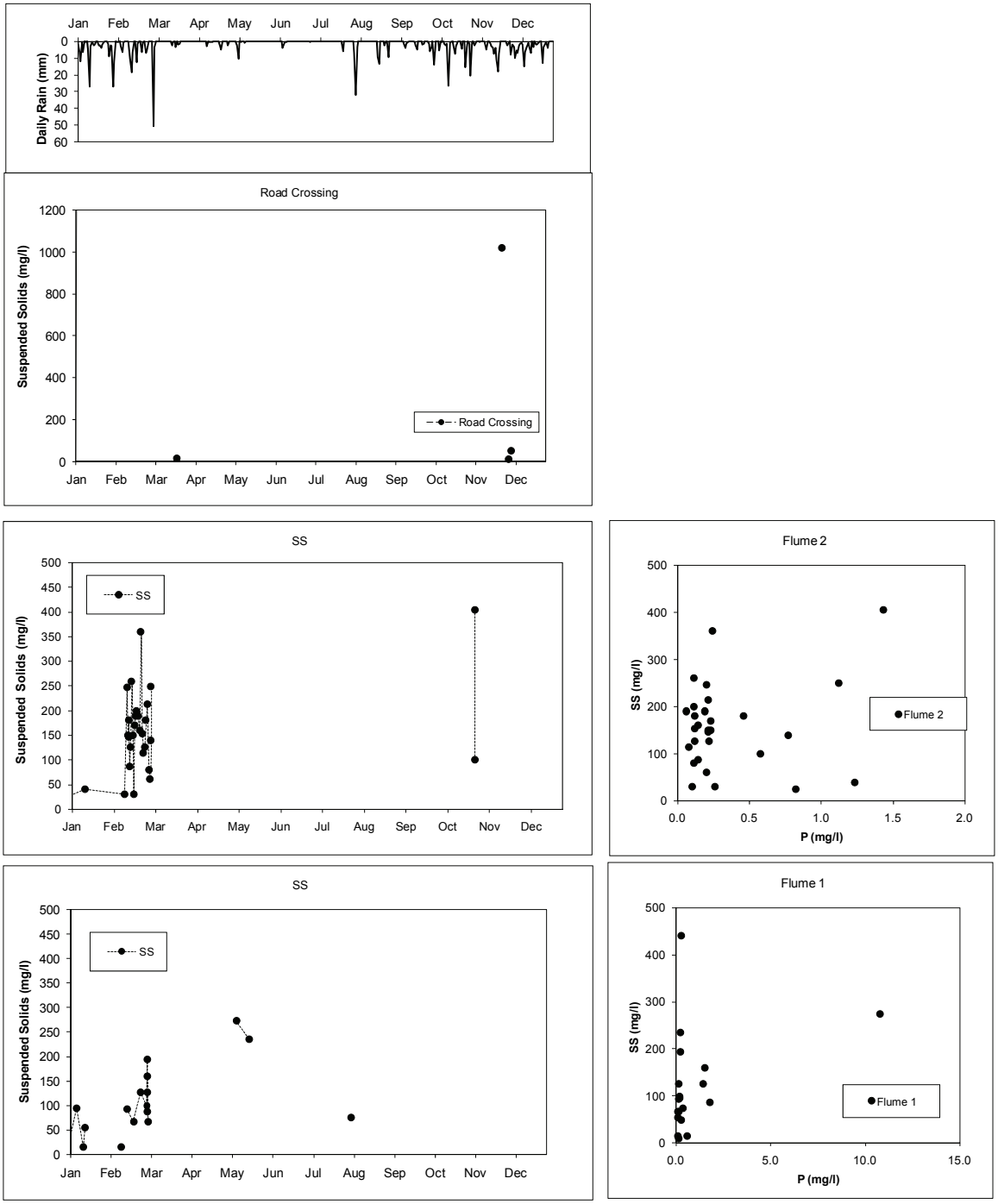

Figure B1.1.2 Rainfall and Suspended solids for 2009 at the monitoring stations: Road Crossing (top), Flume 2 (middle) and Flume 1 (bottom) showing Suspended solids-P relationship (right).

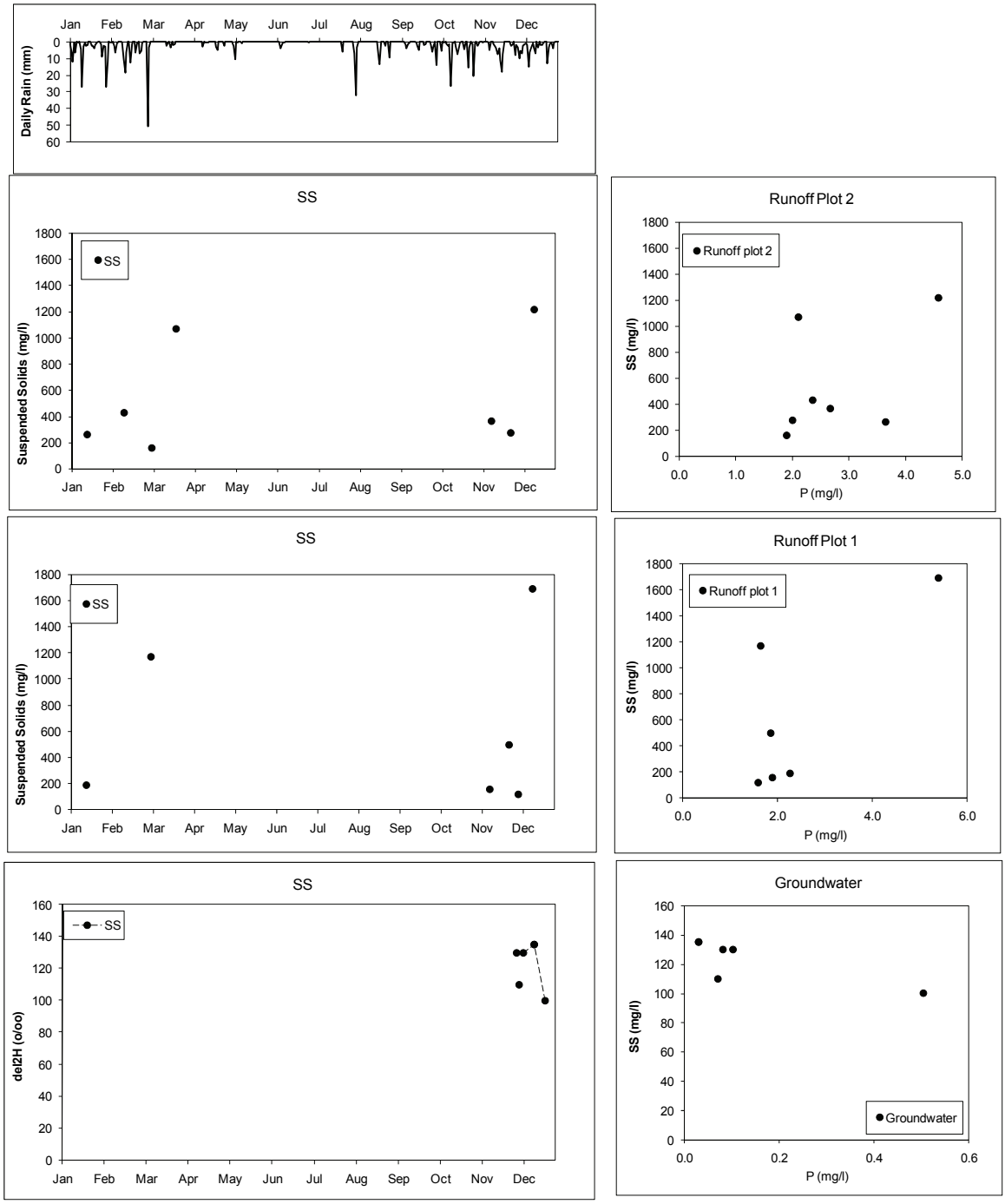

Figure B1.1.3 Rainfall and Suspended solids for 2009 at the monitoring stations: Runoff plot 2 (top), Runoff plot 1 (middle) and Groundwater (bottom) showing Suspended solids-P relationship (right).

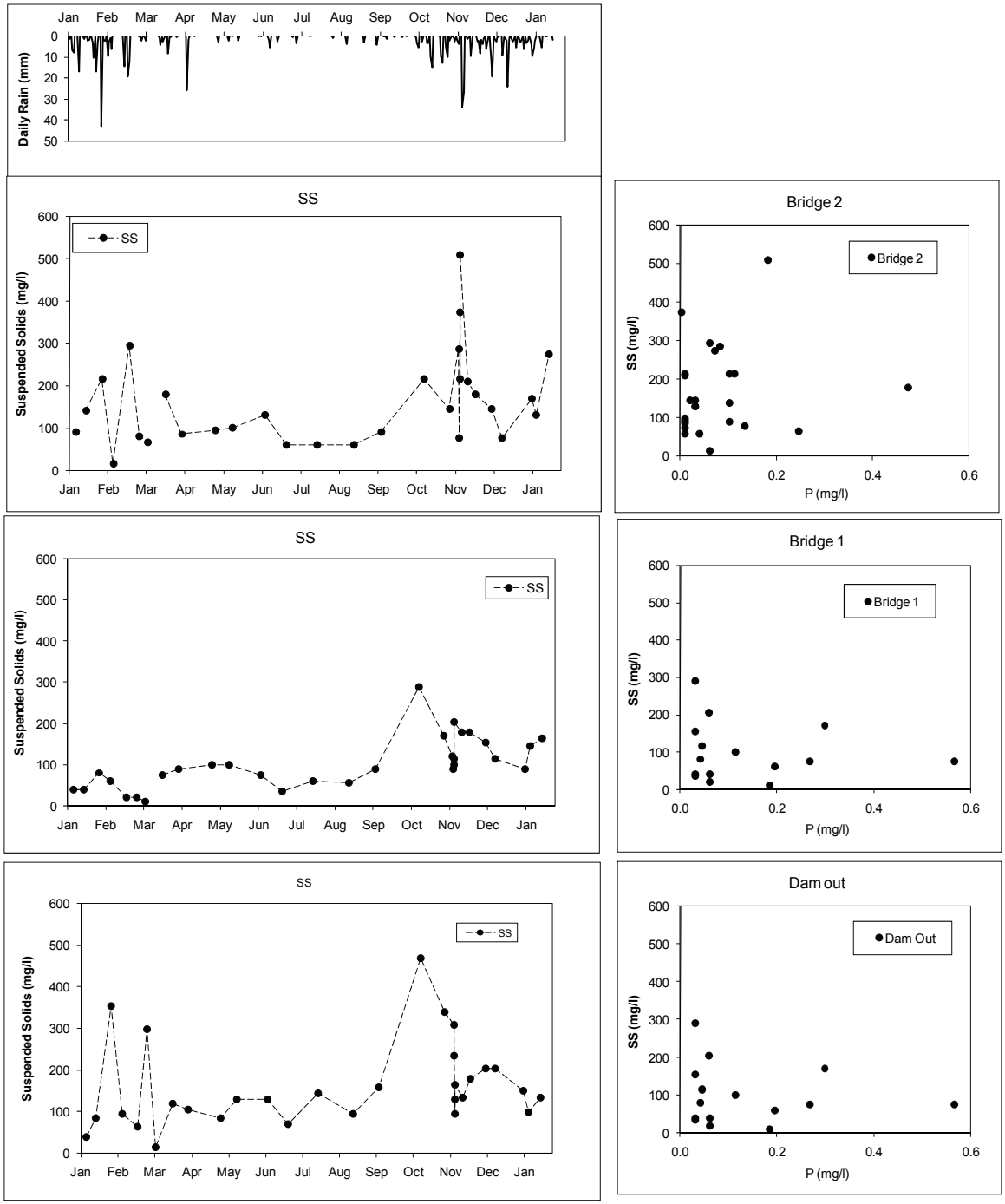

Figure B1.2.1 Rainfall and Suspended solids for 2010 at the monitoring stations: Bridge 2 (top), Bridge 1 (middle) and Dam Out (bottom) showing Suspended solids-P relationship (right).

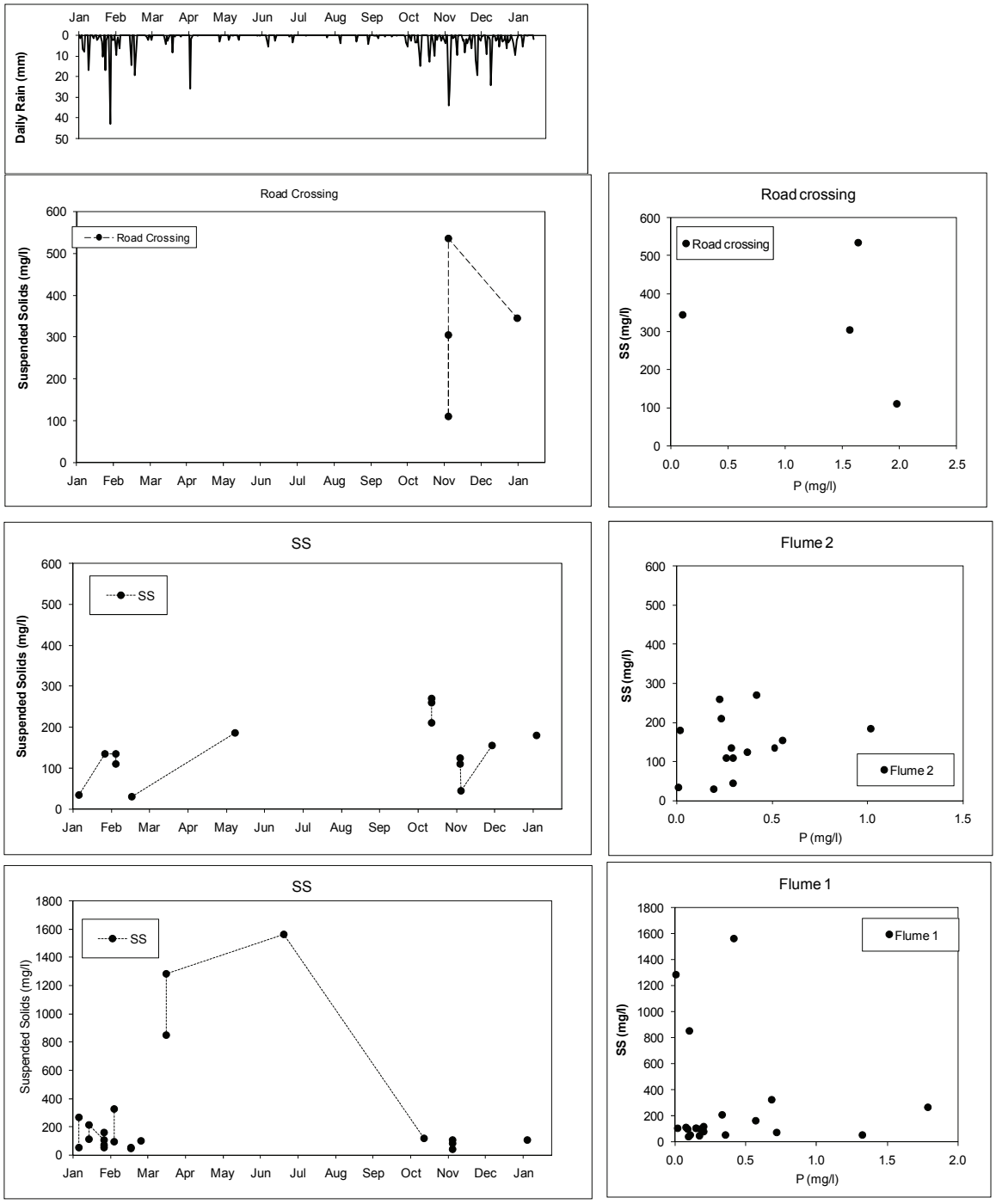

Figure B1.2.2 Rainfall and Suspended solids for 2010 at the monitoring stations: Road Crossing (top), Flume 2 (middle) and Flume 1 (bottom) showing Suspended solids-P relationship (right).

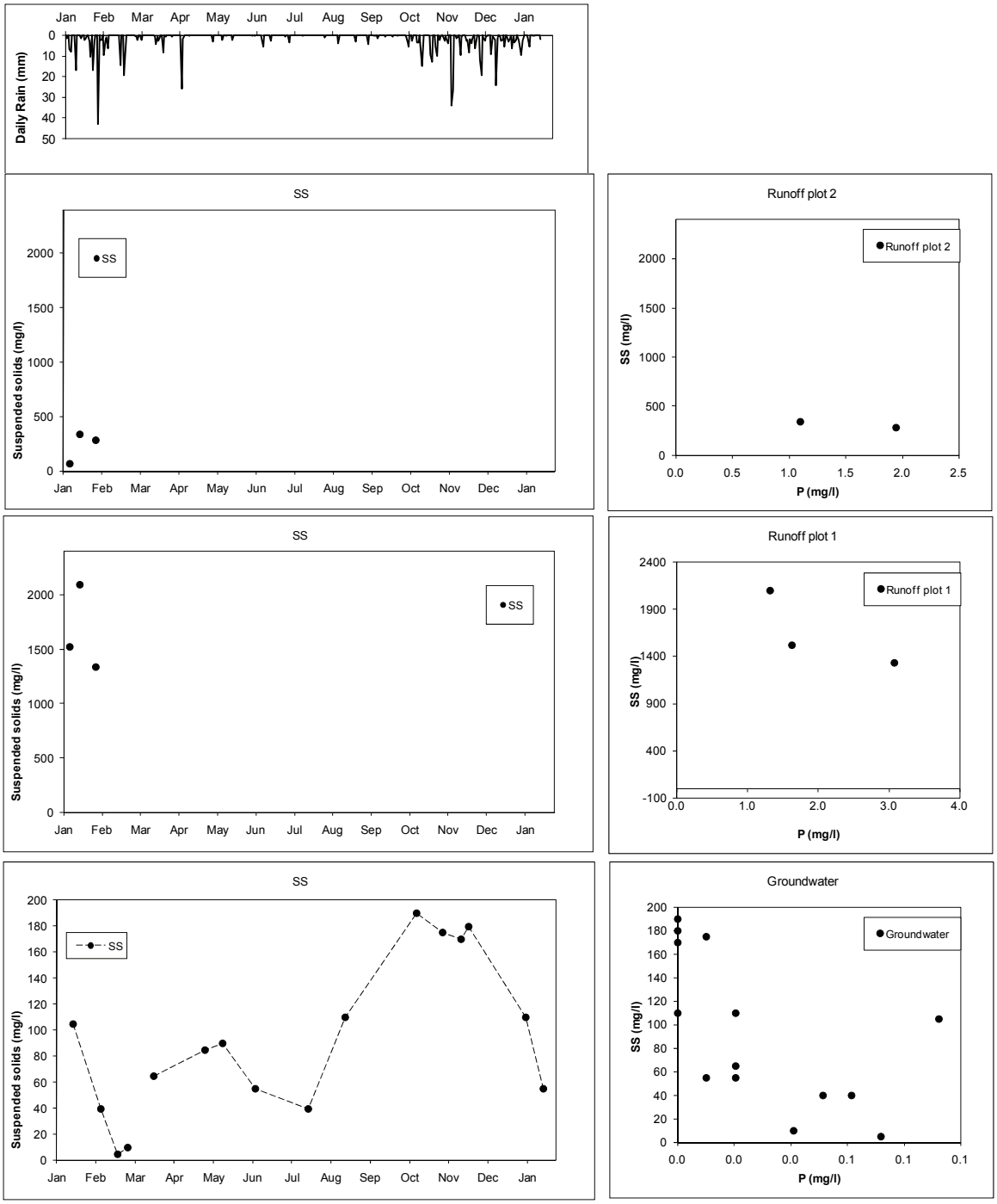

Figure B1.2.3 Rainfall and Suspended solids for 2010 at the monitoring stations: Runoff plot 2 (top), Runoff plot 1 (middle) and Groundwater (bottom) showing Suspended solids-P relationship (right).

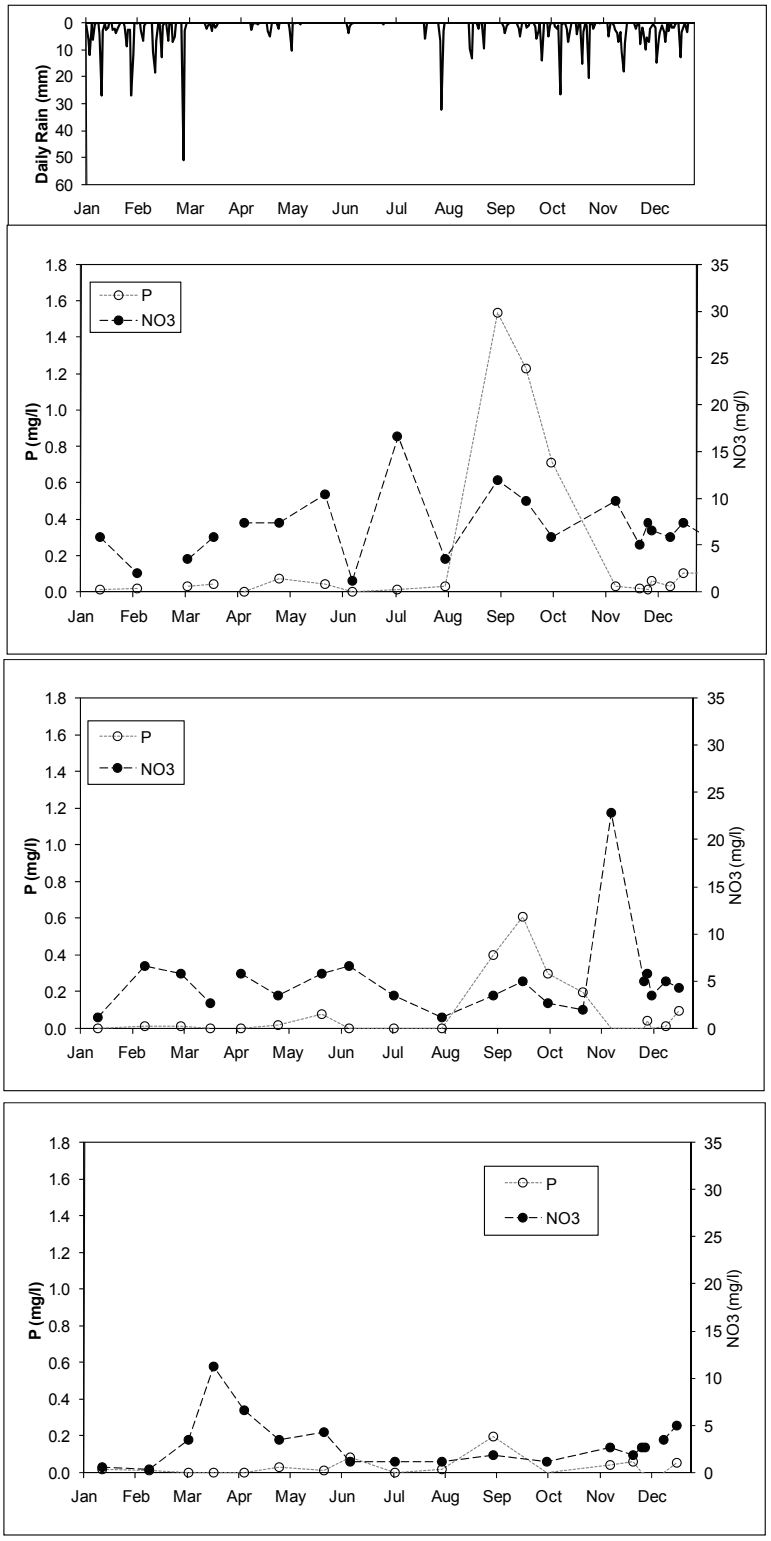

Figure B2.1.1 Rainfall, and NO_3 and P responses for 2009 at the monitoring stations: Bridge 2 (top), Bridge 1 (middle) and Dam Out (bottom).

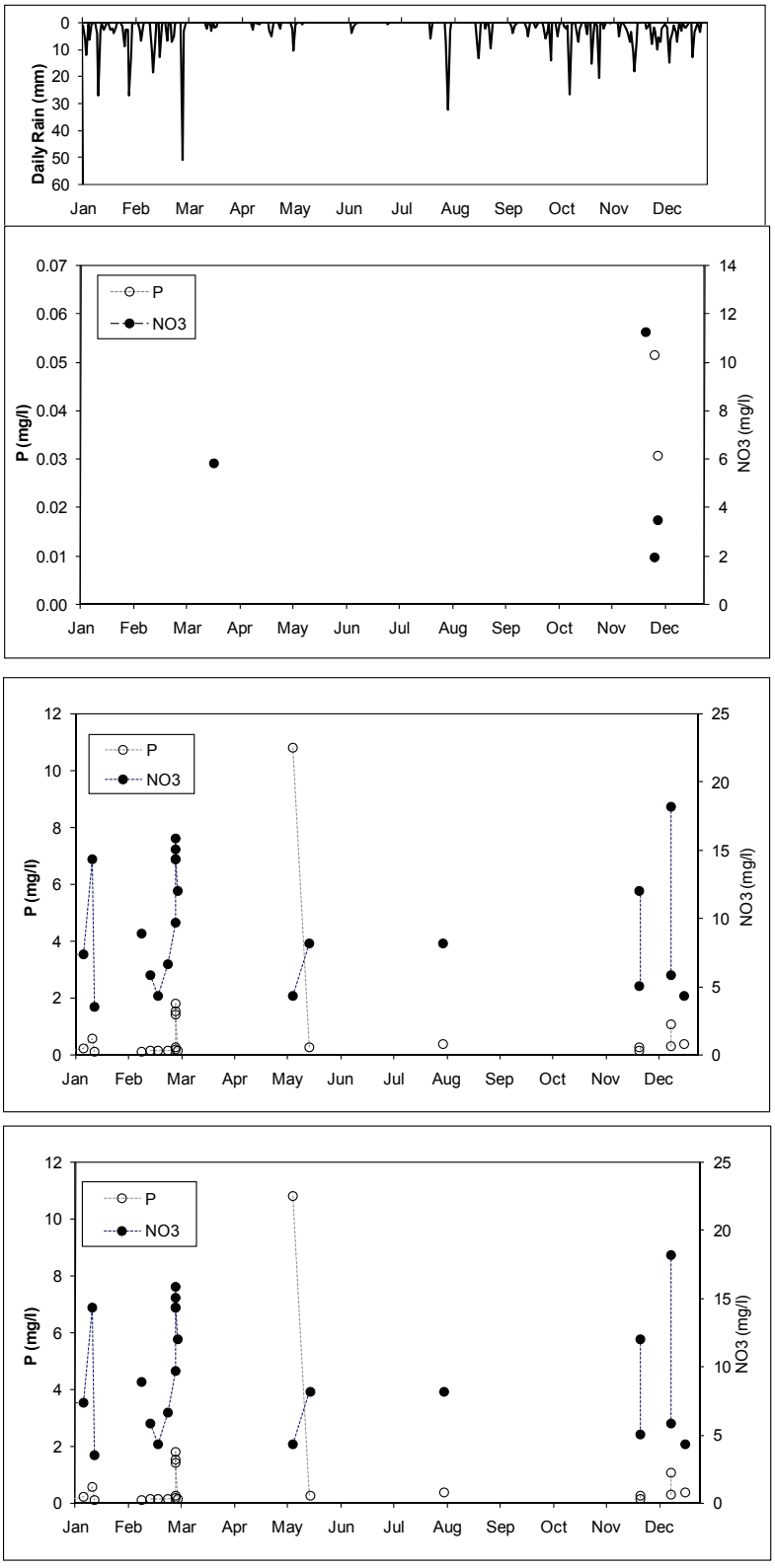

Figure B2.1.2 Rainfall, and NO_3 and P responses for 2009 at the monitoring stations: Road Crossing (top), Flume 2 (middle) and Flume 1 (bottom).

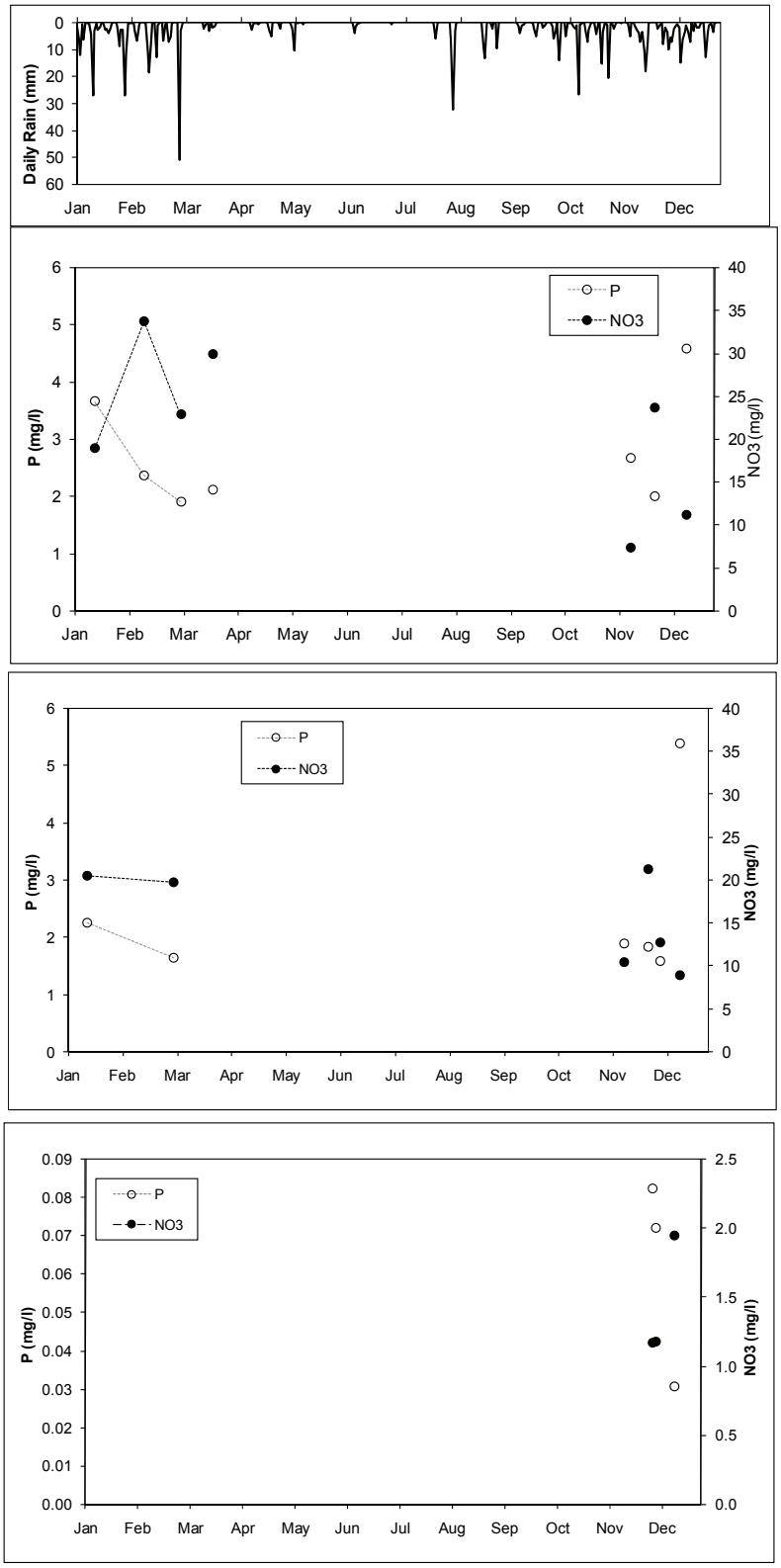

Figure B2.1.3 Rainfall, and NO_3 and P responses for 2009 at the monitoring stations: Runoff plot 2 (top), Runoff plot 1 (middle) and Groundwater (bottom).

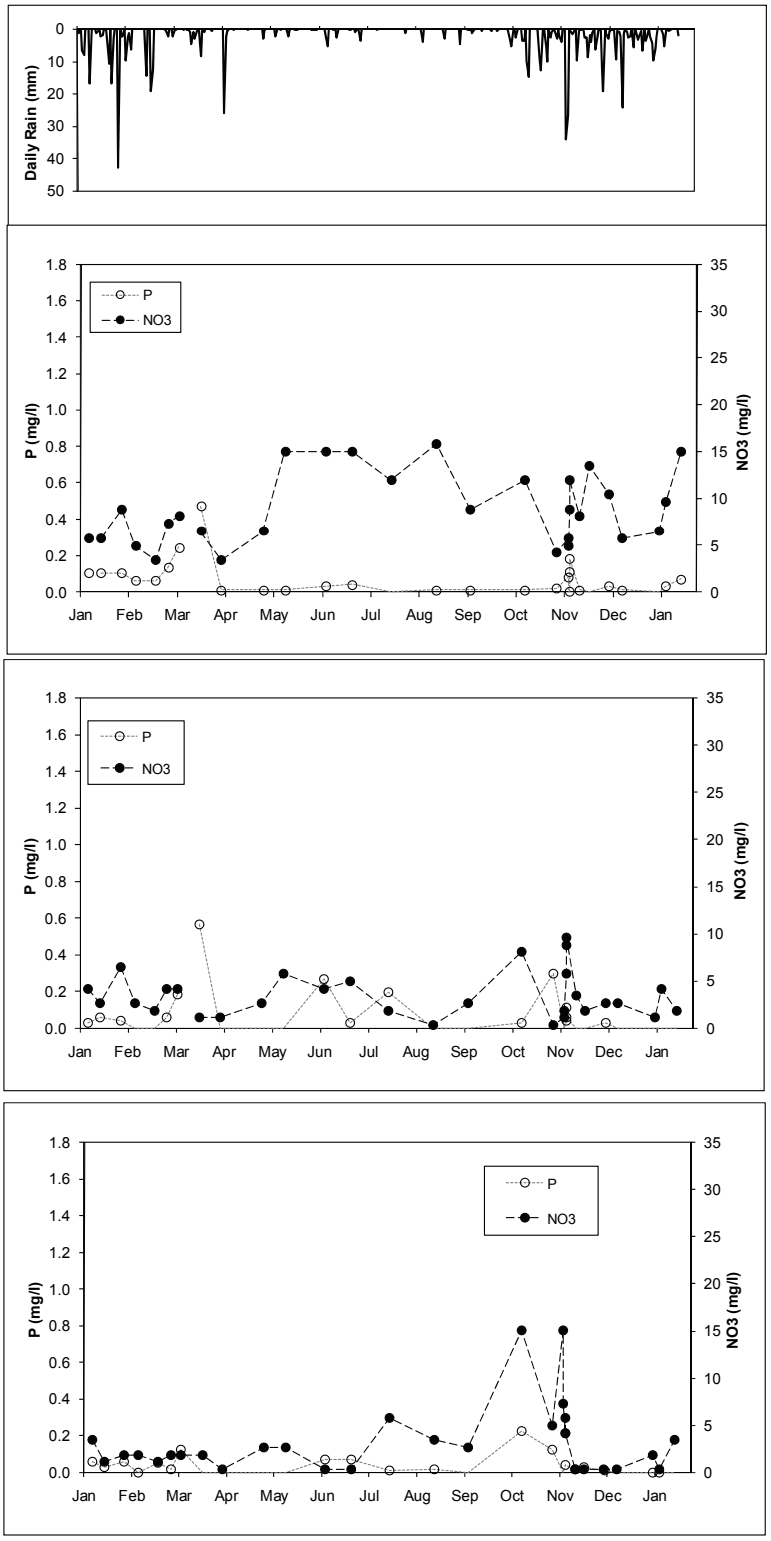

Figure B2.2.1 Rainfall, and NO_3 and P responses for 2010 at the monitoring stations: Bridge 2 (top), Bridge 1 (middle) and Dam Out (bottom).

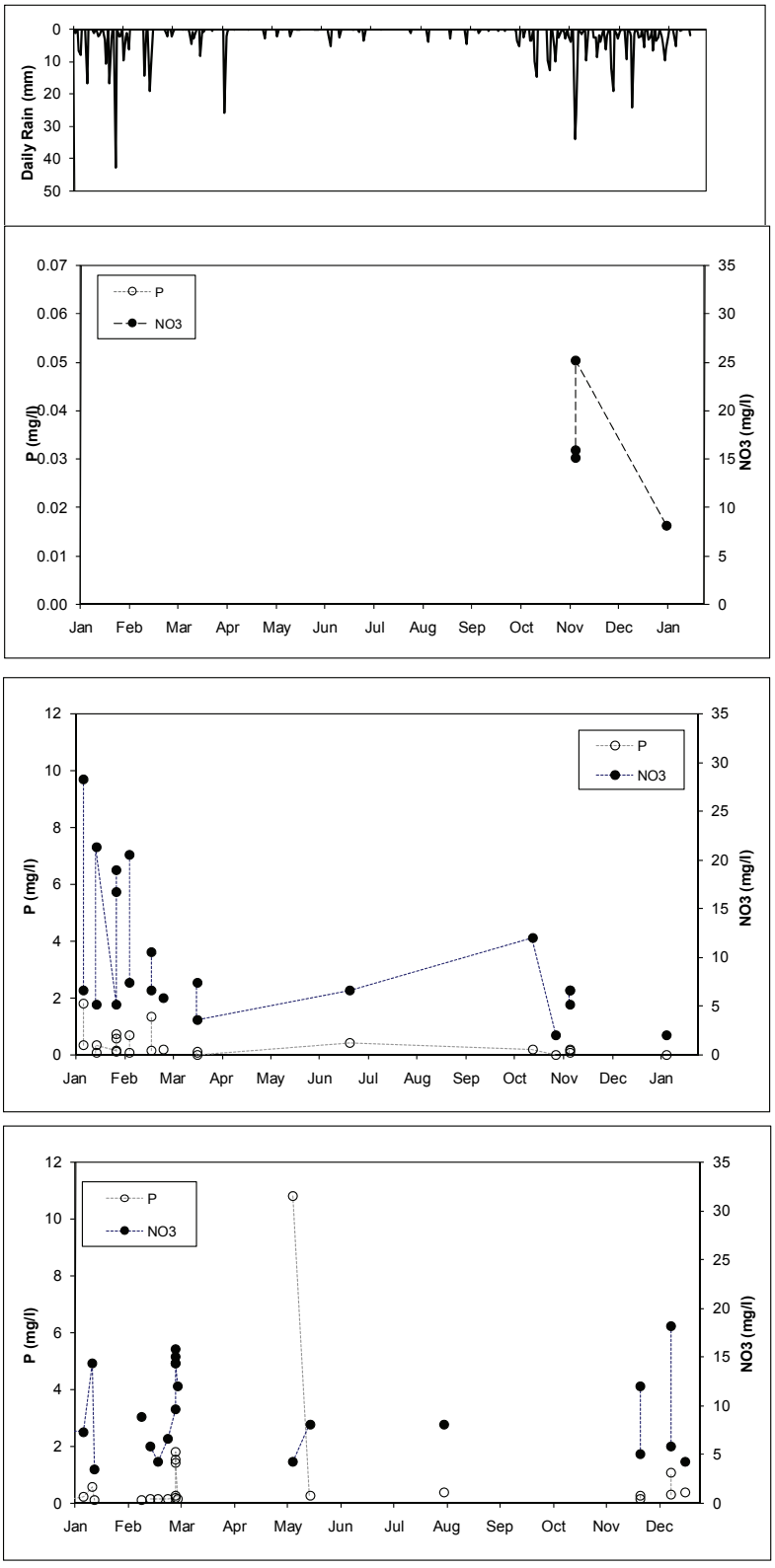

Figure B2.2.2 Rainfall, and NO_3 and P responses for 2010 at the monitoring stations: Road Crossing (top), Flume 2 (middle) and Flume 1 (bottom).

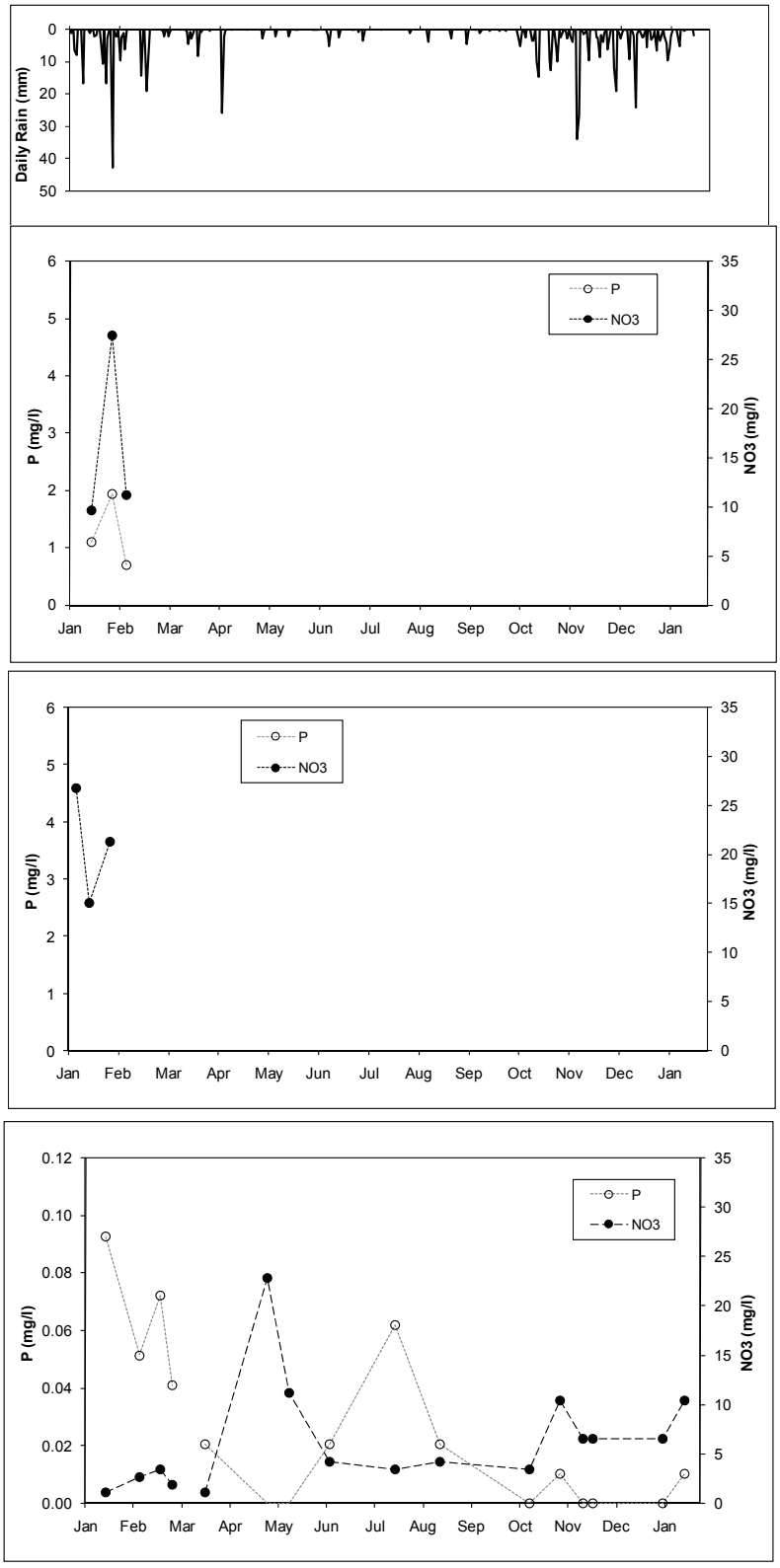

Figure B2.2.3 Rainfall, and NO_3 and P responses for 2010 at the monitoring stations: Runoff plot 2 (top), Runoff plot 1 (middle) and Groundwater (bottom).

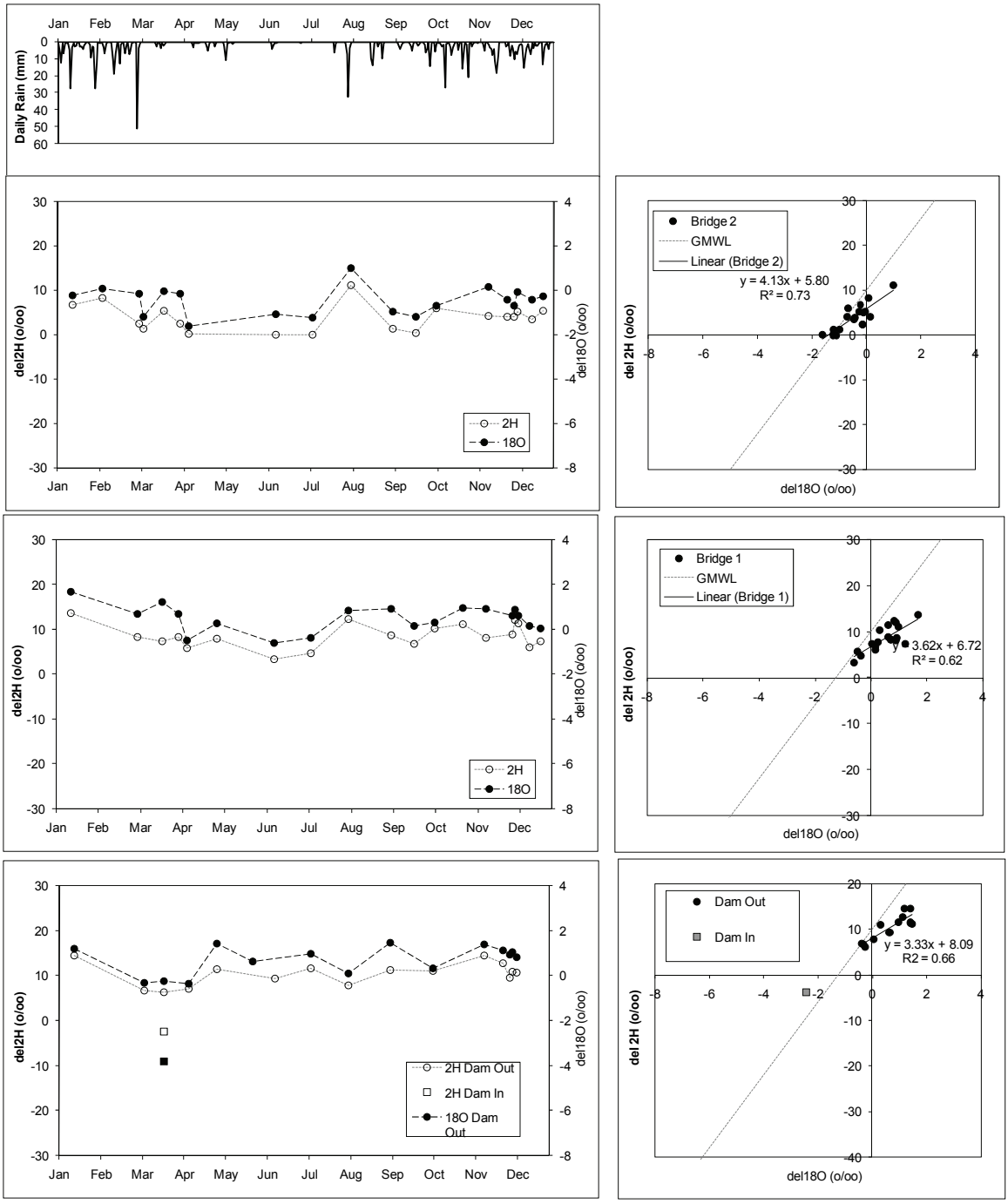

Figure B3.1.1 Rainfall and isotope responses for 2009 at the monitoring stations: Bridge 2 (top), Bridge 1 (middle) and Dam Out (bottom).

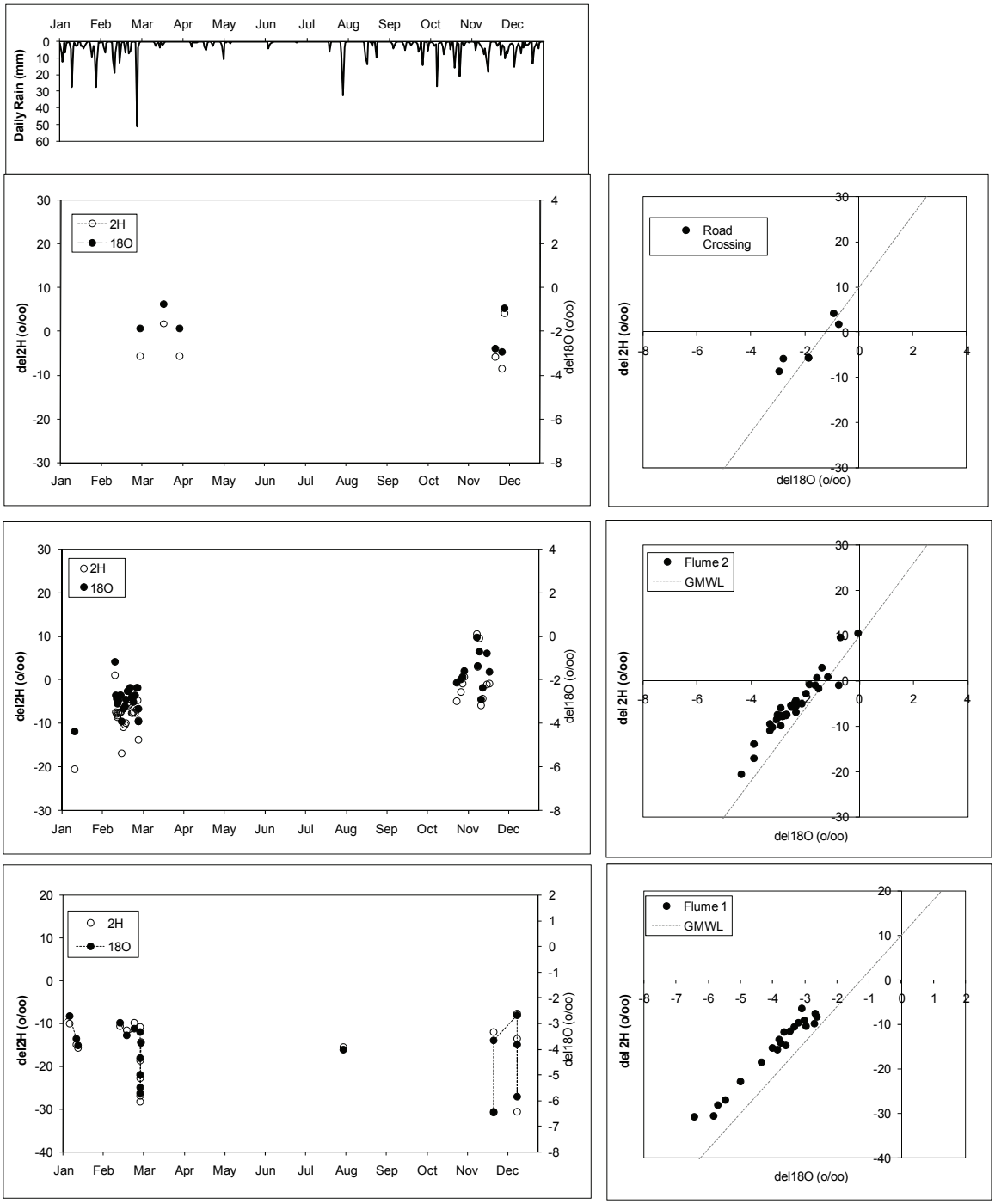

Figure B3.1.2 Rainfall and isotope responses for 2009 at the monitoring stations: Road Crossing (top), Flume 2 (middle) and Flume 1 (bottom).

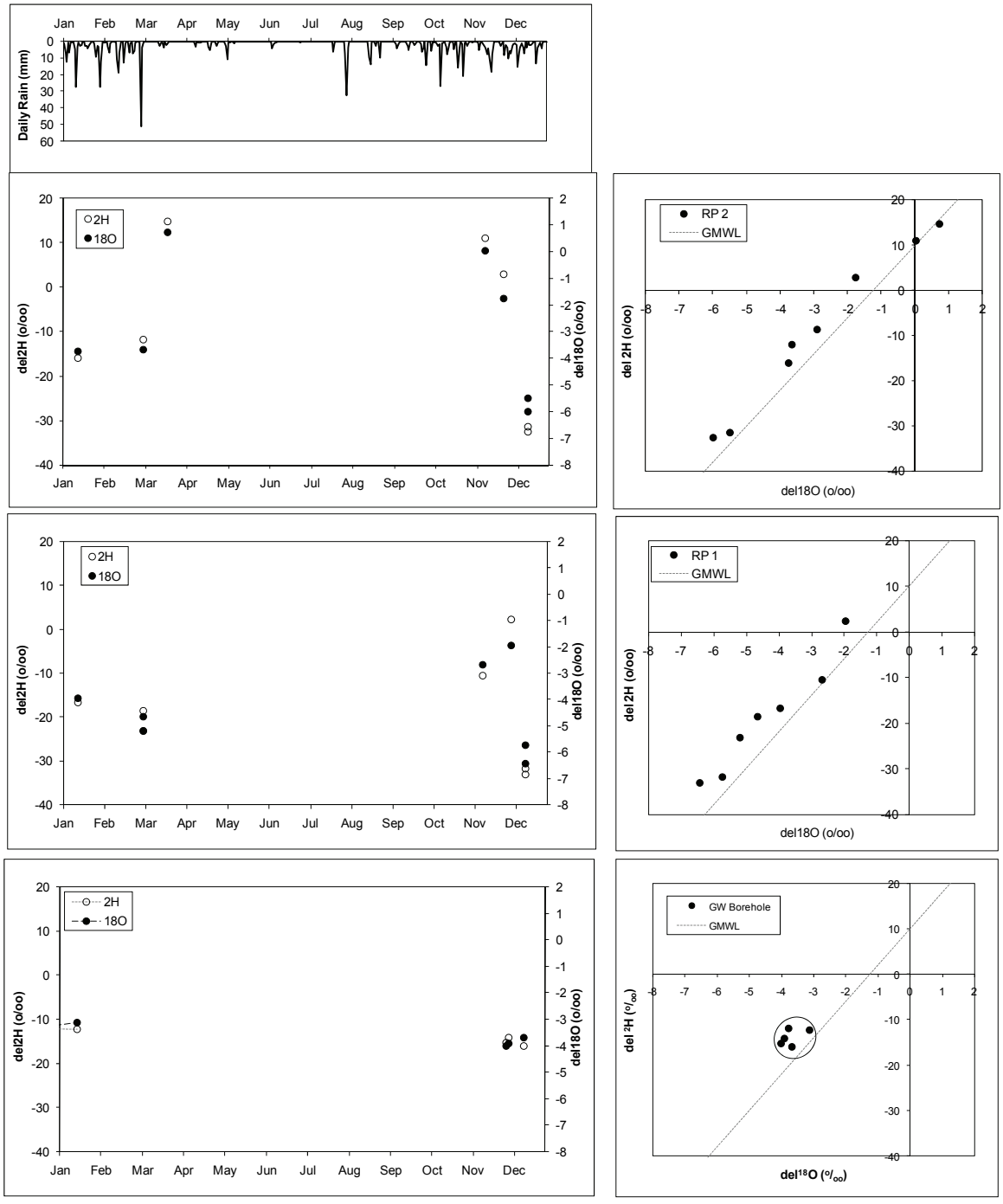

Figure B3.1.3 Rainfall and isotope responses for 2009 at the monitoring stations: Runoff plot 2 (top), Runoff plot 1 (middle) and Groundwater (bottom).

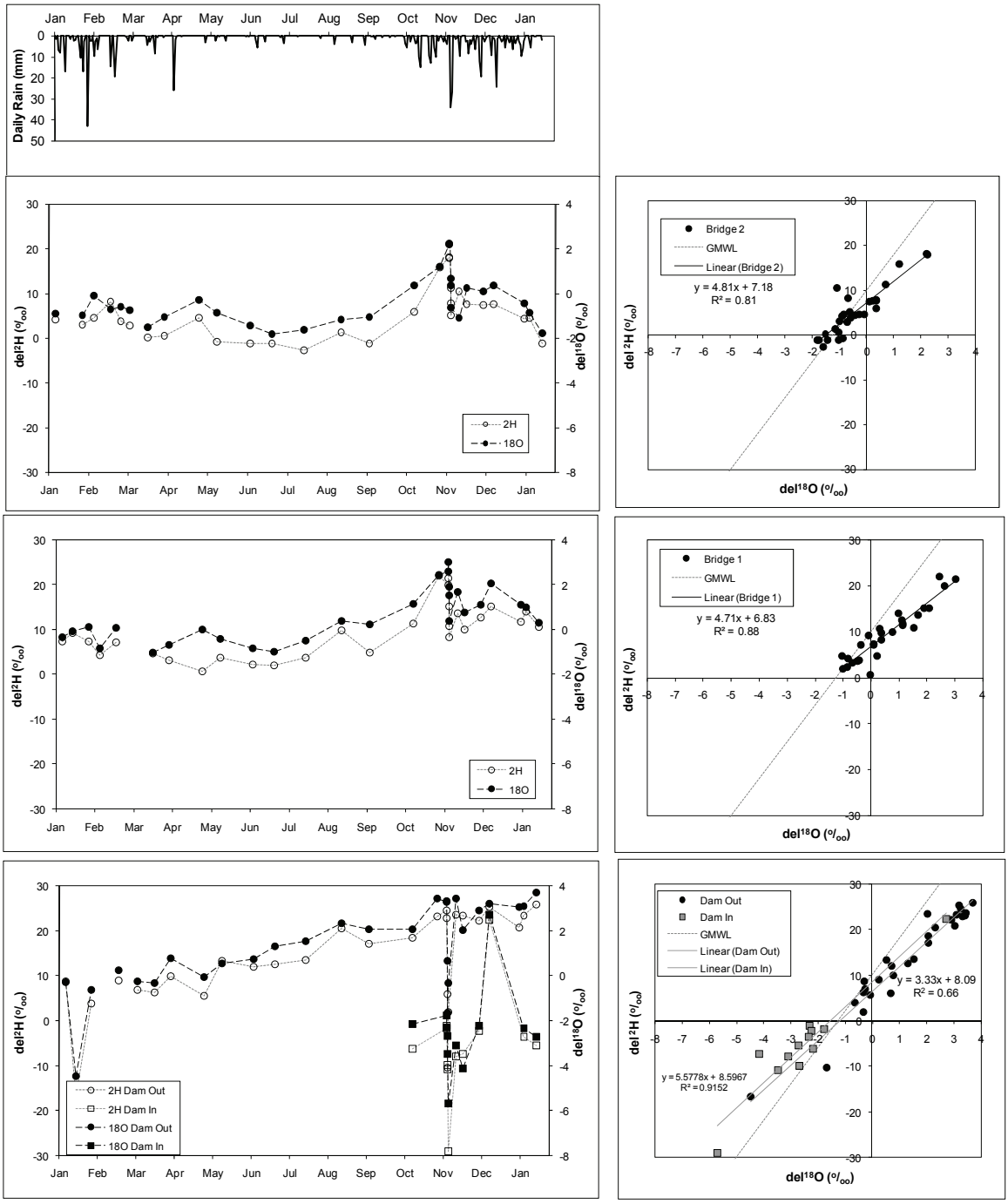

Figure B3.2.1 Rainfall and isotope responses for 2010 at the monitoring stations: Bridge 2 (top), Bridge 2 (middle) and Dam Out/Dam In (bottom).

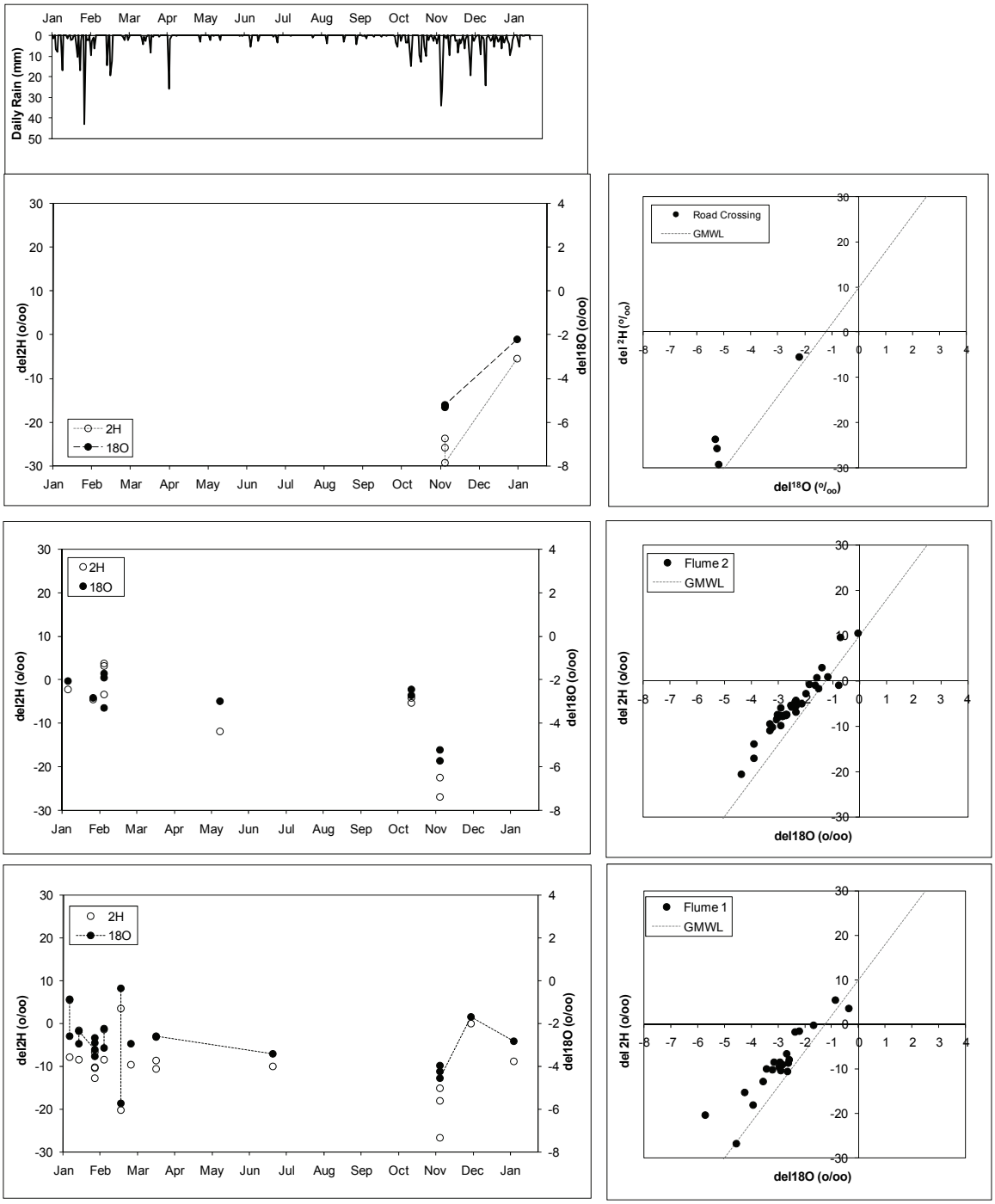

Figure B3.2.2 Rainfall and isotope responses for 2010 at the monitoring stations: Road Crossing (top), Flume 2 (middle) and Flume 1 (bottom).

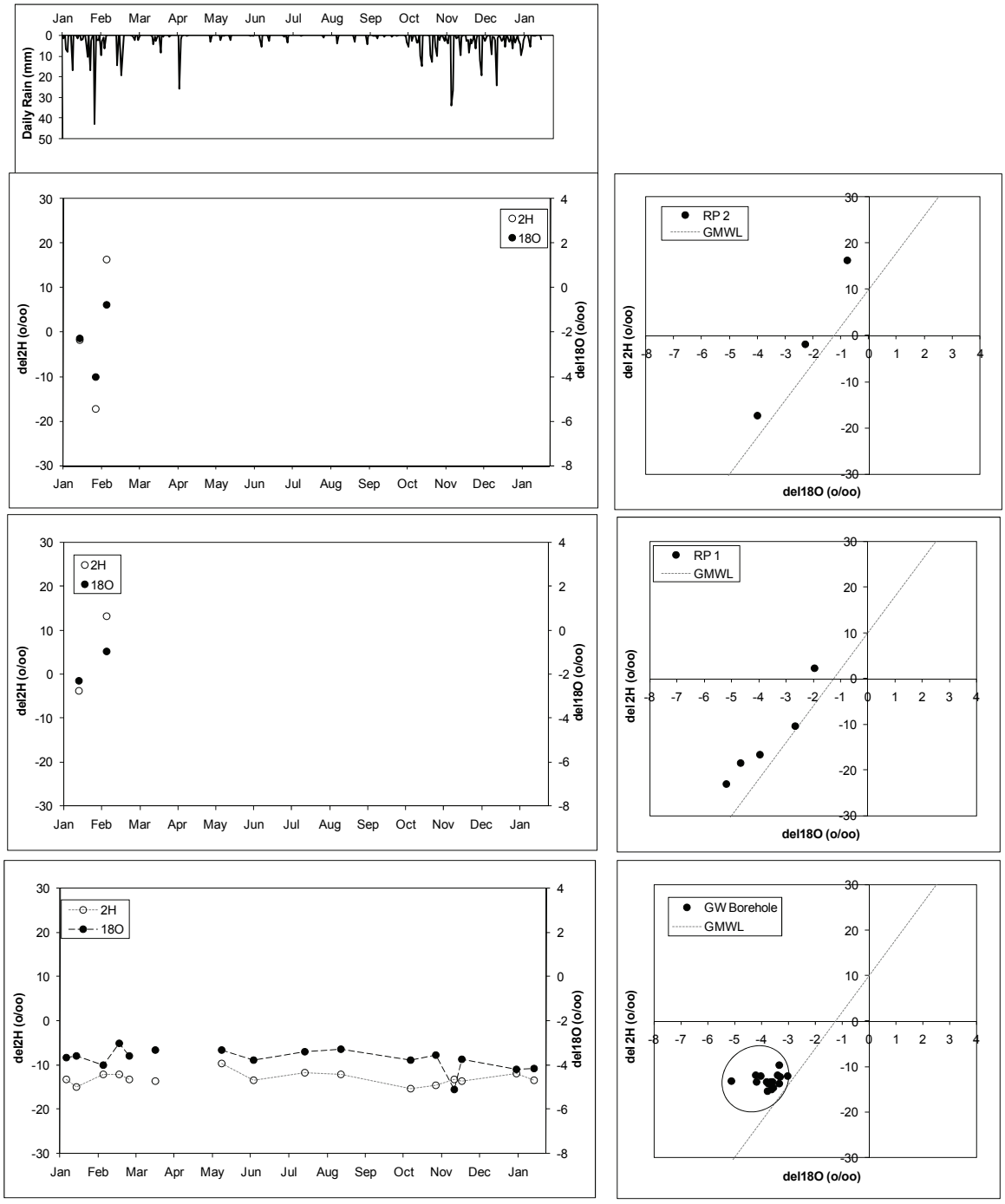

Figure B3.2.3 Rainfall and isotope responses for 2010 at the monitoring stations: Runoff plot 2 (top), Runoff plot 1 (middle) and Groundwater (bottom).

APPENDIX C

EVENTS : RAINFALL, RUNOFF and WATER QUALITY

C1 EVENT 1: 10 January 2009

C1.1 NO_3, P and sediments: Flume 1 and Flume 2

C1.2 Isotopes: Flume 1 and Flume 2

C2 EVENT 2: 28 February 2009

C2.1 NO_3, P and sediments: Flume 1 and Flume 2

C2.2 Isotopes: Flume 1 and Flume 2

C3 EVENT 3: 26 January 2010

C3.1 NO_3, P and sediments: Flume 1

C3.2 Isotopes: Flume 1 and Flume 2

C4 EVENT 4: 10 November 2010

C4.1 NO_3, P and sediments: Flume 1 and Flume 2

C4.2 NO_3, P and sediments: Road Crossing and Dam In

C4.3 NO_3, P and sediments: Dam 1 Out and Dam 2 Out

C4.4 NO_3, P and sediments: Bridge 1 and Bridge 2

C4.5 Isotopes: Flume 1 and Flume 2

C4.6 Isotopes: Road Crossing and Dam In

C4.7 Isotopes: Dam 1 Out and Dam 2 Out

C4.8 Isotopes: Bridge 1 and Bridge 2

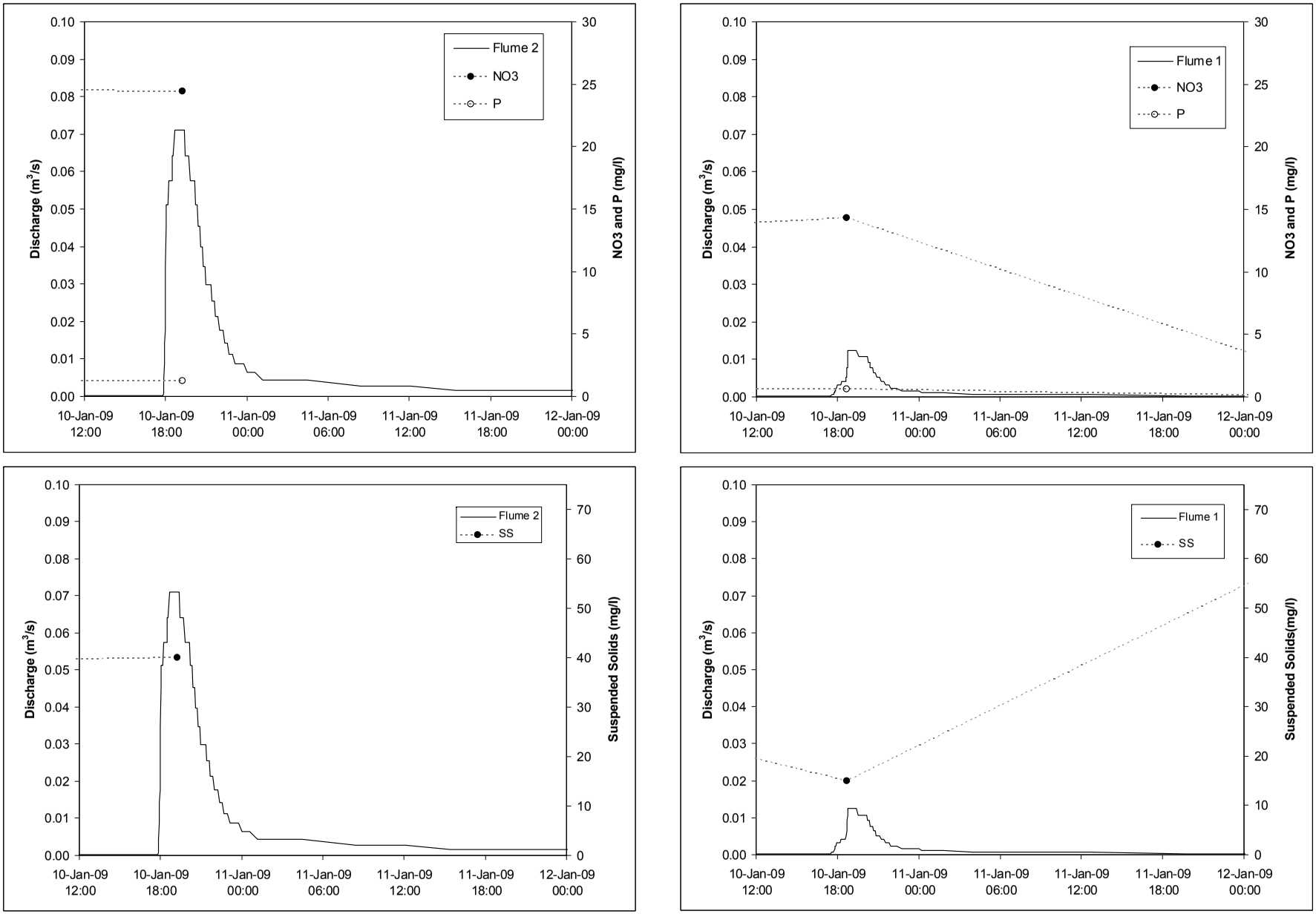

Figure C1.1. Rainfall, runoff Nitrate and P (above) and Suspended Solids (below) responses for Flume 1 (left) and Flume 2 (right) for event of 10 January 2009.

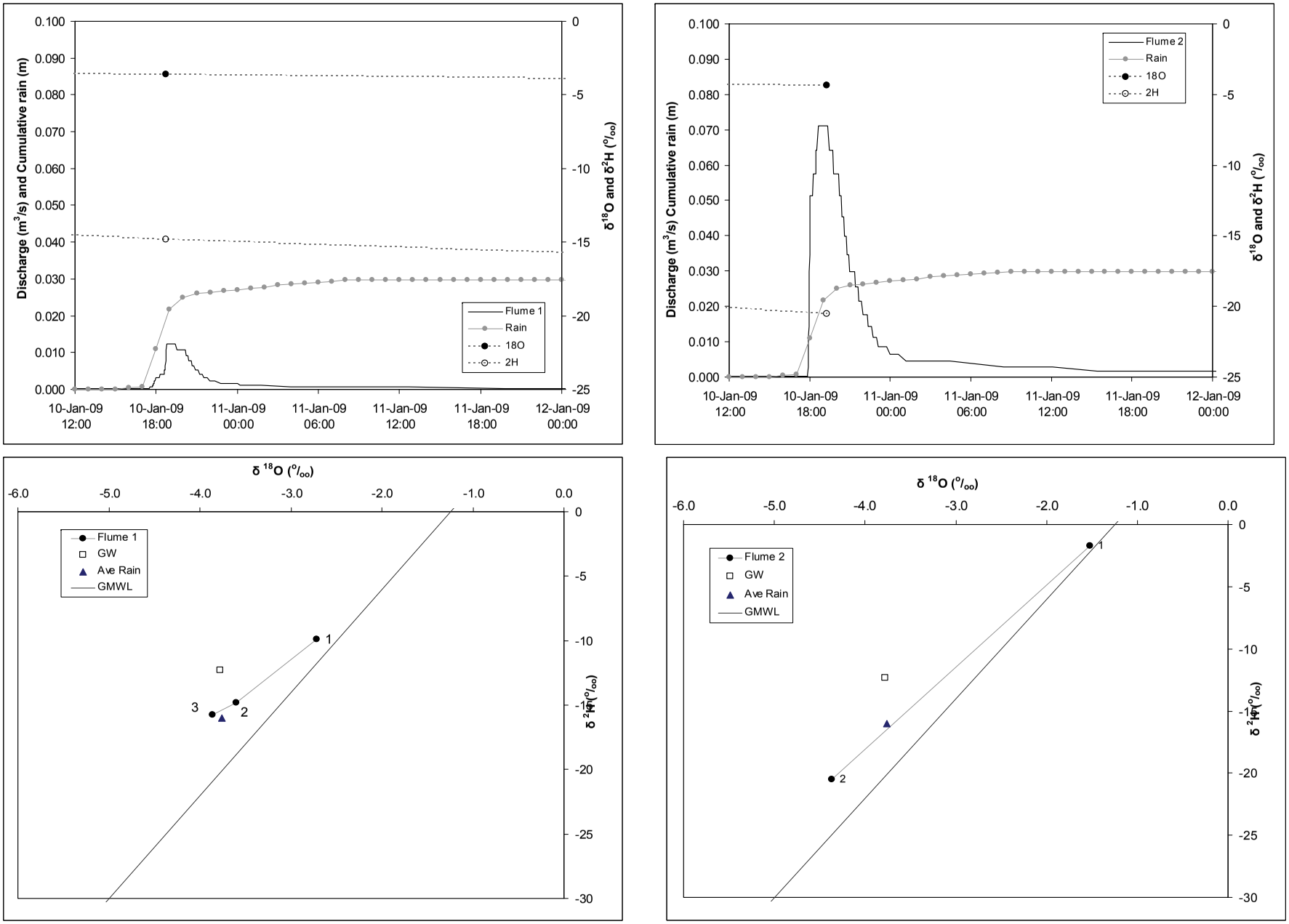

Figure C1.2. Rainfall, runoff and Isotope responses for Flume 1 (left) and Flume 2 (right) for event of 10 January 2009.

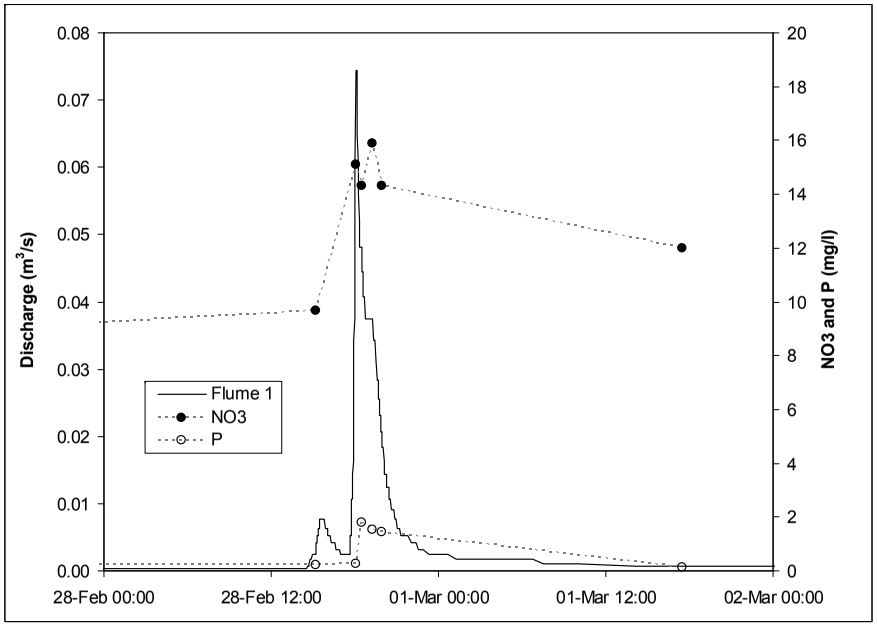

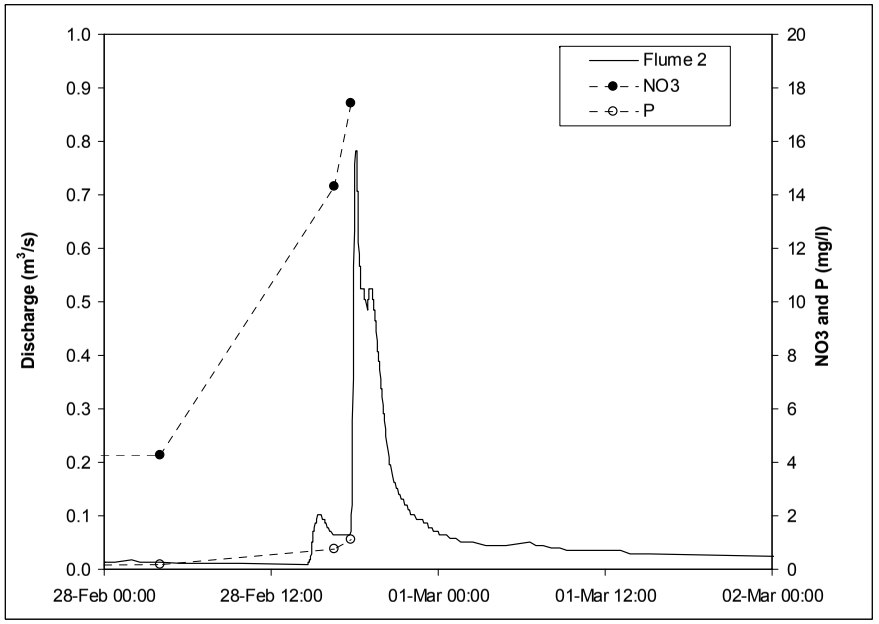

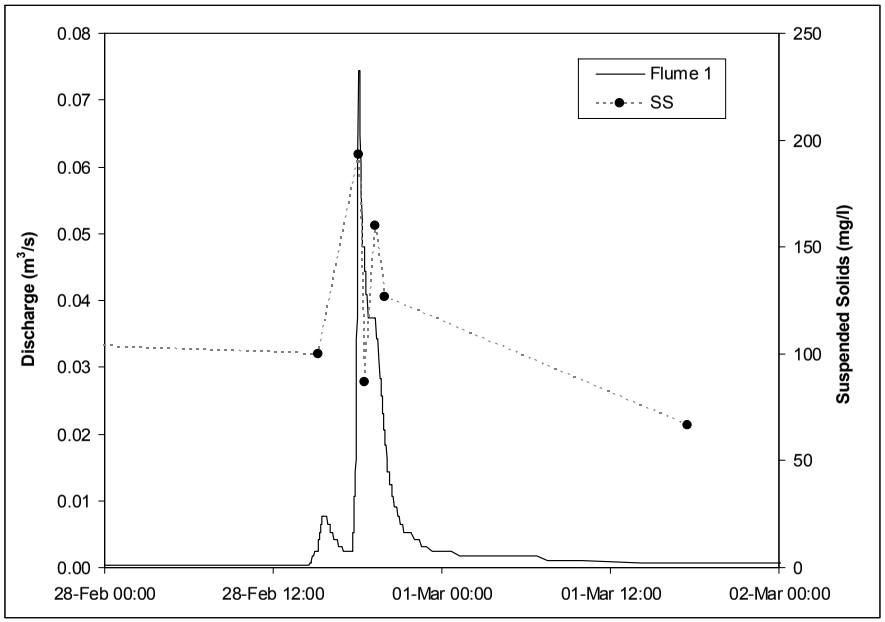

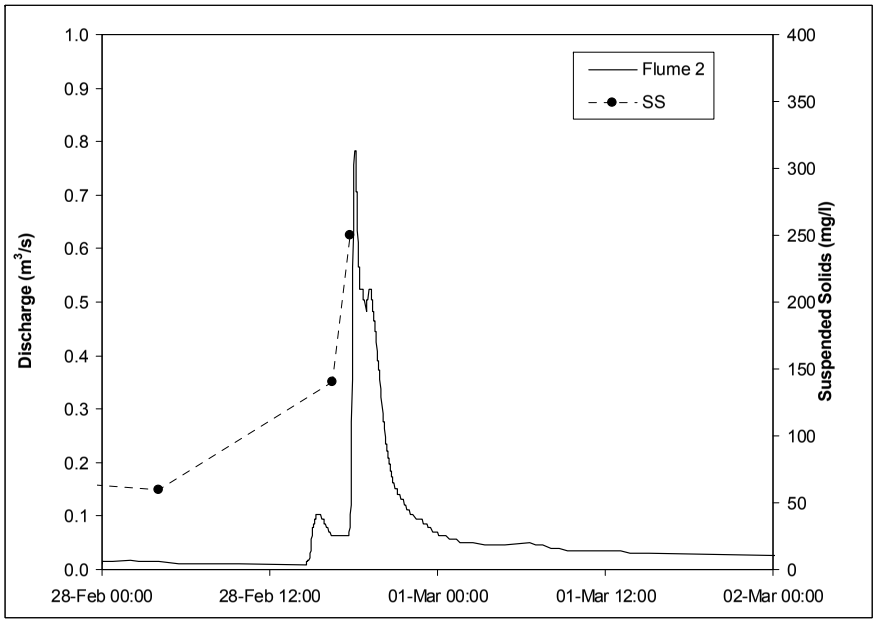

Figure C2.1. Rainfall, runoff Nitrate and P (above) and Suspended Solids (below) responses for Flume 1 (left) and Flume 2 (right) for event of 28 February 2009.

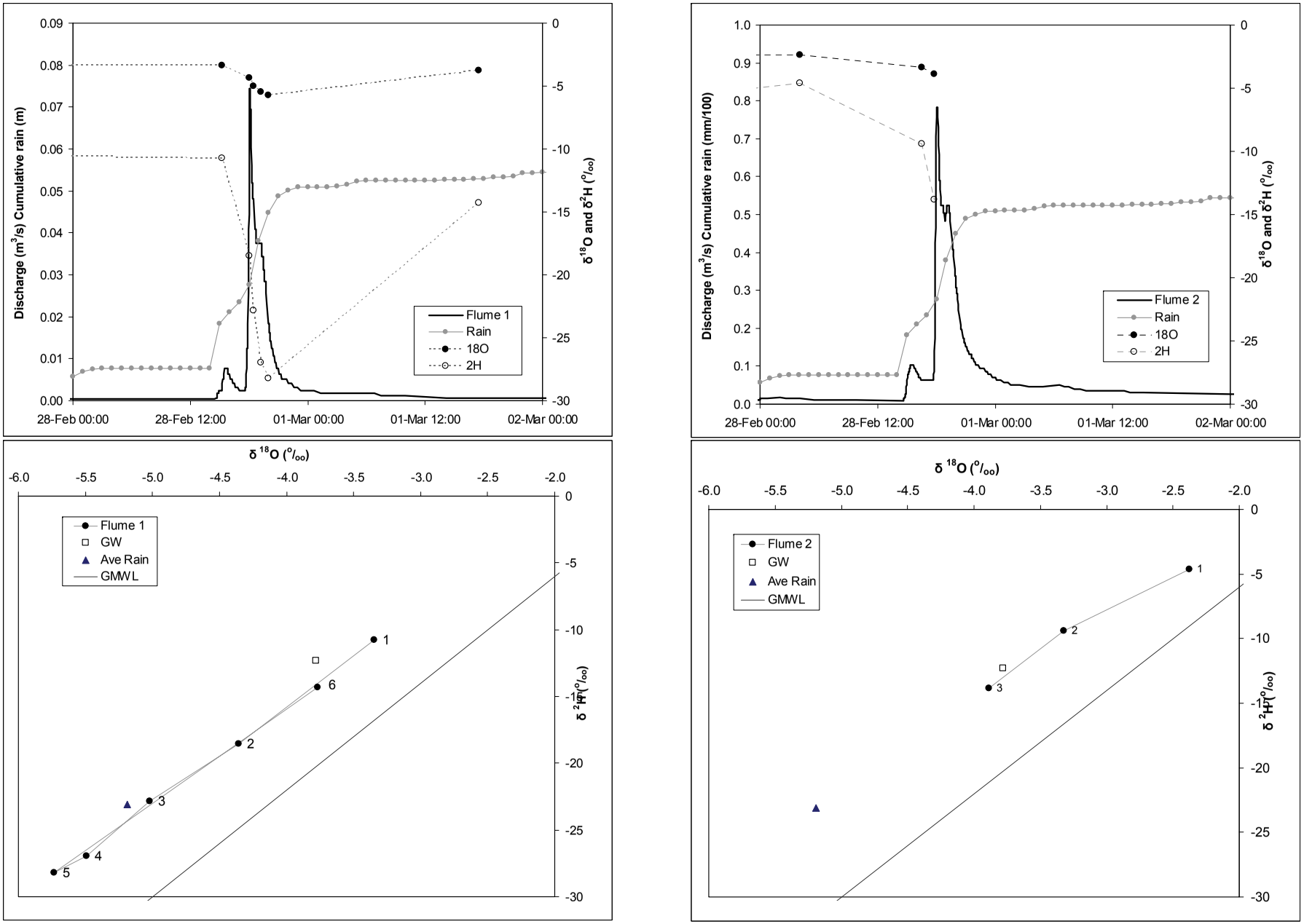

Figure C2.2. Rainfall, runoff and Isotope responses for Flume 1 (left) and Flume 2 (right) for event of 28 February 2009.

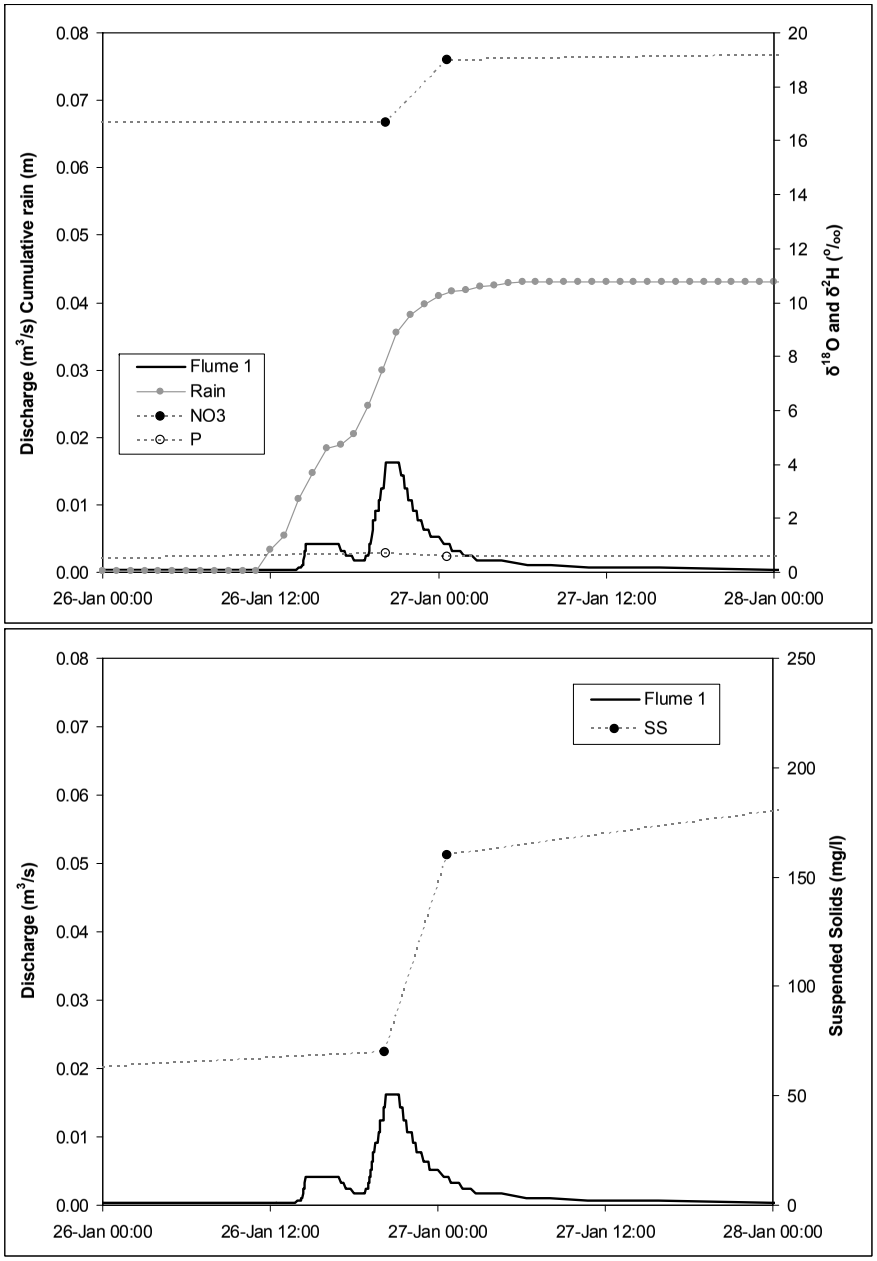

Figure C3.1. Rainfall, runoff Nitrate and P (above) and Suspended Solids (below) responses for Flume 1 for event of 27 January 2010.

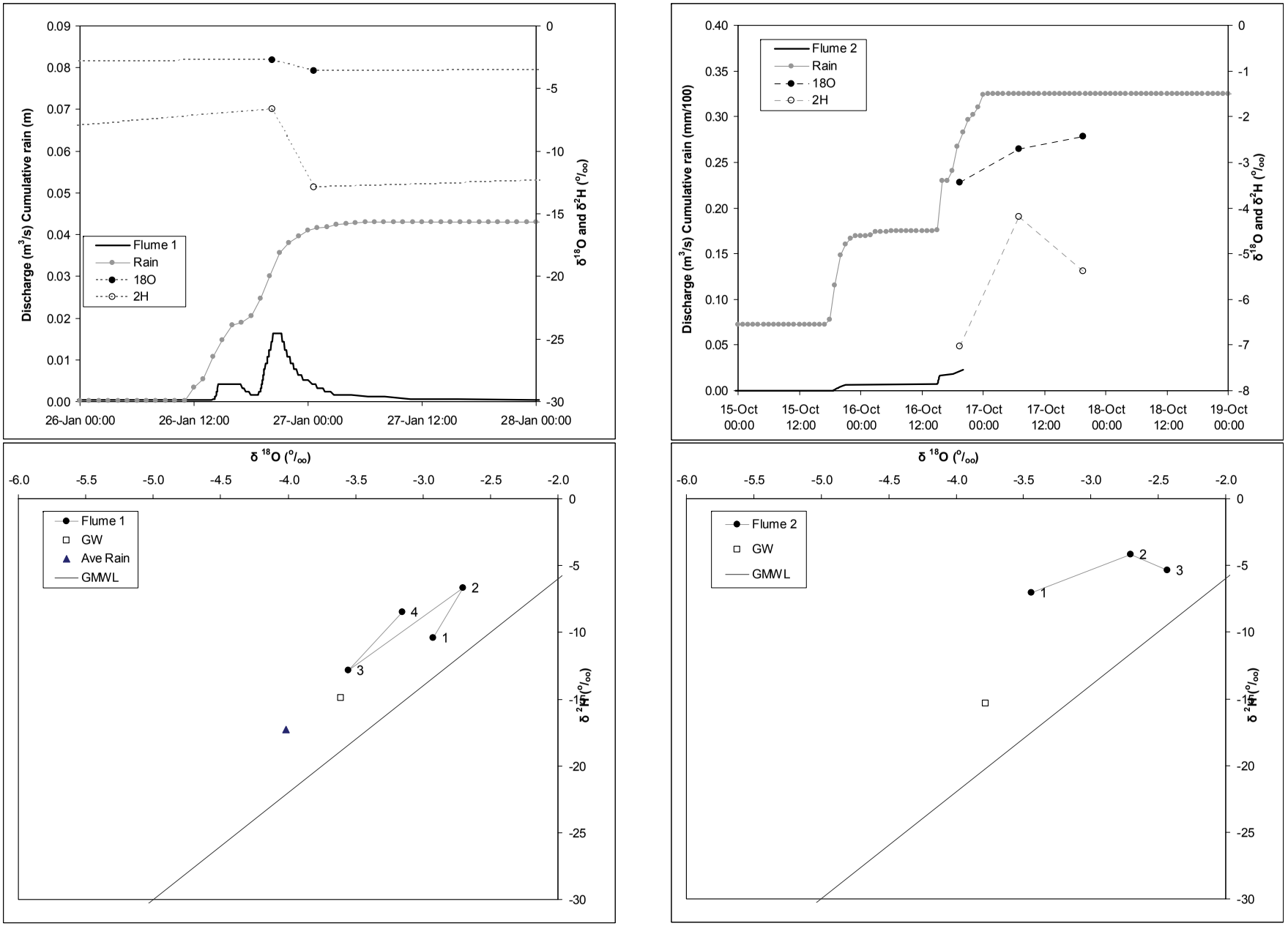

Figure C3.2. Rainfall, runoff and Isotope responses for Flume 1 (left) and Flume 2 (right) for event of 27 January 2010.

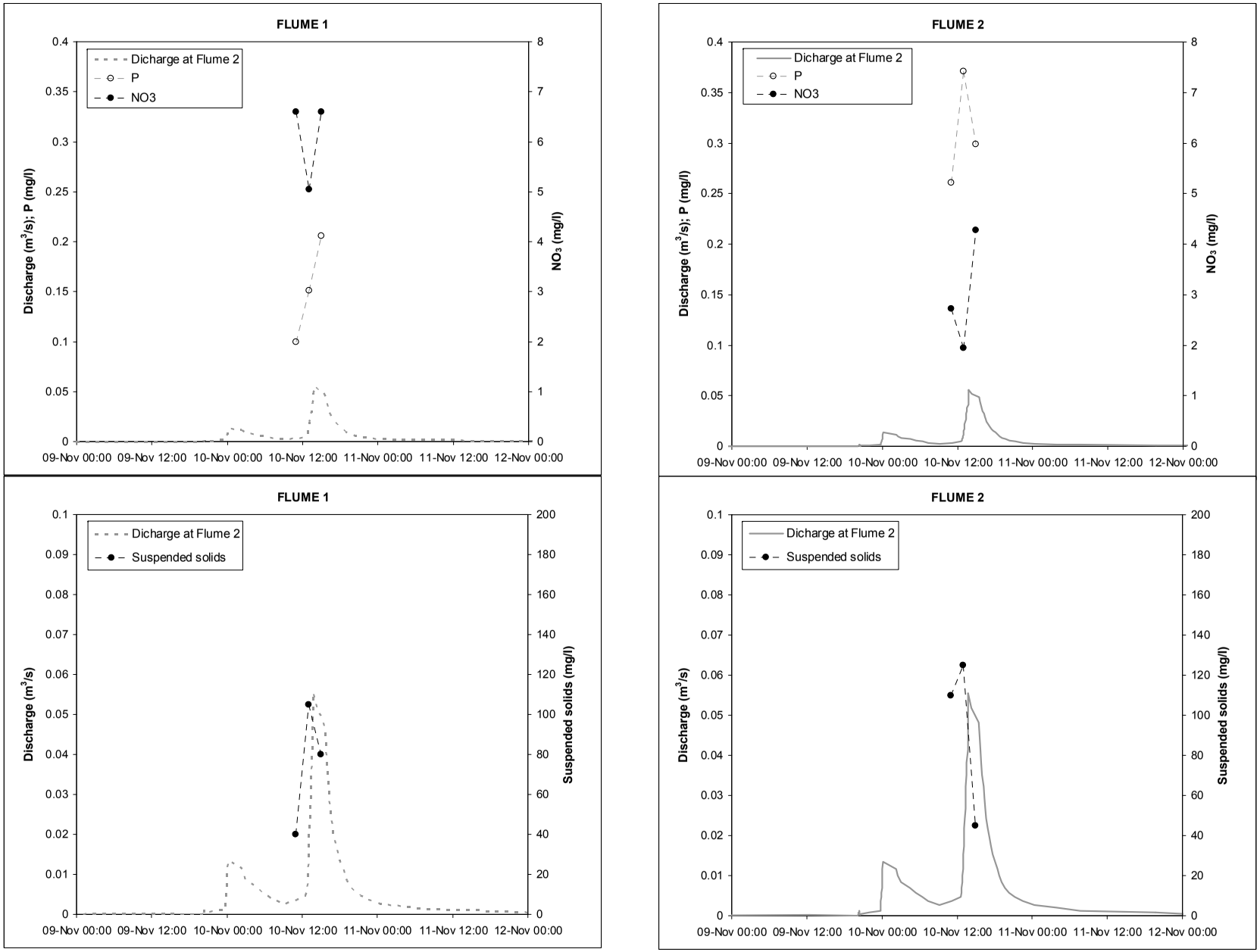

Figure C4.1. Rainfall, runoff Nitrate and P (above) and Suspended Solids (below) responses for Flume 1 (left) and Flume 2 (right) for event of 10 November 2010.

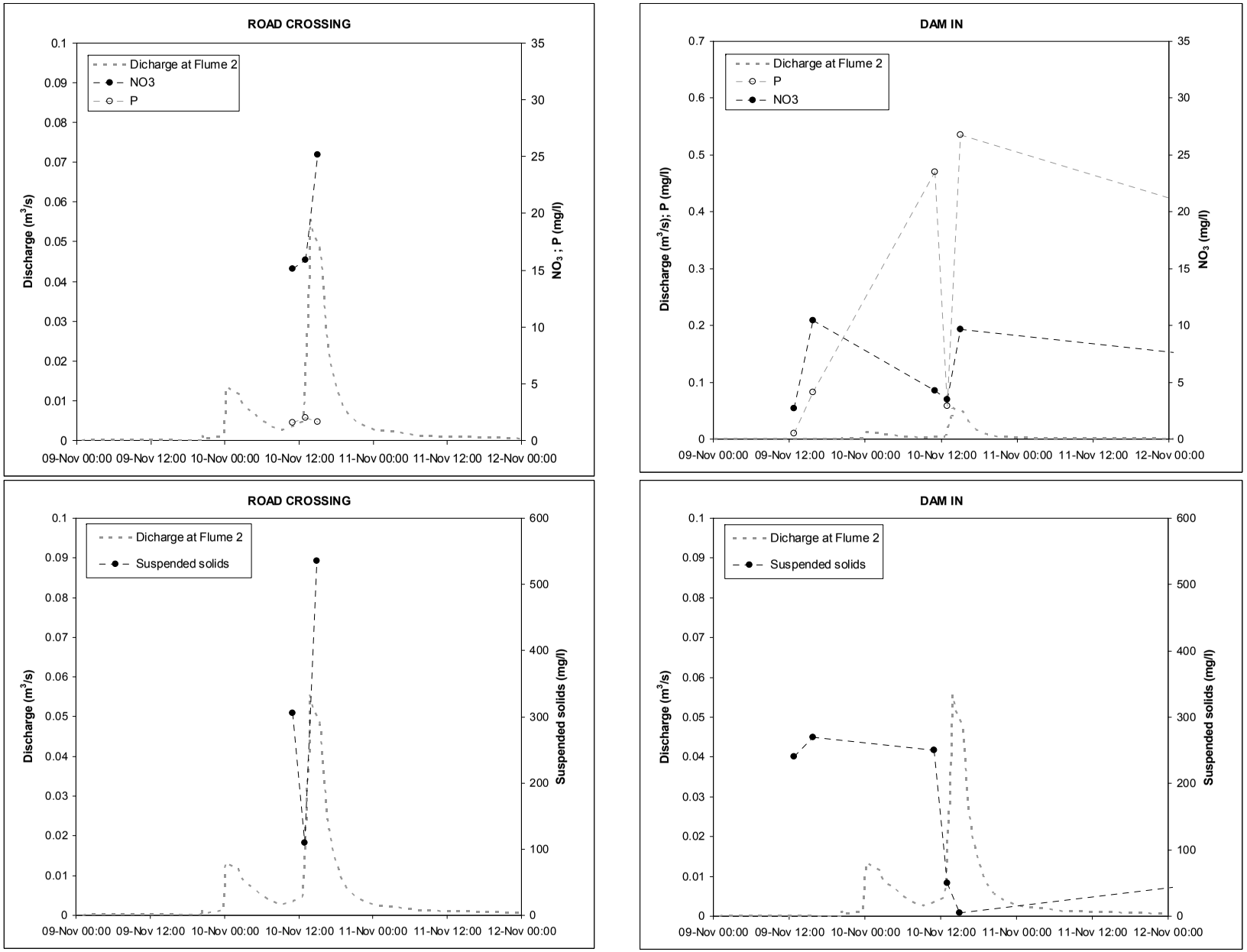

Figure C4.2. Rainfall, runoff Nitrate and P (above) and Suspended Solids (below) responses for Road crossing (left) and Dam In (right) for event of 10 November 2010.

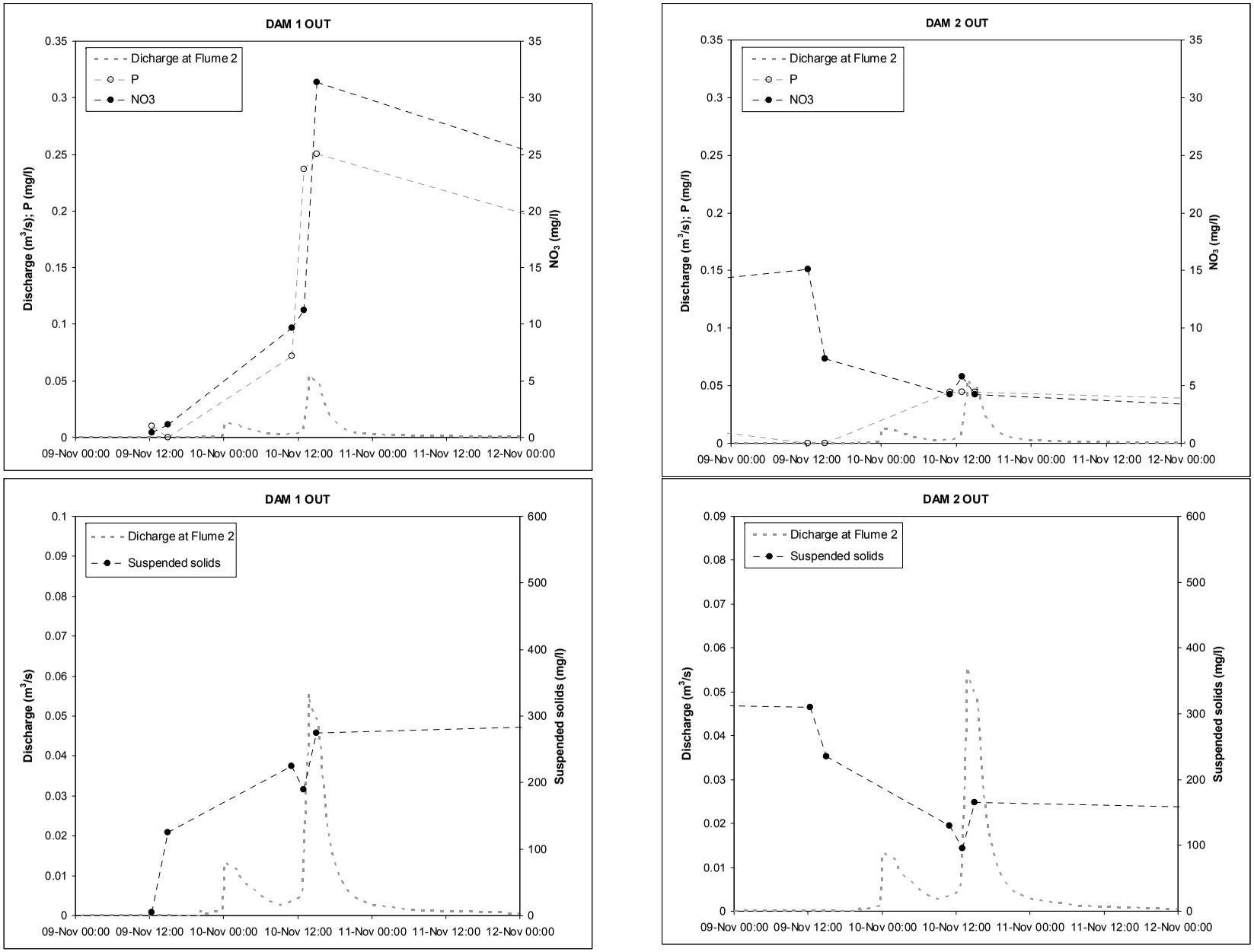

Figure C4.3. Rainfall, runoff Nitrate and P (above) and Suspended Solids (below) responses for Dam 1 Out (left) and Dam 2 Out (right) for event of 10 November 2010.

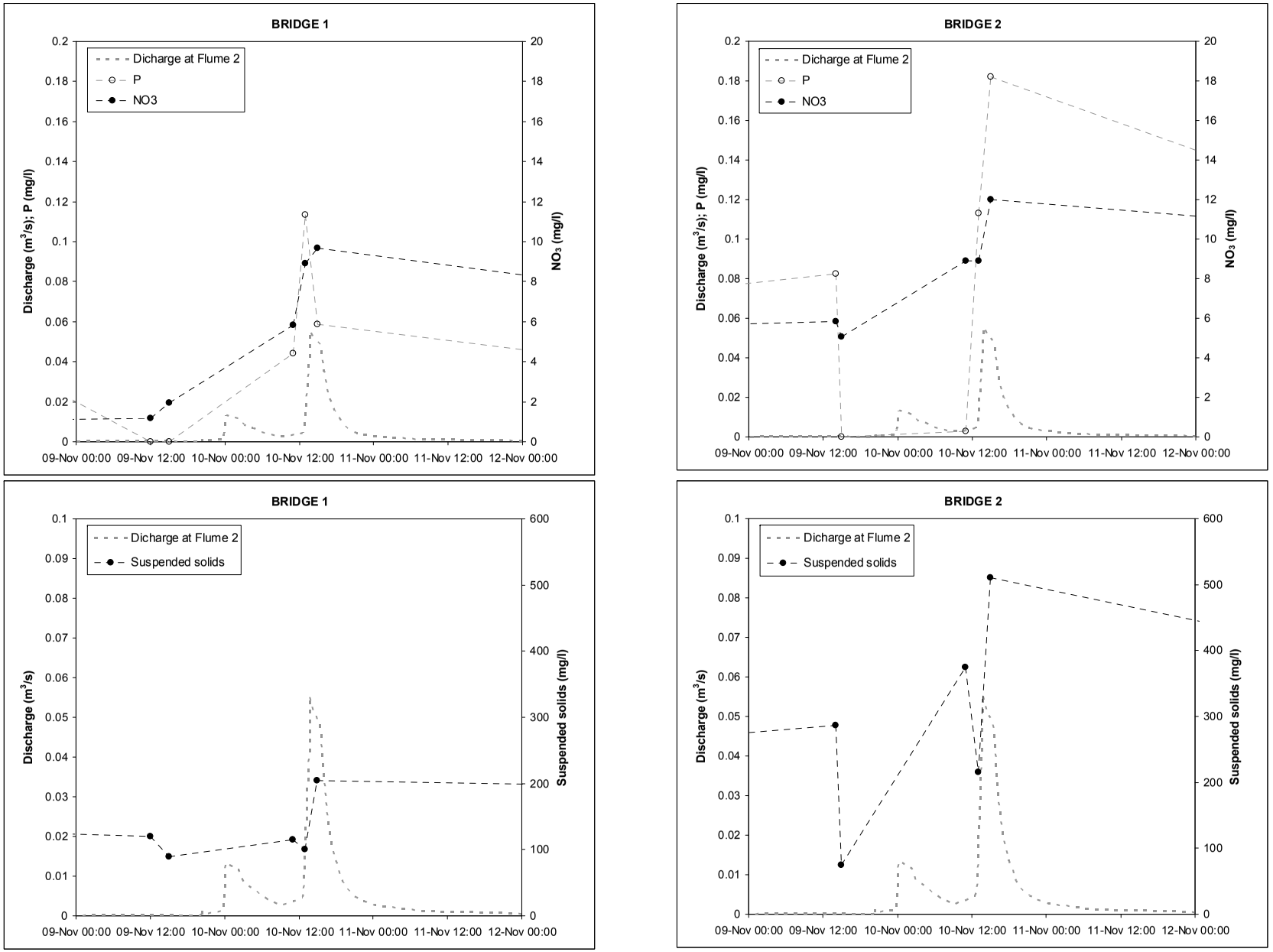

Figure C4.4. Rainfall, runoff Nitrate and P (above) and Suspended Solids (below) responses for Bridge 1 (left) and Bridge 2 (right) for event of 10 November 2010.

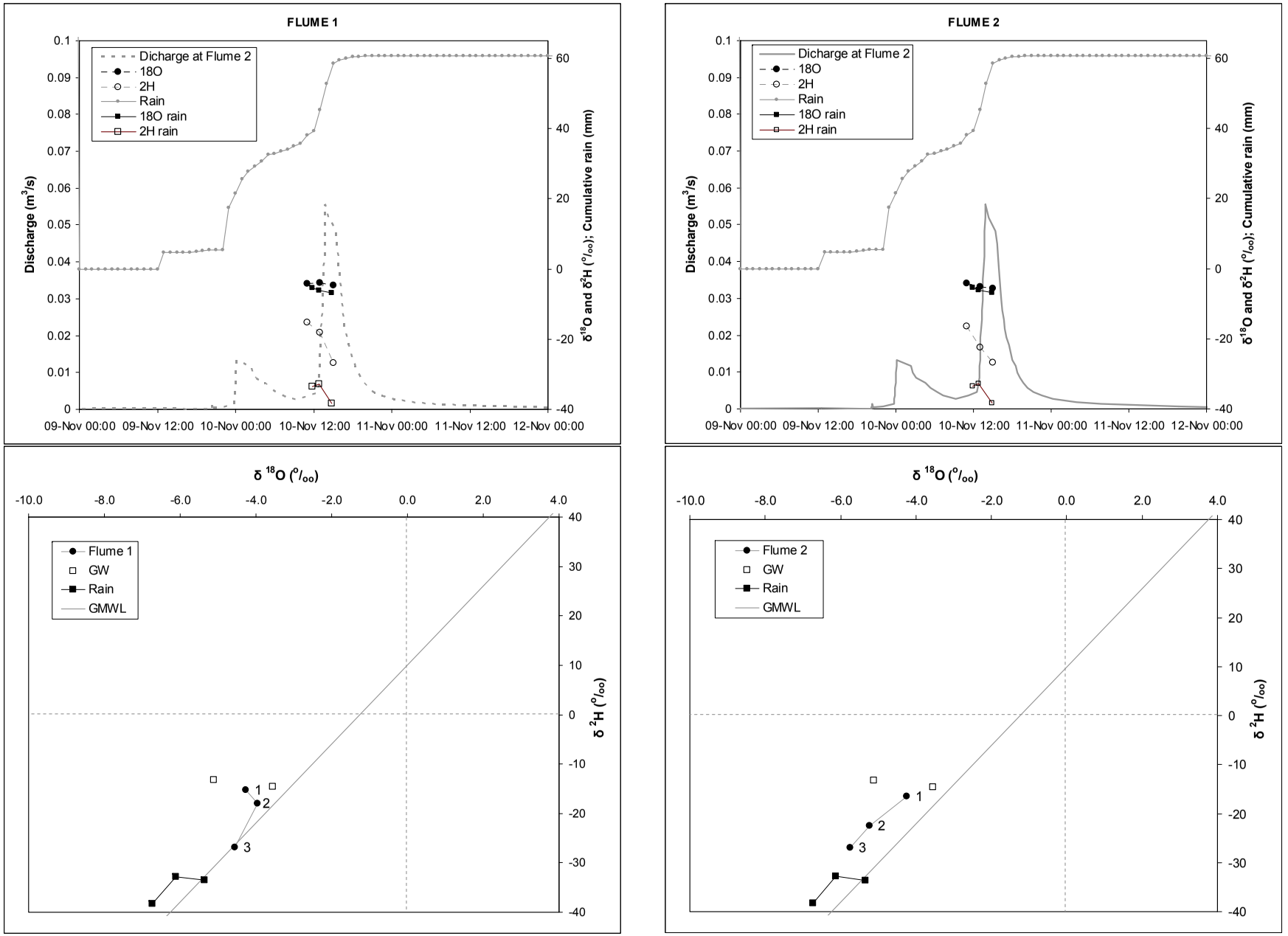

Figure C4.5. Rainfall, runoff and Isotope responses for Flume 1 (left) and Flume 2 (right) for event of 10 November 2010.

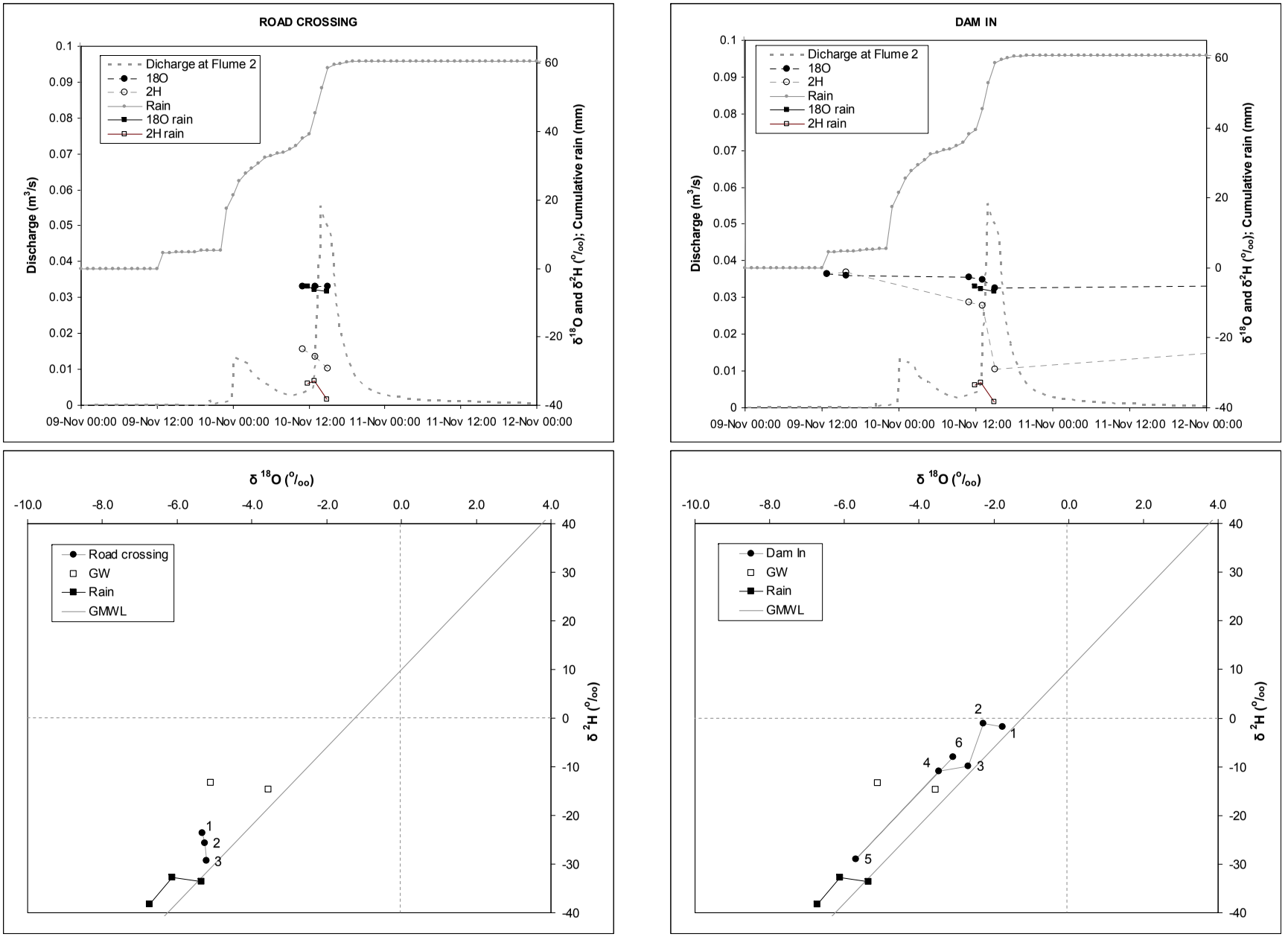

Figure C4.6. Rainfall, runoff and Isotope responses for Road crossing (left) and Dam In (right) for event of 10 November 2010.

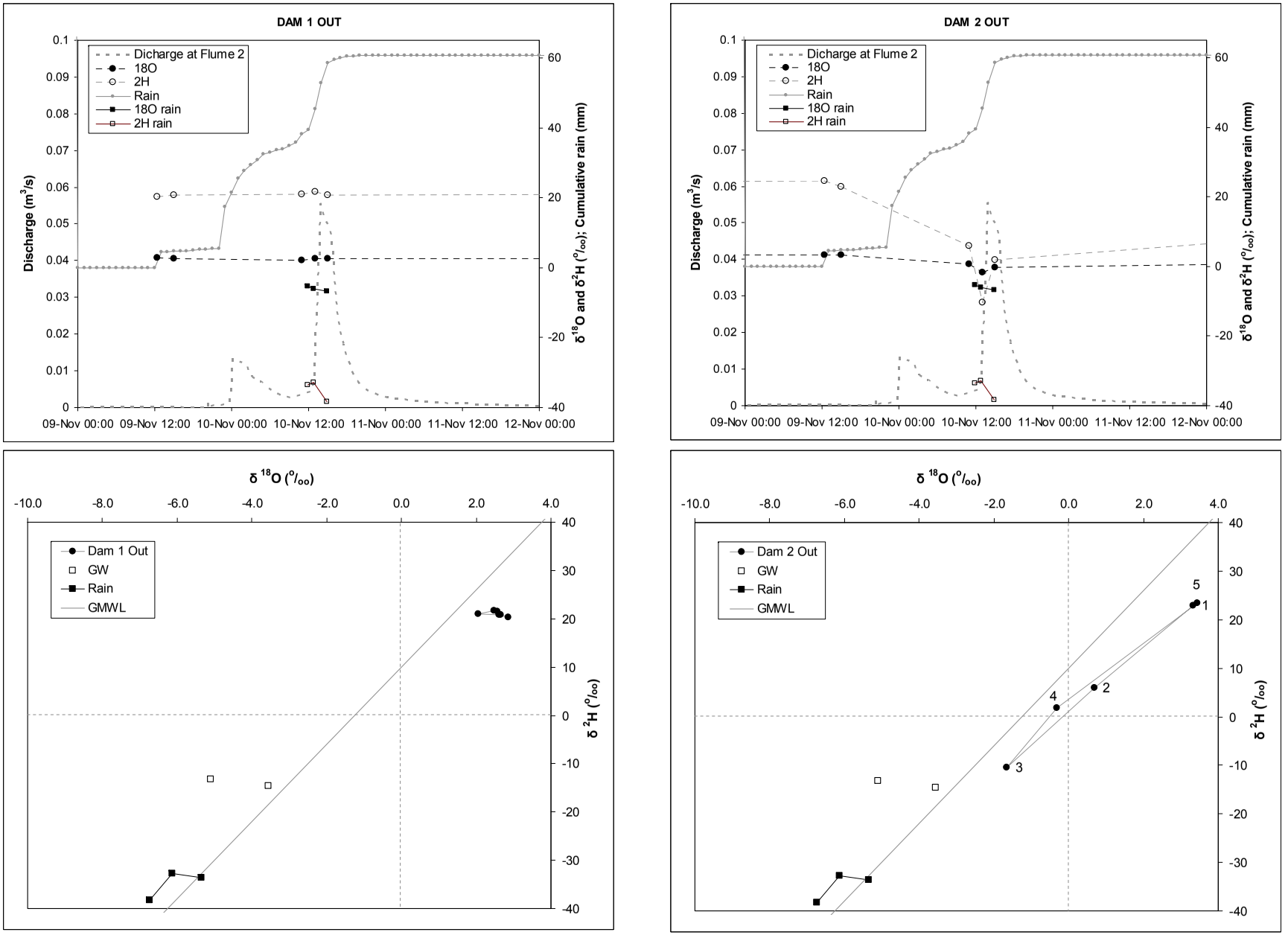

Figure C4.7. Rainfall, runoff and Isotope responses for Dam 1 Out (left) and Dam 2 Out (right) for event of 10 November 2010.

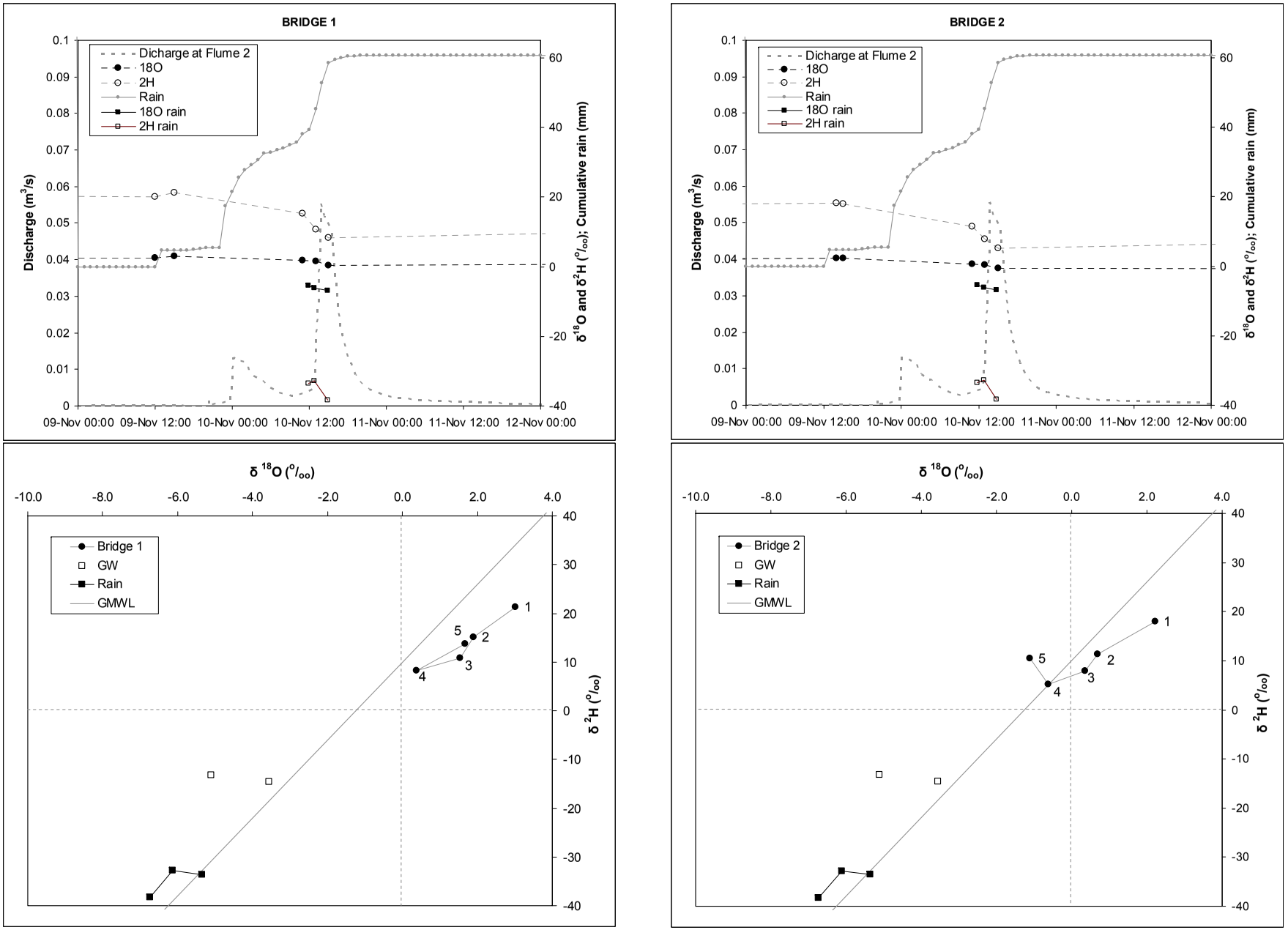

Figure C4.8. Rainfall, runoff and Isotope responses for Bridge 1 (left) and Bridge 2 (right) for event of 10 November 2010.

APPENDIX D

WATER QUALITY EVENTS: STREAM TRANSECTS

D1 SUSPENDED SOLIDS

D1.1 Suspended solids transect January, February and December 2009

D1.2 Suspended solids transect June 2010 and January 2011

D2 NO_3 and P

D2.1 NO_3 and P transect January, February and December 2009

D2.2 NO_3 and P transect June 2010 and January 2011

D3 ISOTOPES

D3.1 Isotopes transect: January and February 2009

D3.2 Isotopes transect: December 2009 and June 2010

D3.3 Isotopes transect: January 2011

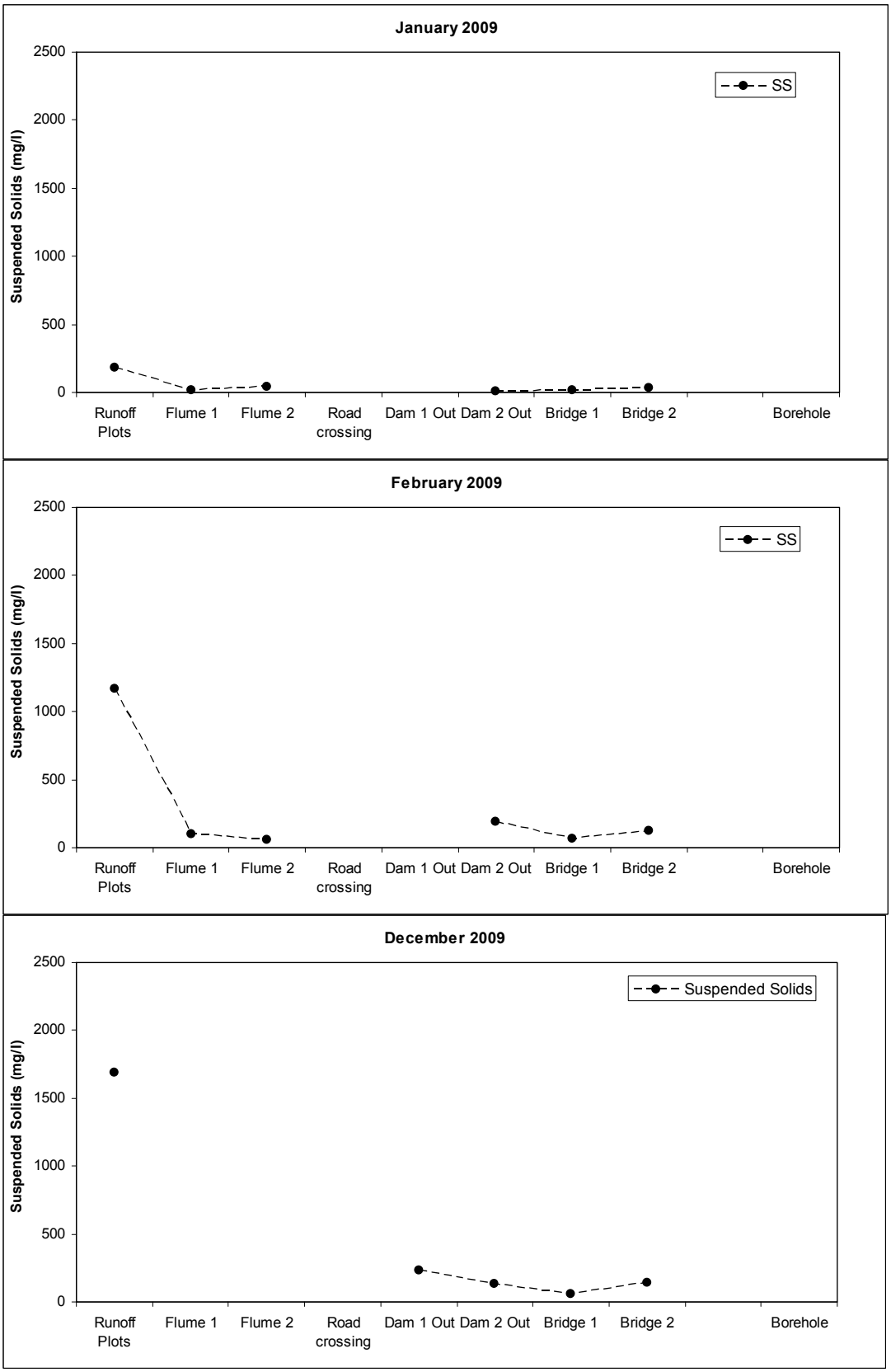

Figure D1.1 Suspended solids concentrations in the stream network for events in January 2009, February 2009 and December 2009.

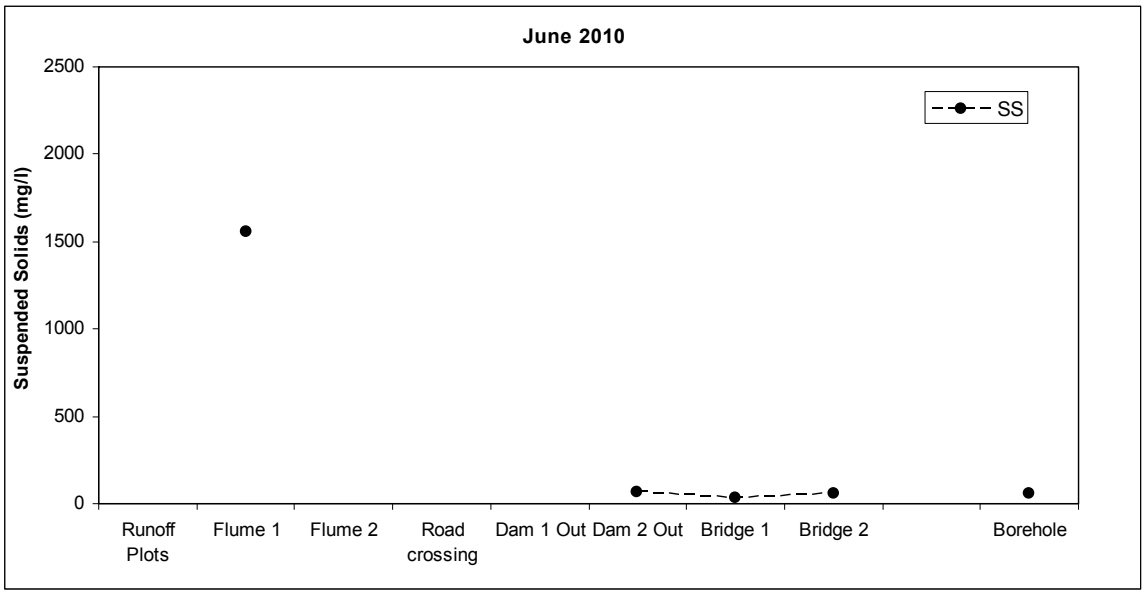

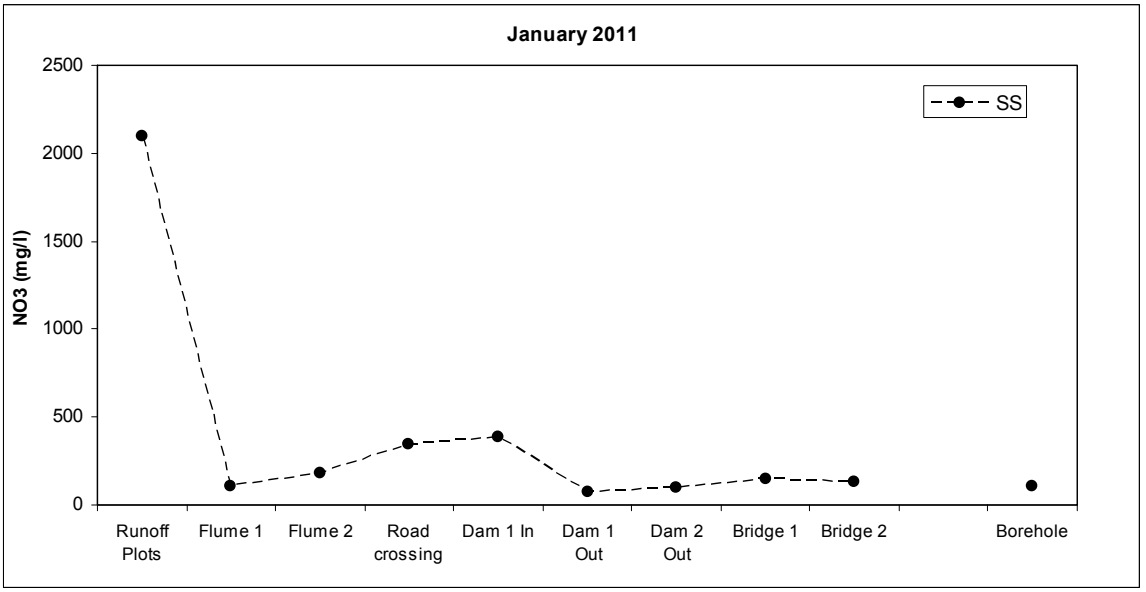

Figure D1.2 Suspended solids concentrations in the stream network for events in June 2010 and January 2011.

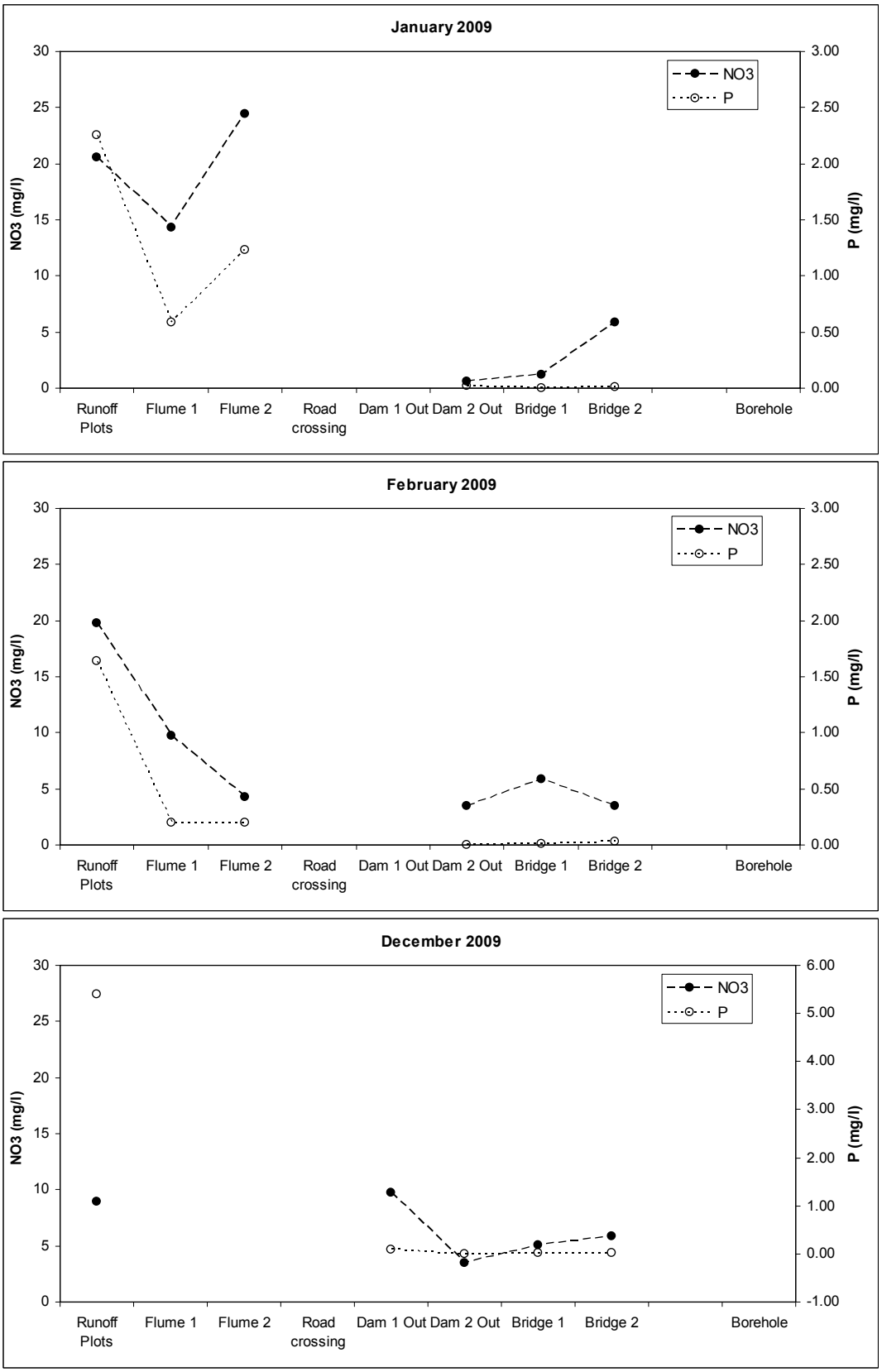

Figure D2.1 NO_3 and P concentrations in the stream network for events in January 2009, February 2009 and December 2009.

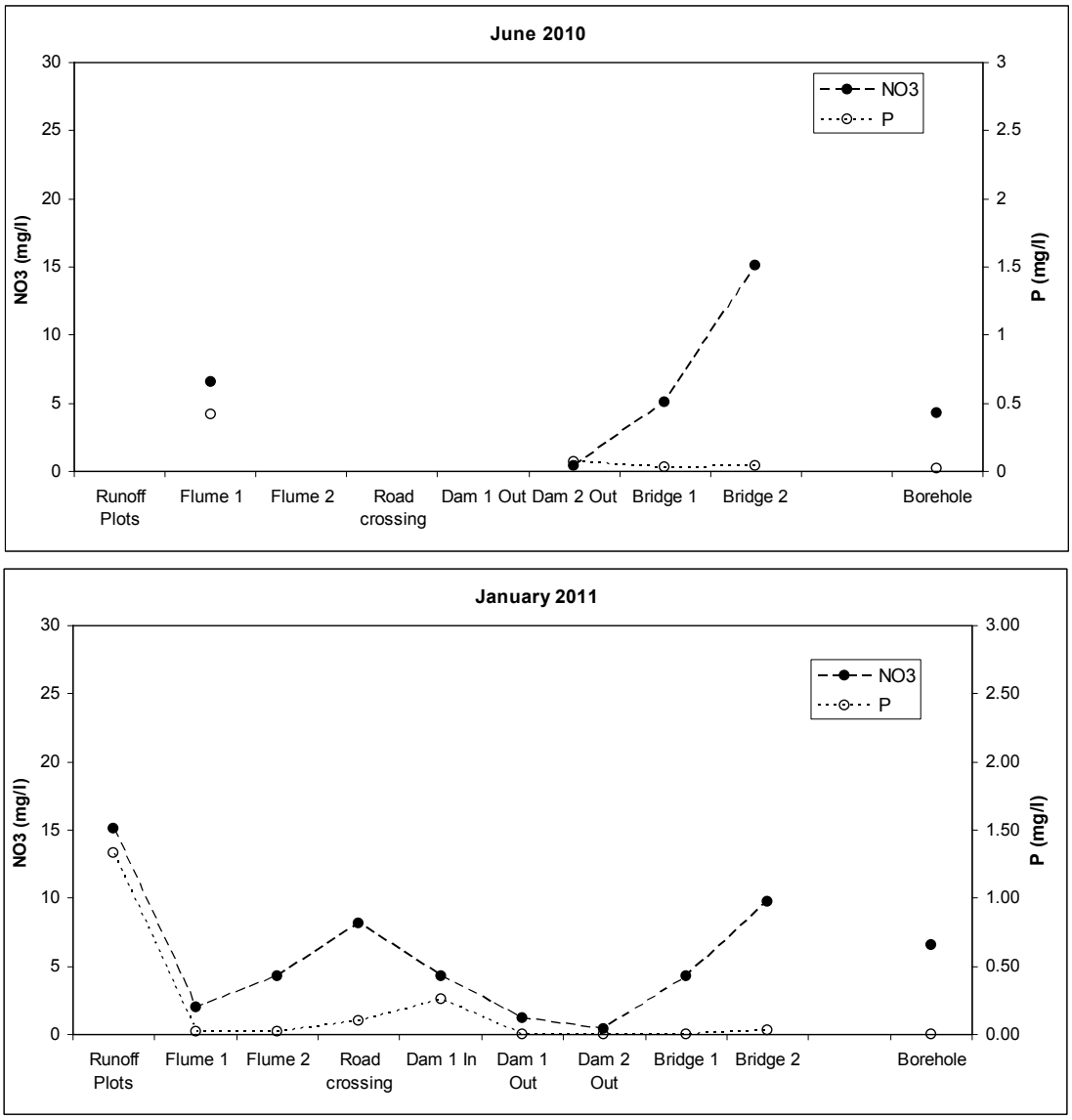

Figure D2.2 NO_3 and P concentrations in the stream network for events in June 2010 and January 2011.

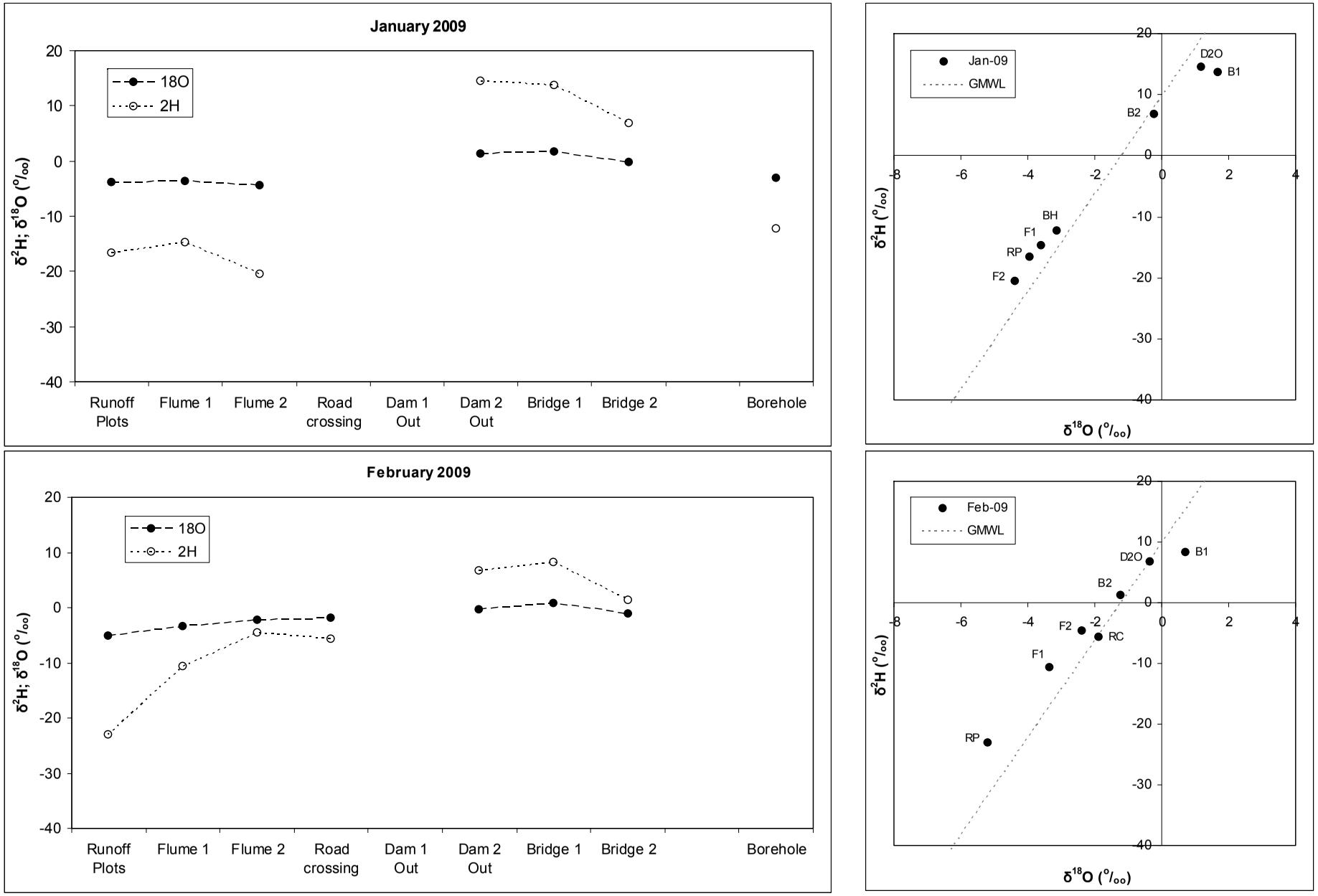

Figure D3.1. Isotope transects for events in January and February 2009.

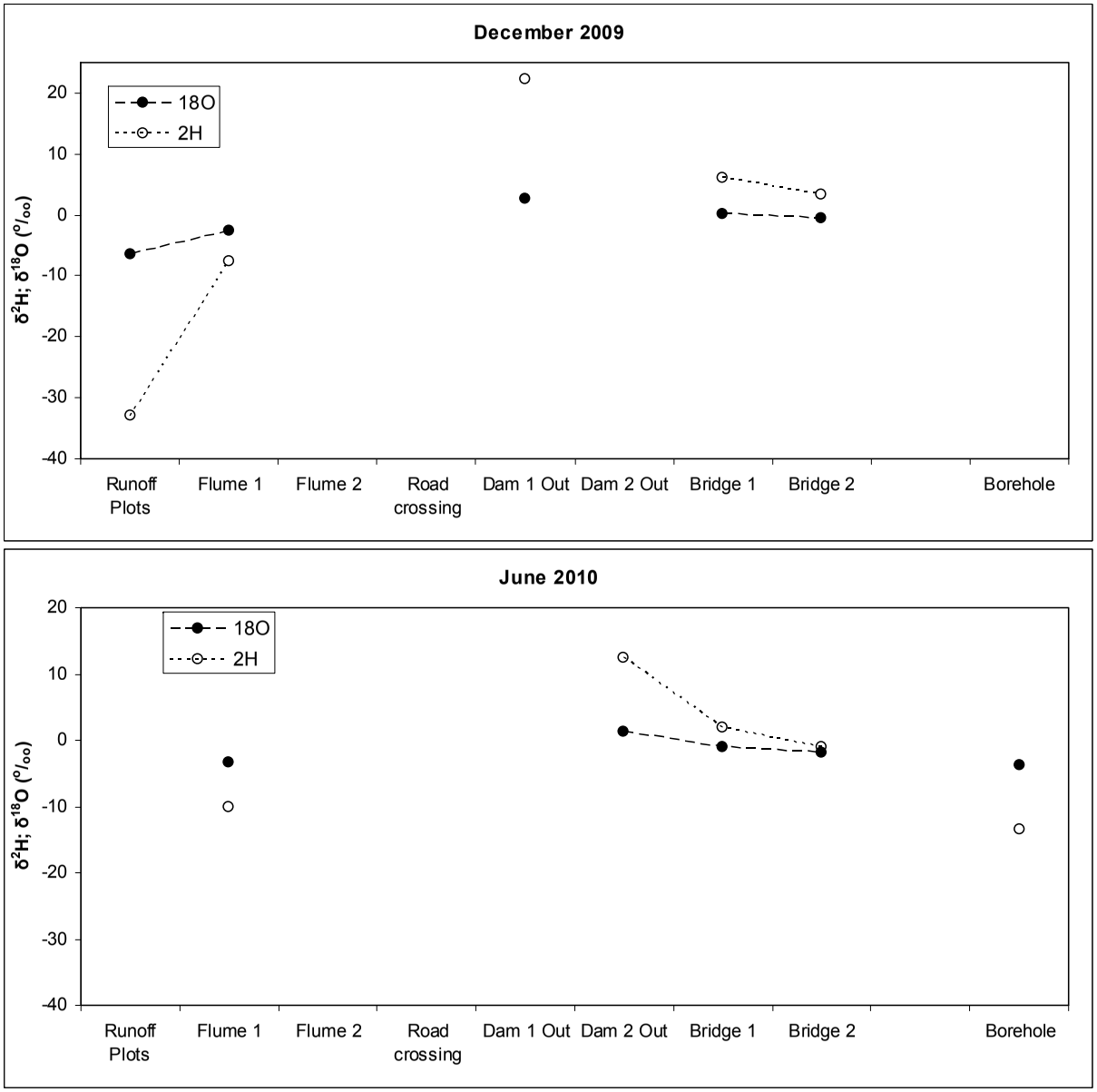

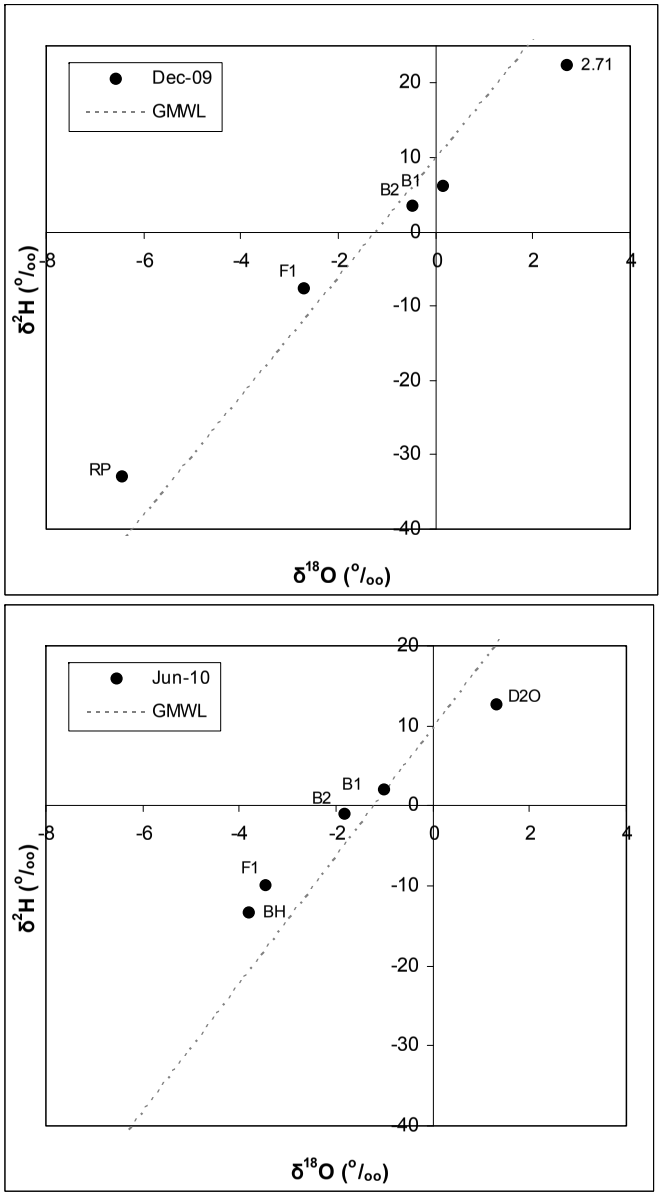

Figure D3.2. Isotope transects for events in December 2009 and June 2010.

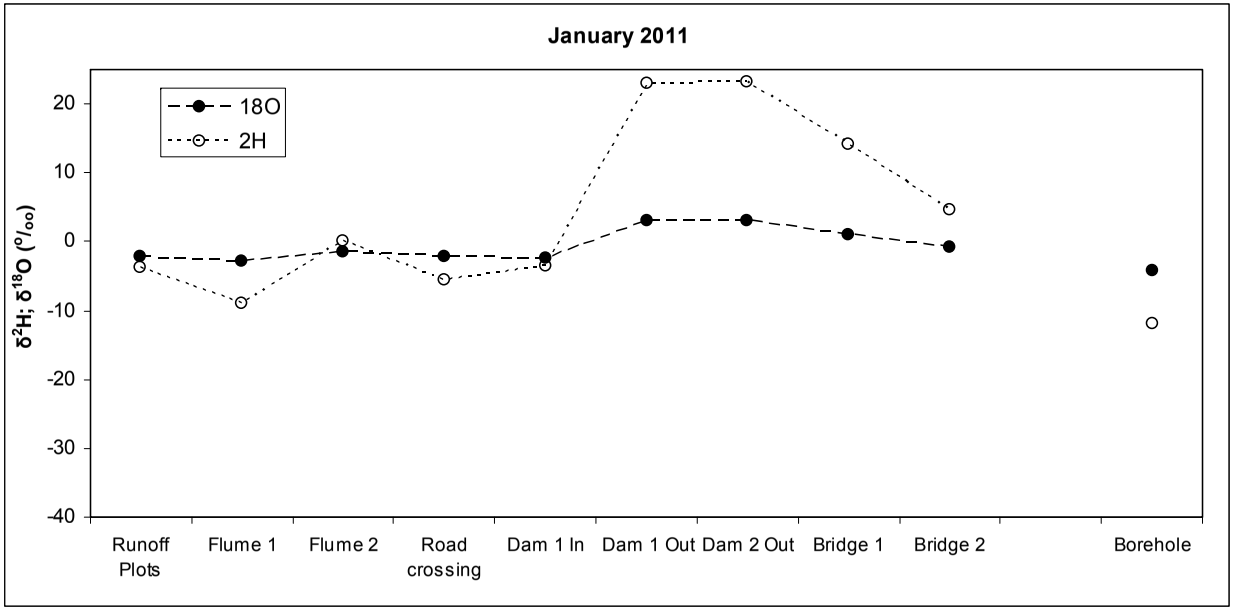

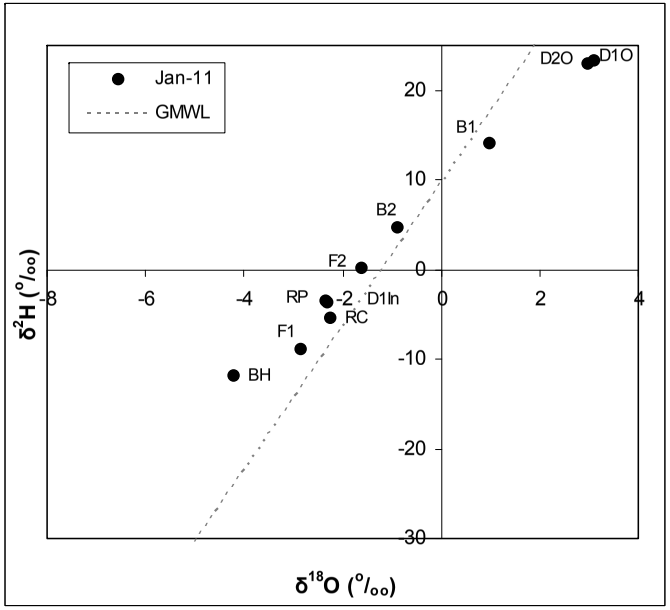

Figure D3.3. Isotope transects for event in January 2011

APPENDIX E
BOREHOLE TIME SERIES

E1 NO_3 and P (2010-2011)

E2 ISOTOPES (2010-2011)

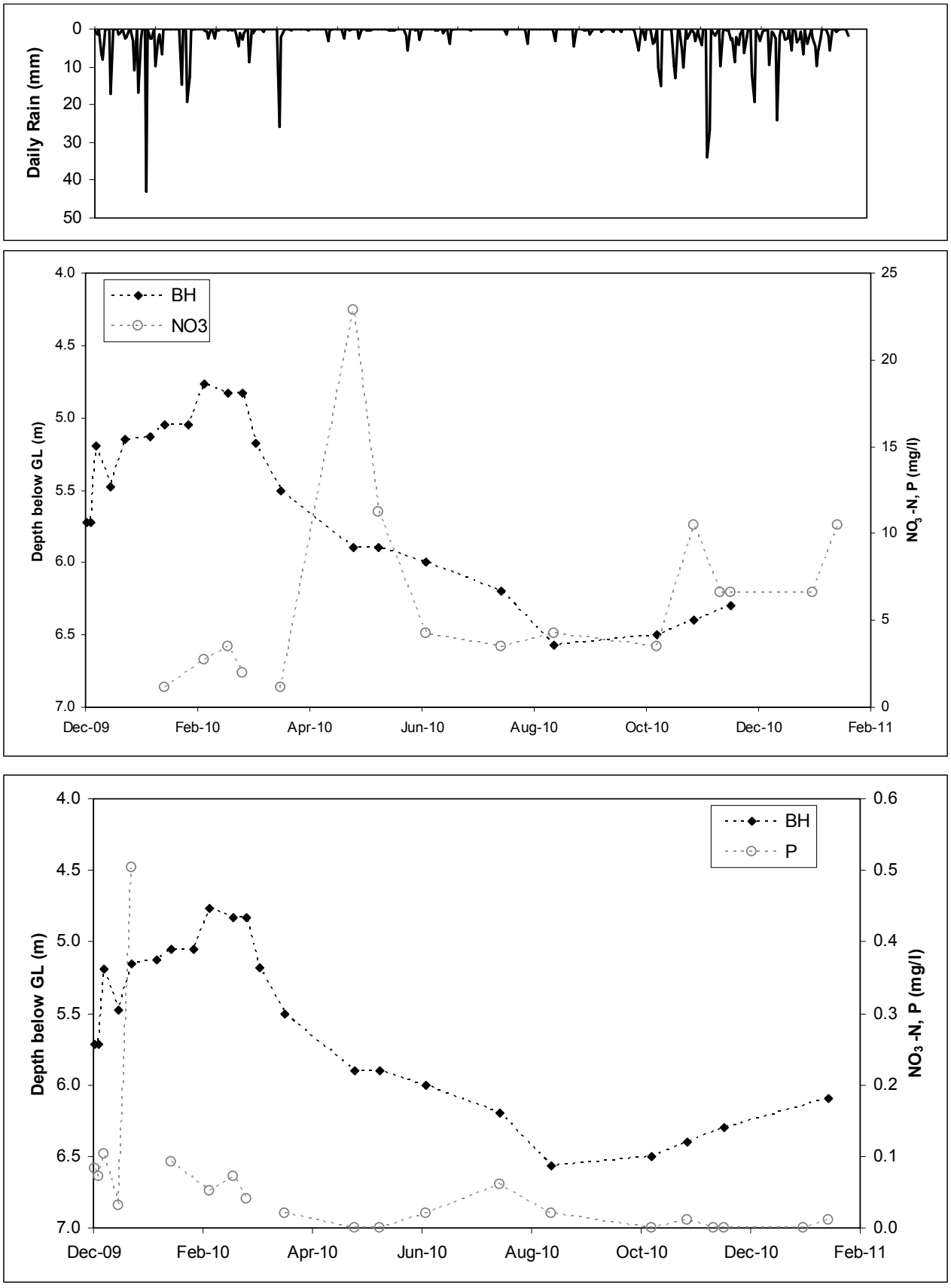

Figure E1. Groundwater depth, NO_3 and P at the BH station December 2009-January 2011.

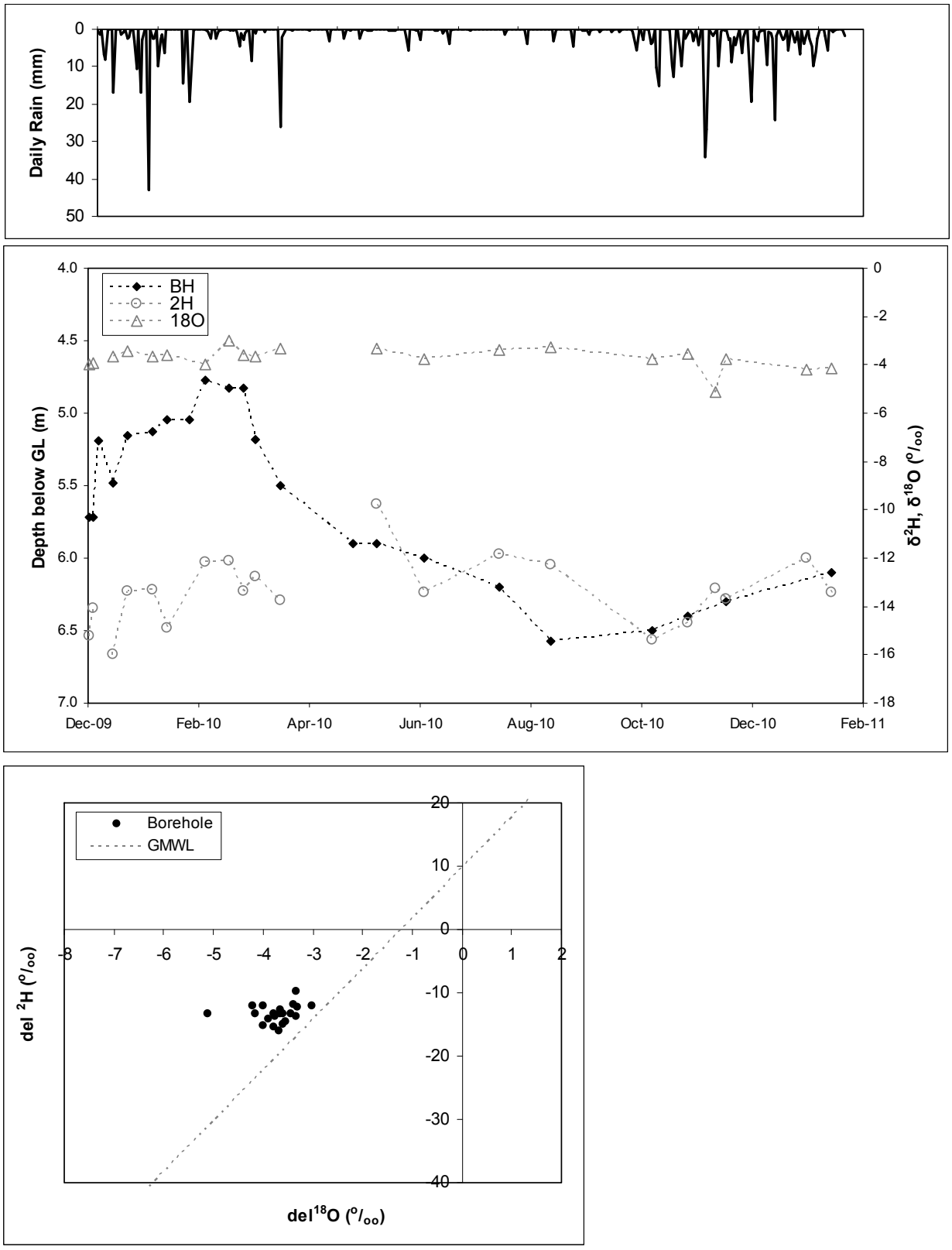

Figure E2. Groundwater depth and isotopes at the BH station December 2009-January 2011.